Application of Submicron Super-fine Powdered Activated Carbon on Mitigating Membrane Fouling in Microfiltration Systems

by
Yuanjun Zhao

A dissertation submitted in partial fulfillment of the requirements for the degree of

Doctor of Philosophy

Hokkaido University
2022

Acknowledgement

I would like to take this chance to express my gratitude to all the people who have worked and helped with this dissertation. Especially, I would like to take this opportunity to thank my supervisor, Professor Yoshihiko Matsui (The Environmental Risk Engineering Laboratory), for his kindness to take me as a member of his laboratory at the first time, for his role model effect to show me his rigor and enthusiasm to research, for his concern and help to my life and future career development planning. During the research in this laboratory, he made me realize and question the problems we ran into, asking as long as respecting my opinion. I could not imagine completing my Ph.D. degree without his guidance.

I would like to thank Associate Professor Taku Matsushita and Nobutaka Shirasaki in this laboratory, for their insights and advice to me at the weekly academic seminar, for their tireless efforts to revise my academic presentations and articles. Matsushita Sensei taught me to treat research and life with a strict but humorous attitude. Shirasaki Sensei made me discipline myself and maintain my motivation for research as long as life.

I would like to thank Dr. Long Pan, Mr. Shun Saito, Dr. Yoshifumi Nakazawa, Dr. Gang Shi, Mr. Ryosuke Kitajima, Mr. Yize Chen, Mr. Yusuke Kinouchi, Mr. Takumu Seko, Mr. Takeo Shimizu and all the rest of the laboratory members from the year 2017 to 2022, not only for their help such as sampling waters, building up experimental equipment and teaching me the operation methods of the analytical instruments, etc., but also being there for me.

I would like to thank my father Jianguo Zhao and my mother Xingqin Pan back in China, for their financial and emotional support during my stay in Japan. I would have felt much more stressful if they were not there supporting me the whole time during the COVID-19.

Finally, I am grateful to Nishihara Cultural Foundation and JST SPRING, Grant Number JPMJSP2119, who provided me with an environment so that I could focus more on my research.

Content

Acknowledgement i
Chapter 1. Introduction 1
1.1. Background 1
1.1.1. Membrane fouling in microfiltration 1
1.1.2. Applications of powdered activated carbon adsorption 1
1.2. Objectives and components of this research 3
1.3. References 4
Chapter 2. Superiority of submicron super-fine powdered activated carbon: straining and high adsorption capacity effects 7
2.1. Chapter introduction 7
2.2. Materials and methods 9
2.2.1. Activated carbons 9
2.2.2. Waters 10
2.2.3. Adsorption isotherm experiments 11
2.2.4. Batch precoat single filtration 11
2.2.5. Batch precoat repeat filtration 11
2.2.6. Lab-scale submerged membrane filtration with AC addition 12
2.3. Results and discussion 17
2.3.1. Adsorption capacities of DOC and biopolymer 17
2.3.2. Batch precoat single filtration on biopolymer removal 20
2.3.3. Batch precoat repeated filtration on biopolymer removal 23
2.3.4. TMP changes during AC addition and membrane filtration 24
2.3.5. Removal of biopolymer and HS during membrane filtration 32
2.4. Chapter conclusions 34
2.5. References 35
Chapter 3. Pulse dosing of submicron super-fine powdered activated carbon: effects of filtration flux, coagulant types, and coagulant-dose timing 37
3.1. Chapter introduction 37
3.2. Materials and methods 39
3.2.1. Waters 39
3.2.2. Activated carbons 39
3.2.3. Coagulants 40
3.2.4. Experiment setup of submerged membrane filtration 42
3.2.5. Filtration with changing precoat filtration flux 43
3.2.6. Filtration with changing coagulant dose timing 45
3.3. Results and discussion 46

3.3.1. Effects of precoat filtration flux on TMP rise 46
3.3.2. Effects of coagulant dose timing on TMP rise 50
3.3.3. Effects of coagulant (PACl) types on TMP rise 53
3.4. Chapter conclusions 58
3.5. References 59
Chapter 4. Pulse dosing of submicron super-fine powdered activated carbon in outside-in-type tubular and inside-out-type monolithic ceramic membranes 61
4.1. Chapter introduction 61
4.2. Materials and methods 64
4.2.1. Waters 64
4.2.2. Activated carbons and coagulants 65
4.2.3. Ceramic membranes 66
4.2.4. Submerged ceramic membrane filtration system 68
4.2.5. Monolithic ceramic membrane filtration system 70
4.2.6. Membrane surface observation 72
4.3. Results 73
4.3.1. Changes of TMP in submerged ceramic membrane systems with pulse and continuous dosing of SSPAC 73
4.3.2. Changes of TMP in a monolithic ceramic membrane system with pulse and continuous dosing of SSPAC 75
4.3.3. Filtrate qualities between pulse and continuous dosing of SSPAC in submerged and monolithic ceramic membrane systems 79
4.3.4. Surface observations of submerged and monolithic ceramic membranes 81
4.4. Discussion 90
4.4.1. Effectiveness of pulse dosing of SSPAC for mitigating hydraulically irreversible membrane fouling 90
4.4.2. Importance of precoat layer formation 94
4.5. Chapter conclusions 98
4.6. References 99
Chapter 5. Conclusions 102

Chapter 1. Introduction

1.1. Background

1.1.1. Membrane fouling in microfiltration

Low-pressure membrane filtration technology (e.g., microfiltration [MF] and nanofiltration [NF]) has become popular over the past few decades in drinking water treatments. However, during the filtration process, natural organic matter (NOM) tends to accumulate on/inside the membrane surface, clogging/constricting membrane pores, and fouls the membrane (Bai et al., 2021; Filloux et al., 2012; Li et al., 2021; Xie et al., 2017; Zhang and Fu, 2018). The accumulation of NOM decreases filterability (increases transmembrane pressure [TMP] in the case of constant filtration flux) and makes the filtration process consume more energy. To reduce the effect of fouling, membrane cleaning methods (e.g., backwashing) are periodically applied, while the TMP still increases as the filtration goes on, reflecting a progress of irreversible fouling.

NOM is present in all of waterbody and plays an important role in membrane fouling. The chemical structure of NOM, however, is not well understood because the composition of NOM is variable and the chemical constituents have a wide range of molecular weights (Adusei-Gyamfi et al., 2019; Amy, 2008). Recently, the introduction of liquid chromatography-organic carbon detection (LC-OCD) used to separate NOM into various fractions (Huber et al., 2011) has revealed that a hydrophilic fraction of the NOM with molecular weights over than 10,000 Da (known as biopolymer) is a major contributor to irreversible membrane fouling (Ayache et al., 2013; Chen et al., 2016; Kimura et al., 2014; Tian et al., 2013; Wang and Li, 2008; Zheng et al., 2010). Therefore, finding a way to remove NOM (especially biopolymer) to protect the membrane during the filtration becomes necessary.

1.1.2. Applications of powdered activated carbon adsorption

Activated carbon (AC) adsorption, coagulation and other pretreatment methods have been widely investigated to remove NOM (particularly biopolymer) prior to membrane filtration and to retard the

long-term buildup of TMP (Cheng et al., 2017; Ding et al., 2018; Fabris et al., 2007; Jarvis et al., 2012; Kimura and Oki, 2017; Lee et al., 2006; Ma et al., 2014; Su et al., 2017; Umar et al., 2016; Wang et al., 2013; Xing et al., 2019). AC adsorption, coagulation, and the combination of both have a long history of application and they are still under study in pilot plants for better performances (Keeley et al., 2016; Kweon et al., 2009). Although pretreatment using only powdered activated carbon (PAC) in an ultrafiltration system has produced a high removal of NOM, the PAC itself has caused severe membrane fouling (Lin et al., 2001, 1999). Recent studies, however, have produced more satisfactory results; when PAC is dosed at the beginning of the filtration or is pre-deposited on the surface of the membrane, membrane fouling is prevented to a certain extent (Campinas, 2010; Kim et al., 2008; Ye et al., 2006). The reasons for these inconsistent results may be the hydrophobicity of the membrane and the diverse characteristics of raw waters. On the other hand, it is reported when AC adsorption is combined with coagulation, larger mitigation of membrane fouling is observed better than applying AC or coagulant alone (Schwaller et al., 2021; Wang et al., 2016; Xing et al., 2019; Yu et al., 2014).

With the development of grinding technology, PAC with median diameter (D50) of ~30 μm can be ground into a superfine size (SPAC, ~1 μm). Such SPAC has been found to have a higher NOM adsorption capacity more rapidly rather than PAC. In addition, the required dosages are smaller (Amaral et al., 2016; Bonvin et al., 2016; Matsui et al., 2007, 2006, 2005, 2004). As a result, dosing with SPAC as a membrane pretreatment method in combination with coagulation has resulted in high rates of NOM removal and the ability to mitigate the buildup of TMP (Matsui et al., 2009). Although biopolymers are efficiently removed through a precoating with SPAC, the SPAC layer itself reduces the permeability of the membrane (Heijman et al., 2009). In the meanwhile, the efficacy of the SPAC precoating with coagulation pretreatment remains unexplored.

Recently the studies on submicron SPAC (SSPAC, ~200 nm) have revealed that the capacity of ACs on adsorbing NOM increases as ACs' sizes decrease from 30 μm to 140 nm (Pan et al., 2017). It is therefore highly interesting that SSPAC might replace PAC as a powerful adsorbent in drinking water treatment while such investigations are highly insufficient.

1.2. Objectives and components of this research

Based on the background above, the study was established to further reveal the potential of SSPAC on removing membrane foulants and its efficacy on mitigating the buildup of TMP during filtration. Specifically, the investigation progress was divided into the following perspectives:

(1) To compare SSPAC with PAC and SPAC on adsorption capacity of NOM and biopolymer, and to approve the straining effect of coated AC layer quantitively.

(2) To find a method for mitigating the buildup of TMP by applying SSPAC, and to determine the optimum experimental condition (e.g., dose timing of coagulant, coating speed of SSPAC, etc.).

(3) To extend the application of SSPAC by applying the method in (2) under varies filtration conditions and different types of membranes (e.g., flat sheet, hollow fiber, monolithic, etc.) with different materials (e.g., Poly Vinylidene DiFluoride [PVDF] and ceramic).

In this dissertation, the discussions were divided into following chapters to achieve the objectives:

Chapter 1 introduced the latest developments on membrane fouling control and AC adsorption. In the meantime, the shortcomings for the current condition and future development directions were presented.

Chapter 2 investigated the adsorption capacity of ACs with a wide range of particle sizes, aiming to prove SSPAC's superiority on NOM removal. For further practice, the effectiveness of coating layer by ACs were estimated to confirm the straining effect on NOM removal. In the latter part of this chapter, coagulant was introduced into the filtration system, and the buildup of TMP was compared.

Based on Chapter 2, Chapter 3 further explored the parameters during the filtration such as precoating speed and precoating efficiency. On the other hand, the type of coagulant and its addition method were further studied to understand their roles in the filtration process combined with SSPAC.

Chapter 4 extended SSPAC with coagulation method into ceramic membranes with different filtration systems. Pilot scale experiments were conducted to assess the feasibility of this method in the context of close-practical application.

Chapter 5 summarized the study findings and presented conclusions.

1.3. References

Adusei-Gyamfi, J., Ouddane, B., Rietveld, L., Cornard, J.P., Criquet, J., 2019. Natural organic matter-cations complexation and its impact on water treatment: A critical review. Water Research 160, 130–147.

Amaral, P., Partlan, E., Li, M., Lapolli, F., Mefford, O.T., Karanfil, T., Ladner, D.A., 2016. Superfine powdered activated carbon (S-PAC) coatings on microfiltration membranes: Effects of milling time on contaminant removal and flux. Water Research 100, 429–438.
Amy, G., 2008. Fundamental understanding of organic matter fouling of membranes. Desalination 231, 44–51.

Ayache, C., Pidou, M., Croué, J.P., Labanowski, J., Poussade, Y., Tazi-Pain, A., Keller, J., Gernjak, W., 2013. Impact of effluent organic matter on low-pressure membrane fouling in tertiary treatment. Water Research 47, 2633–2642.

Bai, Z., Zhang, R., Wang, S., Gao, S., Tian, J., 2021. Membrane fouling behaviors of ceramic hollow fiber microfiltration (MF) membranes by typical organic matters. Separation and Purification Technology 274, 118951.

Bonvin, F., Jost, L., Randin, L., Bonvin, E., Kohn, T., 2016. Super-fine powdered activated carbon (SPAC) for efficient removal of micropollutants from wastewater treatment plant effluent. Water Research 90, 90–99.

Campinas, M., 2010. Assessing PAC contribution to the NOM fouling control in PAC/UF systems. Water Research 44, 1636–1644.

Chen, F., Peldszus, S., Elhadidy, A.M., Legge, R.L., van Dyke, M.I., Huck, P.M., 2016. Kinetics of natural organic matter (NOM) removal during drinking water biofiltration using different NOM characterization approaches. Water Research 104, 361–370.

Cheng, X., Liang, H., Ding, A., Zhu, X., Tang, X., Gan, Z., Xing, J., Wu, D., Li, G., 2017. Application of Fe(II)/peroxymonosulfate for improving ultrafiltration membrane performance in surface water treatment: Comparison with coagulation and ozonation. Water Research 124, 298–307.

Ding, Q., Yamamura, H., Yonekawa, H., Aoki, N., Murata, N., Hafuka, A., Watanabe, Y., 2018. Differences in behaviour of three biopolymer constituents in coagulation with polyaluminium chloride: Implications for the optimisation of a coagulation–membrane filtration process. Water Research 133, 255–263.

Fabris, R., Lee, E.K., Chow, C.W.K., Chen, V., Drikas, M., 2007. Pre-treatments to reduce fouling of low pressure micro-filtration (MF) membranes. Journal of Membrane Science 289, 231–240.

Filloux, E., Gallard, H., Croue, J.P., 2012. Identification of effluent organic matter fractions responsible for low-pressure membrane fouling. Water Research 46, 5531–5540.

Heijman, S.G.J., Hamad, J.Z., Schippers, J., Amy, G., Kennedy, M.D., 2009. Submicron powdered activated carbon used as a pre-coat in ceramic micro-filtration. Desalination and Water Treatment 9, 86–91.

Huber, S.A., Balz, A., Abert, M., Pronk, W., 2011. Characterisation of aquatic humic and non-humic matter with size-exclusion chromatography - organic carbon detection - organic nitrogen detection (LC-OCD-OND). Water Research 45, 879–885.

Jarvis, P., Sharp, E., Pidou, M., Molinder, R., Parsons, S.A., Jefferson, B., 2012. Comparison of coagulation performance and floc properties using a novel zirconium coagulant against traditional ferric and alum coagulants. Water Research 46, 4179–4187.

Keeley, J., Jarvis, P., Smith, A.D., Judd, S.J., 2016. Coagulant recovery and reuse for drinking water treatment. Water Research 88, 502–509.

Kim, J., Cai, Z., Benjamin, M.M., 2008. Effects of adsorbents on membrane fouling by natural organic matter. Journal of Membrane Science 310, 356–364.

Kimura, K., Oki, Y., 2017. Efficient control of membrane fouling in MF by removal of biopolymers: Comparison of various pretreatments. Water Research 115, 172–179.

Kimura, K., Tanaka, K., Watanabe, Y., 2014. Microfiltration of different surface waters with/without coagulation: Clear correlations between membrane fouling and hydrophilic biopolymers. Water Research 49, 434–443.

Kweon, J.H., Hur, H.W., Seo, G.T., Jang, T.R., Park, J.H., Choi, K.Y., Kim, H.S., 2009. Evaluation of coagulation and PAC adsorption pretreatments on membrane filtration for a surface water in Korea: A pilot study. Desalination 249, 212–216.

Lee, J.-W., Choi, S.-P., Moon, H., Shim, W.-G., Thiruvenkatachari, R., 2006. Submerged microfiltration membrane coupled with alum coagulation/powdered activated carbon adsorption for complete decolorization of reactive dyes. Water Research 40, 435–444.

Li, J., Wang, B., Chen, Z., Ma, B., Chen, J.P., 2021. Ultrafiltration membrane fouling by microplastics with raw water: Behaviors and alleviation methods. Chemical Engineering Journal 410, 128174.

Lin, C.F., Huang, Y.J., Hao, O.J., 1999. Ultrafiltration processes for removing humic substances: Effect of molecular weight fractions and PAC treatment. Water Research 33, 1252–1264.

Lin, C.F., Liu, S.H., Hao, O.J., 2001. Effect of functional groups of humic substances on UF performance. Water Research 35, 2395–2402.

Ma, M., Liu, R., Liu, H., Qu, J., 2014. Mn(VII)-Fe(II) pre-treatment for Microcystis aeruginosa removal by Al coagulation: Simultaneous enhanced cyanobacterium removal and residual coagulant control. Water Research 65, 73–84.

Matsui, Y., Aizawa, T., Kanda, F., Nigorikawa, N., Mima, S., Kawase, Y., 2007. Adsorptive removal of geosmin by ceramic membrane filtration with super-powdered activated carbon. Journal of Water Supply: Research and Technology - AQUA 56, 411–418.

Matsui, Y., Fukuda, Y., Inoue, T., Matsushita, T., Aoki, N., Mima, S., 2004. Enhancing an adsorption-membrane hybrid system with microground activated carbon. Water Science and Technology: Water Supply 4, 189–197.

Matsui, Y., Hasegawa, H., Ohno, K., Matsushita, T., Mima, S., Kawase, Y., Aizawa, T., 2009. Effects of super-powdered activated carbon pretreatment on coagulation and trans-membrane pressure buildup during microfiltration. Water Research 43, 5160–5170.

Matsui, Y., Murase, R., Sanogawa, T., Aoki, N., Mima, S., Inoue, T., Matsushita, T., 2005. Rapid adsorption pretreatment with submicrometre powdered activated carbon particles before microfiltration. Water Science and Technology 51, 249–256.

Matsui, Y., Sanogawa, T., Aoki, N., Mima, S., Matsushita, T., 2006. Evaluating submicron-sized activated carbon adsorption for microfiltration pretreatment. Water Science and Technology: Water Supply 6, 149–155.

Pan, L., Nishimura, Y., Takaesu, H., Matsui, Y., Matsushita, T., Shirasaki, N., 2017. Effects of decreasing activated carbon particle diameter from 30 Mm to 140 nm on equilibrium adsorption capacity. Water Research 124, 425–434.

Schwaller, C., Hoffmann, G., Hiller, C.X., Helmreich, B., Drewes, J.E., 2021. Inline dosing of powdered activated carbon and coagulant prior to ultrafiltration at pilot-scale – Effects on trace organic chemical removal and operational stability. Chemical Engineering Journal 414, 128801.

Su, Z., Liu, T., Yu, W., Li, X., Graham, N.J.D., 2017. Coagulation of surface water: Observations on the significance of biopolymers. Water Research 126, 144–152.

Tian, J., Ernst, M., Cui, F., Jekel, M., 2013. Correlations of relevant membrane foulants with UF membrane fouling in different waters. Water Research 47, 1218–28.

Umar, M., Roddick, F., Fan, L., 2016. Impact of coagulation as a pre-treatment for UVC/H2O2-biological activated carbon treatment of a municipal wastewater reverse osmosis concentrate. Water Research 88, 12–19.

Wang, H., Qu, F., Ding, A., Liang, H., Jia, R., Li, K., Bai, L., Chang, H., Li, G., 2016. Combined effects of PAC adsorption and in situ chlorination on membrane fouling in a pilot-scale coagulation and ultrafiltration process. Chemical Engineering Journal 283, 1374–1383.

Wang, S., Liu, C., Li, Q., 2013. Impact of polymer flocculants on coagulation-microfiltration of surface water. Water Research 47, 4538–4546.

Wang, X.M., Li, X.Y., 2008. Accumulation of biopolymer clusters in a submerged membrane bioreactor and its effect on membrane fouling. Water Research 42, 855–862.

Xie, M., Luo, W., Gray, S.R., 2017. Surface pattern by nanoimprint for membrane fouling mitigation: Design, performance and mechanisms. Water Research 124, 238–243.

Xing, J., Liang, H., Cheng, X., Yang, H., Xu, D., Gan, Z., Luo, X., Zhu, X., Li, G., 2019. Combined effects of coagulation and adsorption on ultrafiltration membrane fouling control and subsequent disinfection in drinking water treatment. Environmental Science and Pollution Research 26, 33770–33780.

Ye, M., Zhang, H., Wei, Q., Lei, H., Yang, F., Zhang, X., 2006. Study on the suitable thickness of a PAC-precoated dynamic membrane coupled with a bioreactor for municipal wastewater treatment. Desalination 194, 108–120.

Yu, W., Xu, L., Qu, J., Graham, N., 2014. Investigation of pre-coagulation and powder activate carbon adsorption on ultrafiltration membrane fouling. Journal of Membrane Science 459, 157–168.

Zhang, Y., Fu, Q., 2018. Algal fouling of microfiltration and ultrafiltration membranes and control strategies: A review. Separation and Purification Technology 203, 193–208.

Zheng, X., Ernst, M., Huck, P.M., Jekel, M., 2010. Biopolymer fouling in dead-end ultrafiltration of treated domestic wastewater. Water Research 44, 5212–5221.

Chapter 2. Superiority of submicron super-fine powdered activated carbon: straining and high adsorption capacity effects

2.1. Chapter introduction

Applying PAC (D50 of ~30μm) into microfiltration for drinking water treatment has been decades while the evaluation of its effectiveness is polarized. It is reported that PAC itself has caused severe membrane fouling (Lin et al., 2001, 1999), while other studies reveal that PAC prevents membrane fouling to a certain extent (Campinas, 2010; Kim et al., 2008). The reasons for these inconsistent results may be the hydrophobicity of the membrane and the diverse characteristics of raw waters. PAC causes less fouling with hydrophilic membranes (Crozes et al., 1993), and helps to reduce fouling when its use is combined with coagulation pretreatment, although such a combination does not eliminate fouling completely. As a result, TMP increases gradually during long-term operation (Kweon et al., 2009).

On the other hand, as SPAC and SSPAC can be produced from normal-size PAC, the superiority of smaller particle-size PAC on adsorption capacity towards NOM was gradually explored (Bonvin et al., 2016; Matsui et al., 2013, 2011, 2006; Pan et al., 2017b, 2017a).

To determine SSPAC's adsorption capacity towards NOM (as well as biopolymer), adsorption isotherm experiments using PAC/SPAC/SSPAC and biopolymers in natural river water were conducted. Furthermore, batch-scale membrane filtration was conducted to elucidate the mechanism of the biopolymer removal. Laboratory-scale membrane filtration with treatments combining PAC/SPAC/SSPAC and coagulation under different dosing methods were further investigated to compare the ability of the treatments to prevent a long-term increase of TMP during filtration with periodic backwashes.

This Chapter has been published by Elsevier, and the information is described as follows:

Title: Precoating membranes with submicron super-fine powdered activated carbon after coagulation prevents transmembrane pressure rise: Straining and high adsorption capacity effects

Author: Yuanjun Zhao, Ryosuke Kitajima, Nobutaka Shirasaki, Yoshihiko Matsui, Taku Matsushita

Name of journal: Water Research

Year: 2020

Volume: 177

Pages: 115757

DOI: 10.1016/j.watres.2020.115757

2.2. Materials and methods

2.2.1. Activated carbons

Wood-based PAC (Taiko-W, Futamura Chemical Co., Ltd., Nagoya, Japan) was used to produce SPAC and SSPAC. A PAC slurry was made by dosing PAC into pure water (Milli-Q water, Merck KGaA, Darmstadt, Germany). The PAC concentration was consistently within the range of 10-15% (w/w). The slurry was then milled in a closed chamber with alumina balls with diameter of 5 and 10 mm at 45 rpm for 5 h to reduce the particle size to the D50 of ~4 μm. The milled slurry was then transferred into a bead mill (LMZ015, Ashizawa Finetech, Ltd., Chiba, Japan) with zirconium dioxide beads with diameter of 0.3 mm in recirculation mode at 2,590 rpm for 30 min to produce SPAC with the D50 of ~1 μm. In the case of SSPAC, the beads with diameter of 0.1 mm were applied under a milling speed of 3,884 rpm for 2 h, which produces SSPAC with the D50 of ~200 nm.

The distribution of ACs was analyzed by a laser-light-scattering instrument (Microtrac MT3300EXII, Nikkiso Co., Inc., Tokyo, Japan). A dispersant (Triton X-100, Kanto Chemical Co., Inc., Tokyo, Japan) was dosed into the samples and then sonicated (150W, 19.5 kHz) for approximately 1 min in the case of PAC/SPAC and for 6 min for SSPAC to break up the particle aggregation and to determine the true particle size (Pan et al., 2016). The particle size distributions of the ACs are shown in Fig. 2-1.

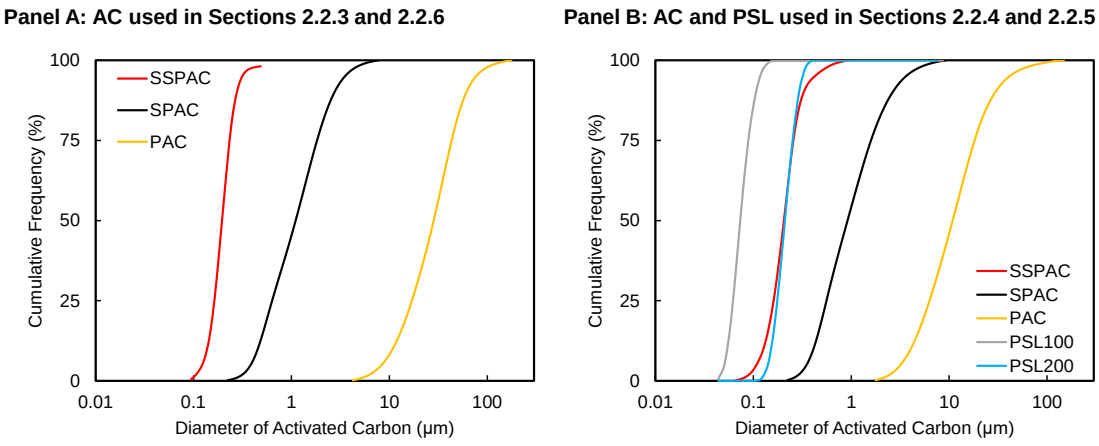

Fig. 2-1. Size distributions of PAC (powdered activated carbon) and PSL (polystyrene latex) particles.

2.2.2. Waters

Wanigawa River (Ibaraki, Japan) that sampled in May (Water-1) and November (Water-2) of 2017 was used as a feed water. Water qualities of the waters are shown in Table 2-1. The samples were shipped to the laboratory and filtered by a mixed cellulose ester (MCE) membrane filters with a pore size of 0.1 μm (φ142 mm, Merck KGaA, Darmstadt, Germany) to obtain a working solution for the adsorption isotherm experiments (Section 2.2.3) and batch precoat filtration experiments (Sections 2.2.4 and 2.2.5). A coated cellulose acetate membrane filter with a pore size of 10 μm (φ142 mm, Toyo Roshi Kaisha, Ltd., Tokyo, Japan) was used to produce 7 L of the water for the experiments involving the AC addition and submerged membrane filtration with a backwash (Section 2.2.6). Ultraviolet absorbance at 260 nm (UV260) and the concentrations of biopolymer, humic substances (HS), and dissolved organic carbon (DOC) were used as metrics of the concentrations (water samples were passed through a 0.45 μm polytetrafluoroethylene [PTFE] membrane so that the total organic carbon [TOC] value that been measured is supposed to be DOC). DOC concentration was determined by a TOC analyzer (Model 900. Sievers Instruments, Boulder, CO, USA). UV260 was analyzed by a UV spectrophotometer (UV-1800, Shimadzu, Kyoto, Japan). Biopolymer and HS concentrations were determined by an HPLC system (1100 series, Agilent Tech, Tokyo, Japan) equipped with a column (Toyopearl HW-50S, 250 mm × 20 mm, Tosoh Inc., Tokyo, Japan) followed by an auto sampling and injecting system with the injection rate of 1.2 mL/min and a UV detector and a TOC analyzer (M9e, Central Kagaku Corp., Tokyo, Japan). This system was developed by Huber's laboratory (Huber et al., 2011).

Table 2-1.
Water quality of Water-1 and Water-2 (the water was pre-filtrated by 0.1-μm MCE membrane).

	pH	DOC (mg/L)	UV260 (cm^{-1})	Biopolymer (mg/L)	Alkalinity (mg/L as $CaCO_3$)	Na^+ (mg/L)
Water-1	8.07	2.61	0.06	0.0725	71	52.7
Water-2	7.62	2.66	0.06	0.0770	72	43.7
	K^+ (mg/L)	Mg^{2+} (mg/L)	Ca^{2+} (mg/L)	Cl^- (mg/L)	NO_3^- (mg/L)	SO_4^{2-} (mg/L)
Water-1	6.03	11.0	19.0	70.7	13.3	24.4
Water-2	5.84	9.18	18.0	54.0	13.8	22.3

2.2.3. Adsorption isotherm experiments

The PAC/SPAC/SSPAC particles were injected into shaking flasks containing 100 mL of Water-2 at fixed carbon dosages of 0, 5, 10, 20, 30 and 40 mg/L. The sealed flasks were then shaken at room temperature of 20 ºC for one week. Then the treated water was centrifuged, and the supernatant was filtered through two stacked PVDF membrane filters with a pore size of 0.2 μm (Dismic-25CS, Advantec Toyo Kaisha, Ltd., Tokyo, Japan) to remove residual AC that may interfere analysis afterwards.

2.2.4. Batch precoat single filtration

The PAC, SPAC and SSPAC as well as two kinds of polystyrene latex spheres (D50 of 100 nm and 200 nm, henceforth referred as PSL-100 and PSL-200, Micromod Partikeltechnologie GmbH, Rostock, Germany) were separately dosed into 50 mL of Water-1. Each suspension was poured into a membrane filter funnel with a flat sheet MCE membrane with pore size of 0.1 μm (φ47 mm, effective membrane filtration area of 9.6 cm^2, Merck KGaA, Darmstadt, Germany). The filtration system was motivated by a consistent vacuum suction force (-80 kPa) so that the first 40 mL of the suspension was filtered through the membrane from upstream to downstream and an initial deposition mass of dosed particles was formed with 0.17, 0.35 or 0.53 mg/cm^2 on the membrane surface. There is still 10 mL of the suspension remained in the funnel to prevent the membrane and the coating layer from drying out. Subsequently, another 50 mL of Water-1 was poured carefully into the funnel without breaking the precoating layer, and the filtration was resumed. The 50 mL of filtrate was taken then for biopolymer analysis. The increase in the AC deposition mass during the 50-mL filtration was small (10%).

2.2.5. Batch precoat repeat filtration

Fifty milliliters of Water-1 that contains 84 mg/L of AC suspension was poured into a membrane filter funnel and 40 mL was filtered through the membrane to form a precoating layer as in Section 2.2.4. Then 50 mL of Water-1 was added into the funnel and passed through the filter. Such process was repeated until the total filtrate volume reached to 2,090 mL per filter. The filtrates were then analyzed

for biopolymer concentration. In some of the experiments, the first 50 mL of suspension with AC particles was sonicated (150 W, 19.5 kHz) for 3 min before the addition.

2.2.6. Lab-scale submerged membrane filtration with AC addition

Fig. 2-2 is a schematic diagram of the experimental setup of submerged membrane filtration system. Water-2 was feed through a peristaltic pump into a rectangular tank with interior dimensions of 1.1 × 1.1 × 27.5 cm (depth) where a hollow fiber PVDF membrane fiber with pore size of 0.1 μm (Asahi Kasei Corp., Tokyo, Japan) with its tip closed was set and submerged (A membrane module containing such PVDF fibers was purchased and cut to a length of 14 cm with an effective filtration area of 6 cm^2). Every cut fiber was measured and tested to make sure the fibers that been used in the experiment maintain a similar permeability. Filtration flux was set at 70.8 L m^{-2} h^{-1} by applying a vacuum suction force from the inside of the membrane. After 0.6 h of water filling, the filtration was proceeded for 7 h with a hydraulic backwash of 30 s that introduced pure water at 50 kPa from the filtrate side, then the suspension in the tank was drained and the second cycle from water filling starts. The filtrate was collected automatically every 30 min intervals for analysis.

In Methods A, B in Fig 2-3 and 2-4, AC was added in a direct pulse dose at the beginning of the filtration right after water filling and followed by a 3-min bubbling for better mixing. In Method C in Fig. 2-5, AC was indirectly pulse dosed as AC and water were mixed vigorously in a bottle and the mixture was injected into the membrane tank as the suspension. Those two methods were compared in Fig. 2-6. In Methods D and E in Fig 2-7 and 2-8, AC was added continuously throughout the filtration process. Among all experiments, the dosage of AC was fixed at 5 mg-C/L in the case of continuous doing, which means the dosage in the case of pulse dose was calculated as the total mass amount of the AC in continuous dose.

Experiments with coagulation were equipped with a static mixer in the feed line. Polyaluminum chloride coagulant (PACl, basicity 2.1; sulfate ion 2% [w/w], Taki Chemical Co., Hyogo, Japan) was dosed at 2 mg-Al/L. In Methods B and C of pulse AC dose, coagulants were applied before AC dose. In

Methods D and E of continuous dose, coagulants were applied either before or after AC dose. The pH was adjusted when the water was fed into the line and kept at 7.5. The pressure was recorded based on the voltage using a digital pressure meter (GC61, Nagano Keiki Products, Tokyo, Japan) and converted into pressure using calibration curves determined during the test experiment. The experiment was conducted with a room temperature of ~25 ºC and the water temperature was monitored by a digital thermometer (LR5011, Hioki E.E Copr., Nagano, Japan). TMP was normalized to 25 ºC to avoid the influence of changes of viscosity.

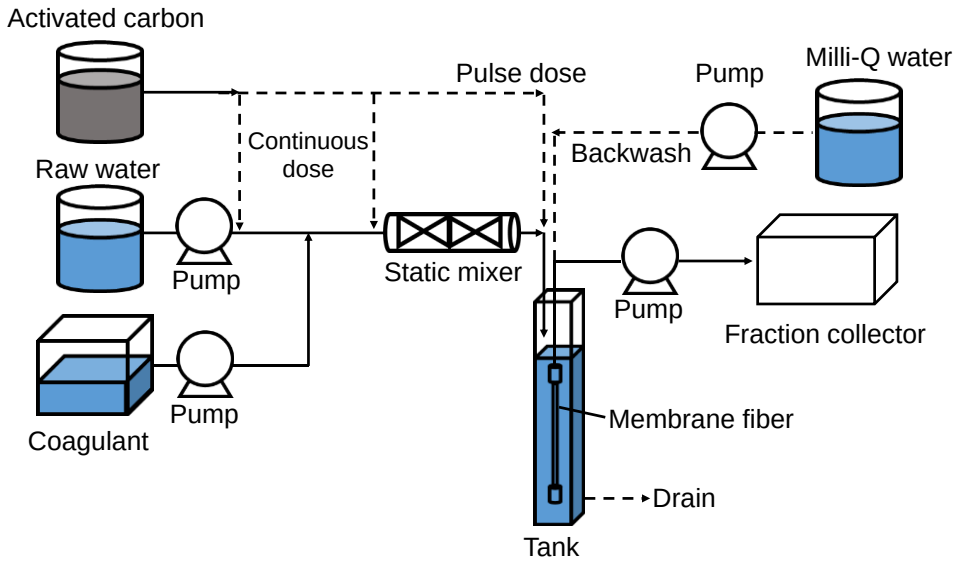

Fig. 2-2. Laboratory setup for additions of activated carbon and coagulant and for submerged membrane filtration with backwash.

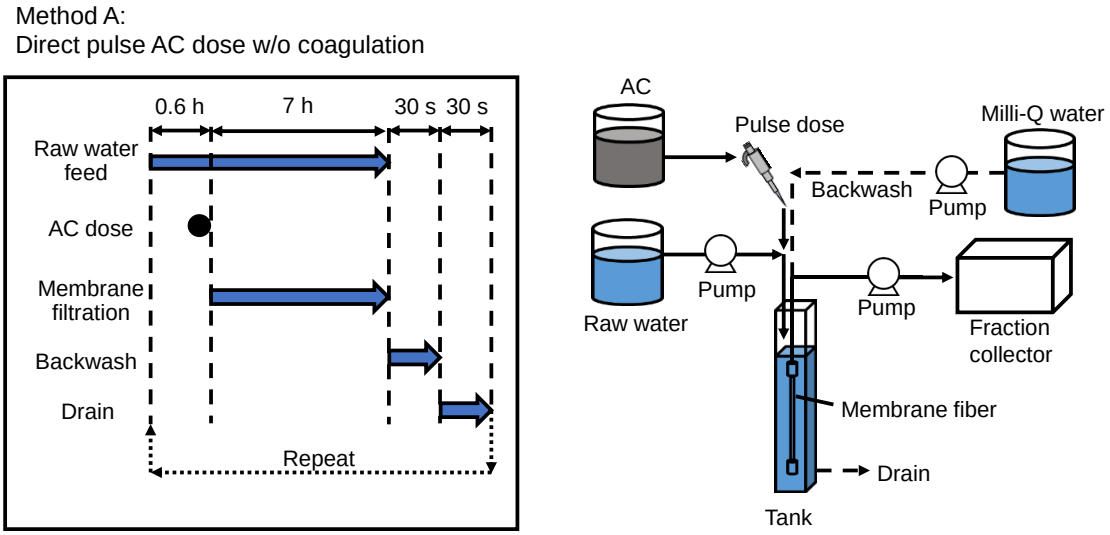

Fig. 2-3. Method A: Process flow and time flow of the direct pulse AC dose without coagulation. (The process was repeated four rounds in every experiment)

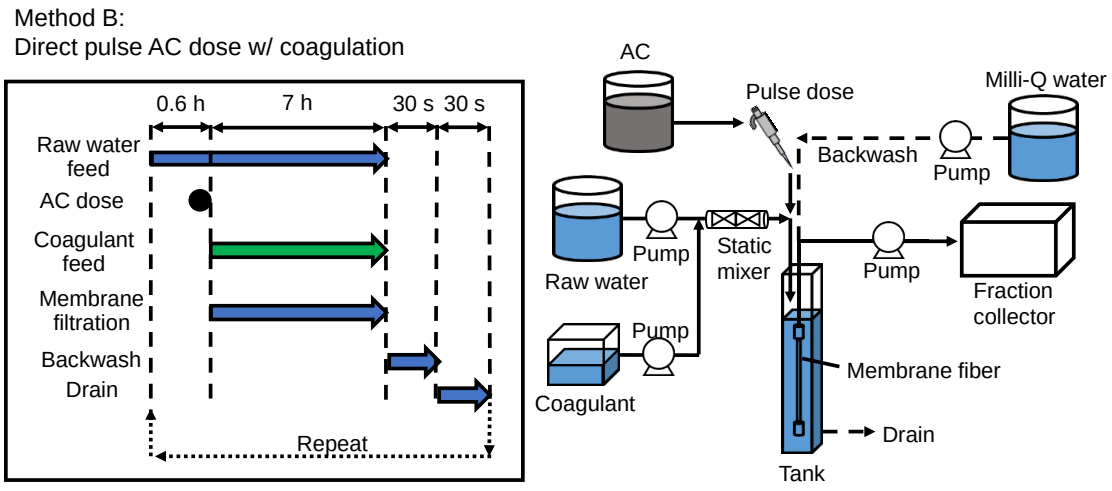

Fig. 2-4. Method B: Process flow and time flow of the direct pulse AC dose with coagulation. (The process was repeated four rounds in every experiment)

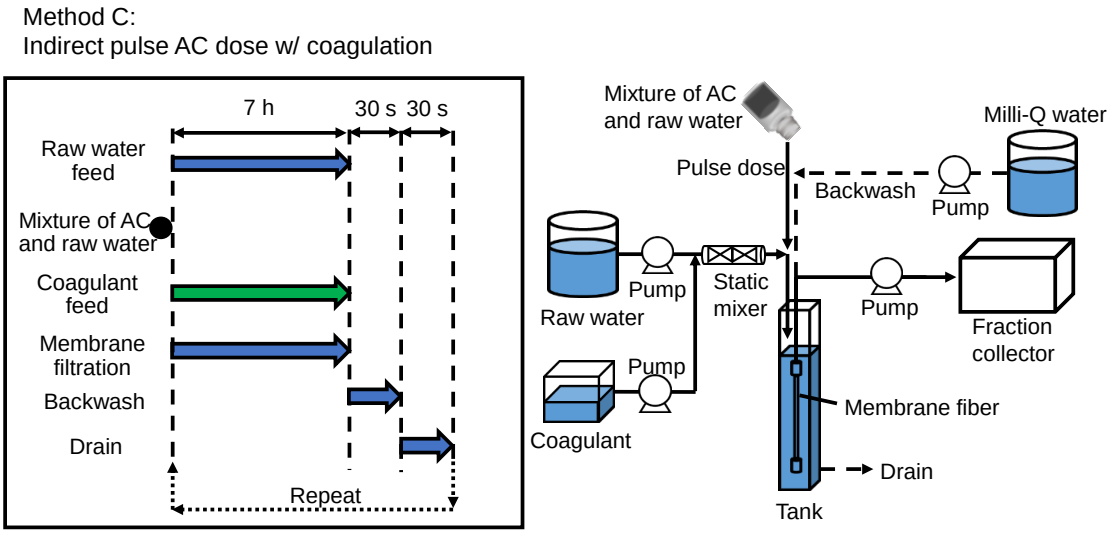

Fig. 2-5. Method C: Process flow and time flow of the indirect pulse AC dose with coagulation. (The process was repeated four rounds in every experiment)

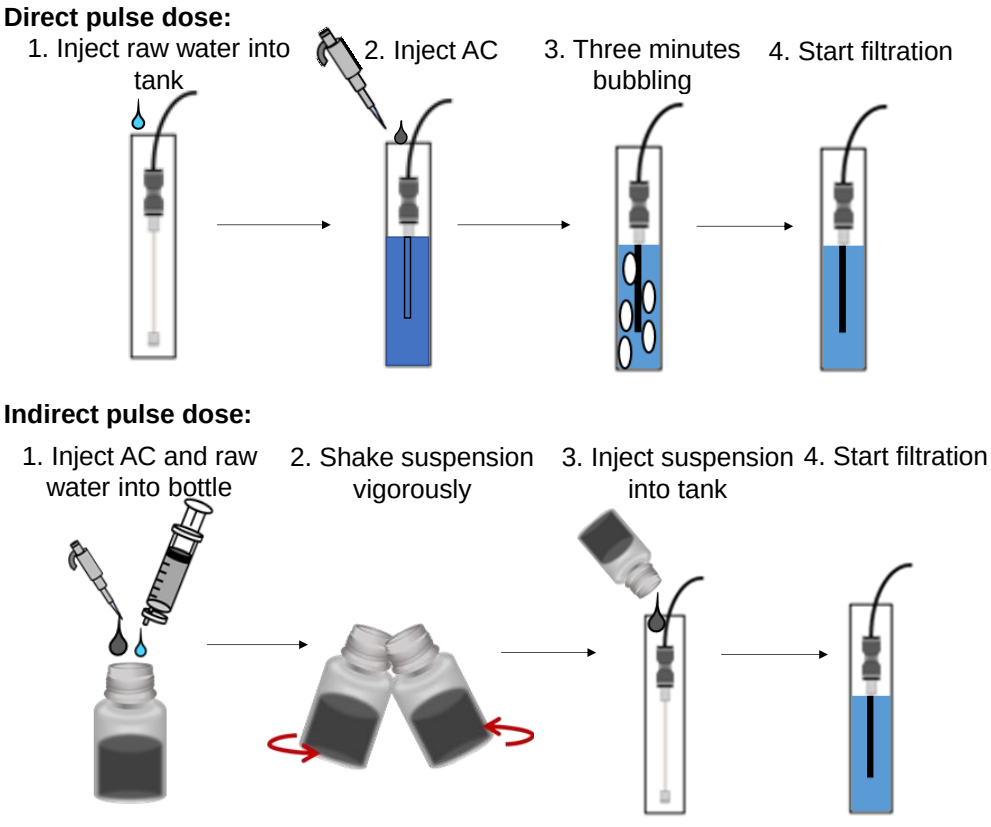

Fig. 2-6. Direct and indirect pulse dose method explanation.

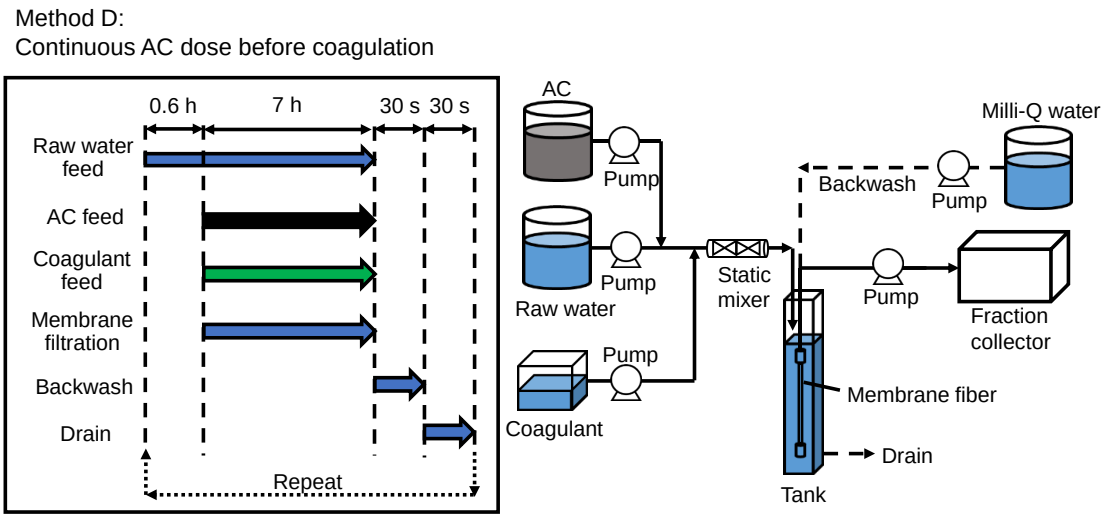

Fig. 2-7. Method D: Process flow and time flow of continuous AC dose before coagulation. (The process was repeated four rounds in every experiment)

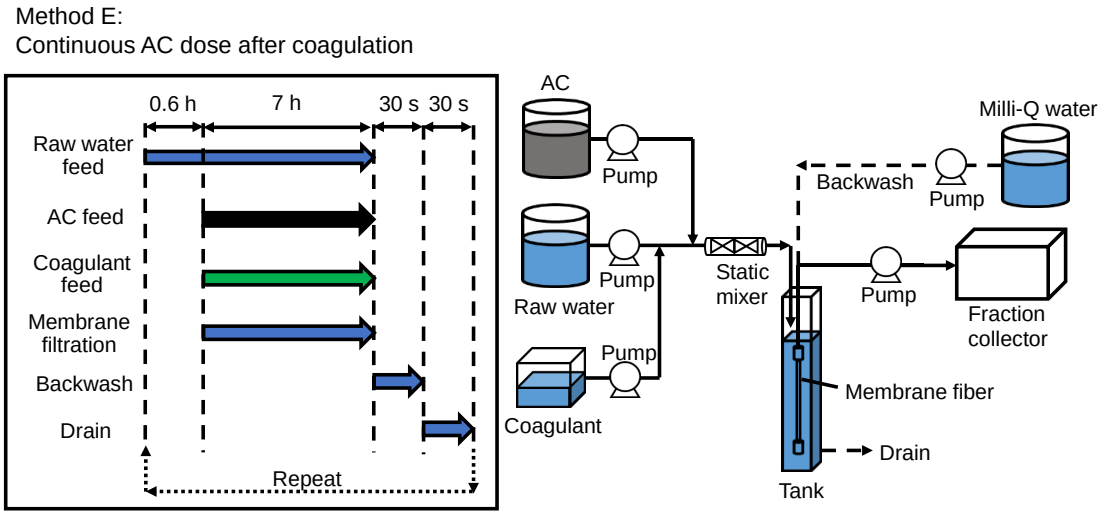

Fig. 2-8. Method E: Process flow and time flow of continuous AC dose after coagulation. (The process was repeated four rounds in every experiment)

2.3. Results and discussion

2.3.1. Adsorption capacities of DOC and biopolymer

Adsorption isotherm of biopolymer, DOC and UV260 were obtained by PAC/SPAC/SSPAC in Fig. 2-9, 2-10 and 2-11. The adsorption capacities of the three ACs for biopolymer, DOC and UV260 follows the order of PAC < SPAC < SSPAC, which corresponds to the descending order of particle size. Adsorption capacities were enhanced as the particle size of ACs decreased is in accordance with the recent discovery that the adsorption capacity of AC toward adsorbates with a high molecular weight increases as the particle size of the AC decreases with D50 from 30 μm to 140 nm (Pan et al., 2017a), which can be explained as that the molecules are mostly adsorbed on the exterior of the AC particles (Ando et al., 2011; Matsui et al., 2014, 2013, 2011) and the milling procedure does not affect internal pore area.

For a better understanding about the dependence of the adsorption capacity on the AC particle size, a solid-phase concentration at equilibrium with a liquid-phase concentration at DOC value of 1.8 mg/L and biopolymer value of 0.02 mg/L was plotted against the D50 of AC particles in Fig. 2-12. The adsorption capacity of the AC for biopolymer was smaller than that for DOC because biopolymers are a portion of NOM and therefore their concentrations are commonly lower than NOM concentrations which are determined by DOC. It is found in this study that as the D50 of the ACs decreased, their capacities to adsorb both biopolymers and DOC increased while the dependency of biopolymer to AC size is much stronger than DOC to the size. The capacity dependency on AC particle size is explained as that the adsorption of high molecular-weight compounds mainly occurred on the exterior of AC particles owing to their limited intraparticle diffusion distances, and it was reported that the capacity dependency is large for large molecules (Ando et al., 2011; Matsui et al., 2011). In this study, therefore, the strong dependence of the biopolymer adsorption capacity on AC particle size was likely related to the large molecular size of biopolymers in NOM. Since the capacity dependency between the biopolymer and NOM (from a total view), biopolymer/DOC concentration ratio after AC contact

decreased with SSPAC and SPAC dosages but increased with PAC dosage (Fig. 2-13). Moreover, the biopolymer/DOC concentration ratio decreased more rapidly after SSPAC rather than SPAC, which indicates that SSPAC selectively adsorbs the biopolymer from NOM with a more obvious preference than PAC and SPAC.

These results suggest that adsorption pretreatment by SSPAC will mitigate the membrane fouling and attenuate the buildup of TMP more efficiently than PAC and SPAC since biopolymer is considered as a major contributor to membrane fouling (Huber et al., 2011; Kimura et al., 2014; Myat et al., 2014; Tian et al., 2013; Zheng et al., 2010). It was reported that a higher biopolymer removal by SPAC over than PAC was observed (Heijman et al., 2009). In this study, however, SSPAC is clearly superior to SPAC on biopolymer removal.

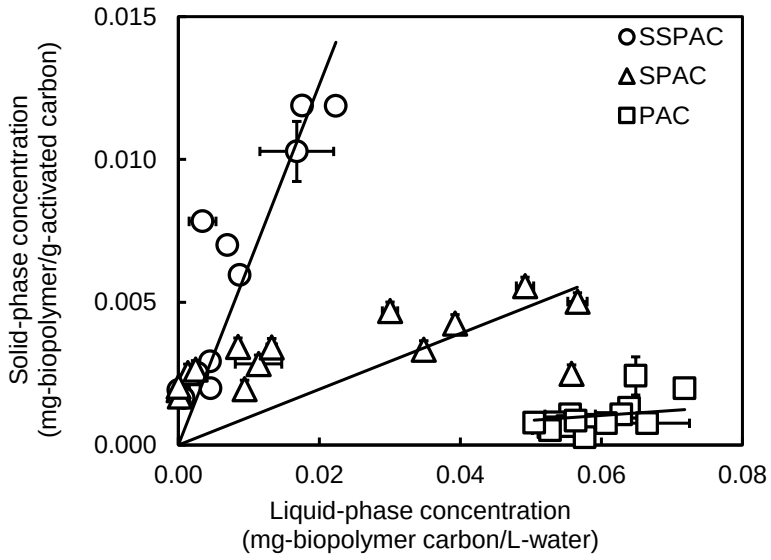

Fig. 2-9. Solid-phase concentration versus liquid-phase concentration of biopolymer for different forms of powdered activated carbon (PAC). Water-2 was used in this experiment. The symbols indicate the data points. The lines are regression lines with an intercept of 0. The error bars indicate ranges of two measurements by liquid chromatography–organic carbon detection methodology (for the x axis) and consequent changes of calculated concentrations (for the y axis). Error bars indicate standard deviations of measurements. Some error bars are hidden behind the symbols.

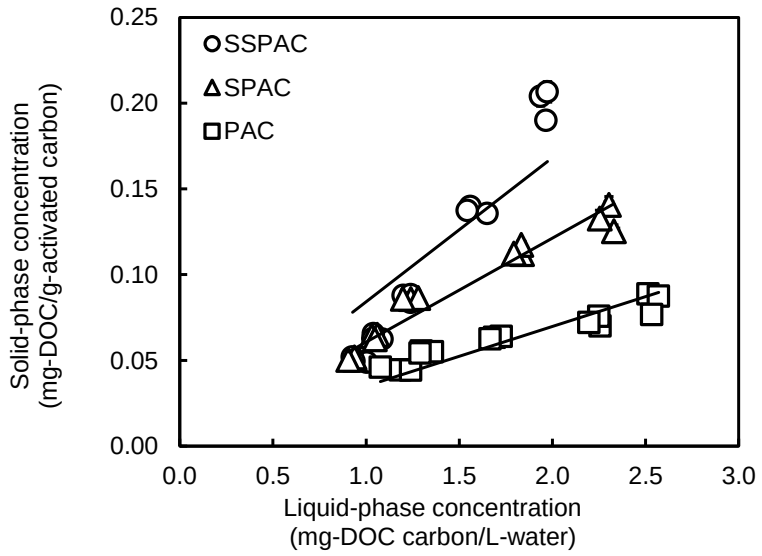

Fig. 2-10. Solid-phase concentration versus liquid-phase concentration of dissolved organic carbon (DOC) for different forms of powdered activated carbon (PAC). Water-2 was used in this experiment. The lines are regression lines with an intercept of 0. Error bars, which indicate standard deviations of measurements, are hidden by the plots.

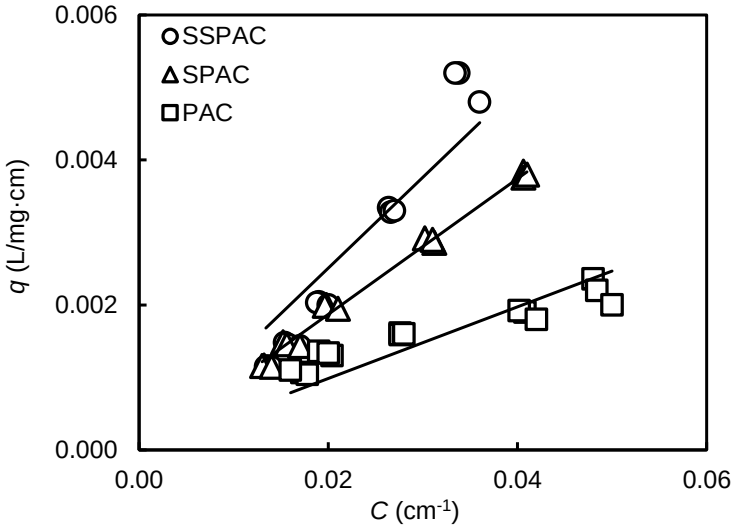

Fig. 2-11. Solid-phase concentration (q) versus liquid-phase concentration (C) of UV260 for different forms of powdered activated carbon (PAC). Water-2 was used in this experiment. The lines are regression lines with an intercept of 0.

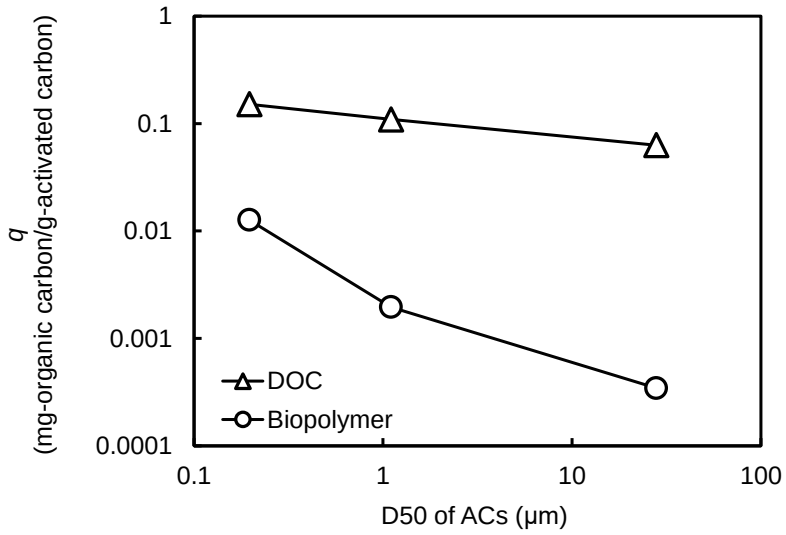

Fig. 2-12. Plots of solid-phase concentration (q) at an equilibrium liquid-phase dissolved organic carbon (DOC) concentration of 1.8 mg/L and a biopolymer concentration of 0.02 mg/L versus the median diameter (D50) of the activated carbons (ACs). The data are taken from Figs. 2-9 and 2-10. Water-2 was used in this experiment.

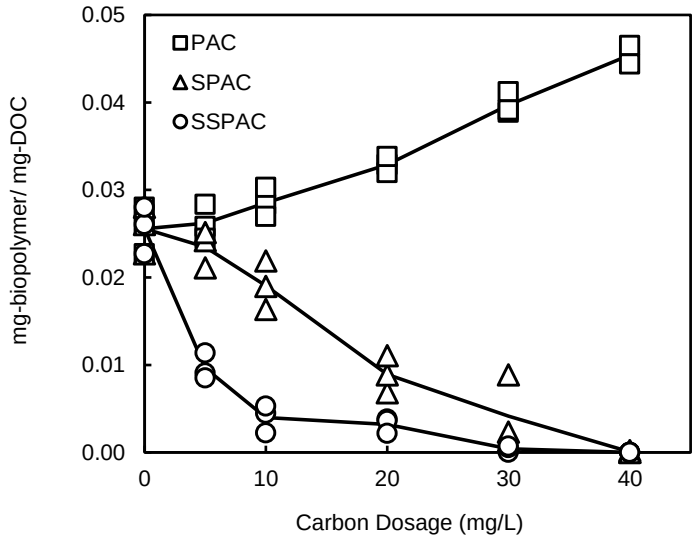

Fig. 2-13. Biopolymer/dissolved organic carbon (DOC) mass ratio versus carbon dosage for different kinds of activated carbon (AC). Water-2 was used in this experiment.

2.3.2. Batch precoat single filtration on biopolymer removal

Fig. 2-14 shows the results of precoat experiments by PAC, SPAC, SSPAC, PSL-100 and PSL-200 particles deposited on a 0.1-μm MCE flat sheet membrane. A procoat layer was produced and the water containing biopolymers passed through the membrane. As described in Section 2.2.2, the water was pre-

filtered by a 0.1-μm MCE membrane so biopolymers in this water cannot be simply removed by membrane filtering (Fig. 2-15). Therefore, it became much more clear that the biopolymer removal in this study was only possible for the adsorption from ACs or the straining effect from precoated layers.

The biopolymer removal increased as the amount of particles precoating the membrane increased. However, the removal by PSL-precoated membrane reached a plateau after a certain amount. The plateau of the biopolymer removal was higher in the case of PSL-100 rather than PSL-200. On the other hand, biopolymer removals by SPAC/SSPAC-precoated membranes were high and can be attributed to the adsorption of biopolymers onto the AC. However, the removal by PSL precoating layer cannot be explained as adsorption since PSL cannot adsorb biopolymers (Fig. 2-16). It is therefore possible that biopolymers were removed by a straining effect from precoated PSL-100 layer. It is reported that when the ratio of particle diameter to media diameter is greater than 0.15, the particle will then be strained by the media (Crittenden et al., 2012). Therefore, the PSL-100 with D50 of 100 nm could strain particles with size over 15 nm. On the other hand, biopolymers have a wide range of molecular weight while the ones with large molecular weights (> 1 million Da) tend to foul the membrane in MF system (Kimura et al., 2018), and such molecular weights could be approximately converted to molecular diameters > 17 nm(Weiss et al., 2018). Although the type and diameter distribution of biopolymer varies from sample to sample, and it is difficult to quantify the diameter distribution of biopolymer in each water sample, the estimation of the molecular diameters > 17 nm is in accordance with the particle size distribution of the biopolymer determined by membrane filtration in this study (Fig. 2-17). Therefore, it is possible to say that most of the biopolymer molecules would be greater than 15 nm in size in the water sample used in this experiment. When a PSL precoat layer forms, biopolymer molecules are too large to pass through the interstitial spaces between the PSL particles and then been captured as the flow of water moves them through the particles. The higher rate of biopolymer removal by precoating PSL-100 over than PSL-200 could be therefore explained by this postulated straining mechanism. The interstitials spaces are smaller in precoated PSL-100 layer than PSL-200 layer, which enabled the former to strain out biopolymer molecules over a wider range of molecular sizes including relatively small ones. The fact that the

straining effect can remove biopolymer molecules larger than a certain size but not the small ones explain why the biopolymer removal plateaued even when the amount of PSL precoating increased. On the other hand, SSPAC achieved the highest removal of biopolymer followed by SPAC and PAC. This result reflects the higher adsorption capacity as well as the higher straining effect of SSPAC.

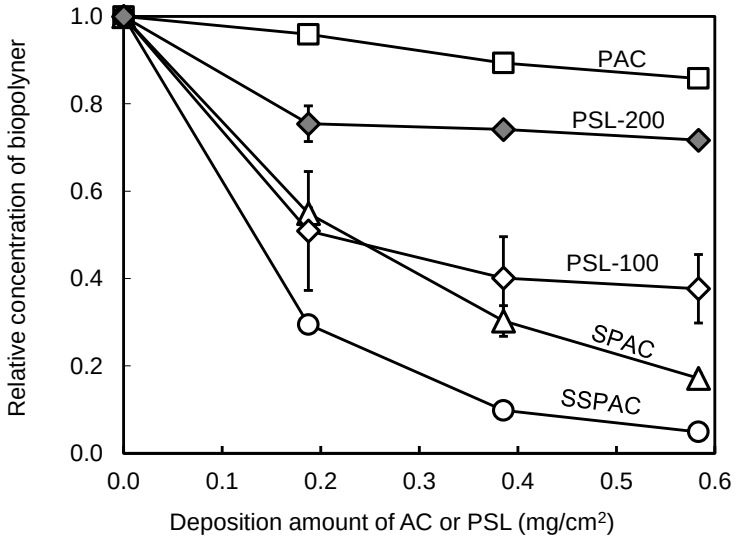

Fig. 2-14. Fractions of biopolymers that remained after passing through a precoated membrane versus amounts of AC or PSLs precoat the membrane. Biopolymer concentration was determined for 50-mL filtrate samples taken after precoating by filtering a 40-mL sample. Error bars indicate ranges of two measurements by liquid chromatography-organic carbon detection methodology. Water-1 was used in this experiment.

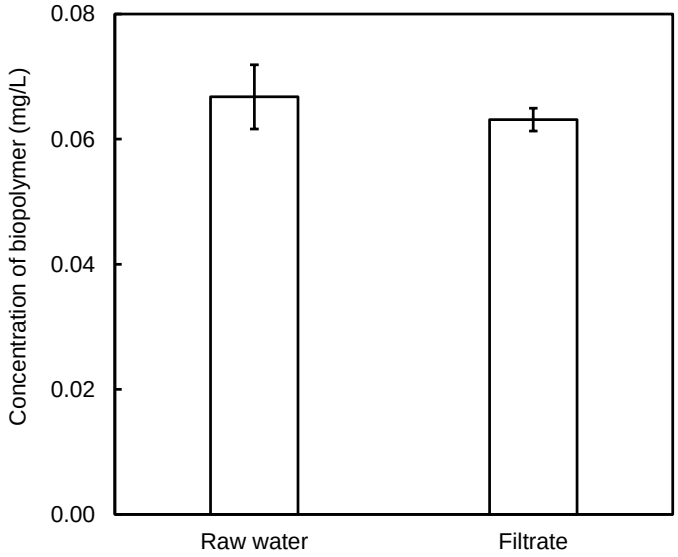

Fig. 2-15. Biopolymer concentrations of water samples before and after passing through a membrane with a pore size of 0.1 μm. Water-2, which was prepared by filtration through a 0.1-μm pore-size membrane, was used in this filtration experiment. Error bars indicate standard deviations of measurements.

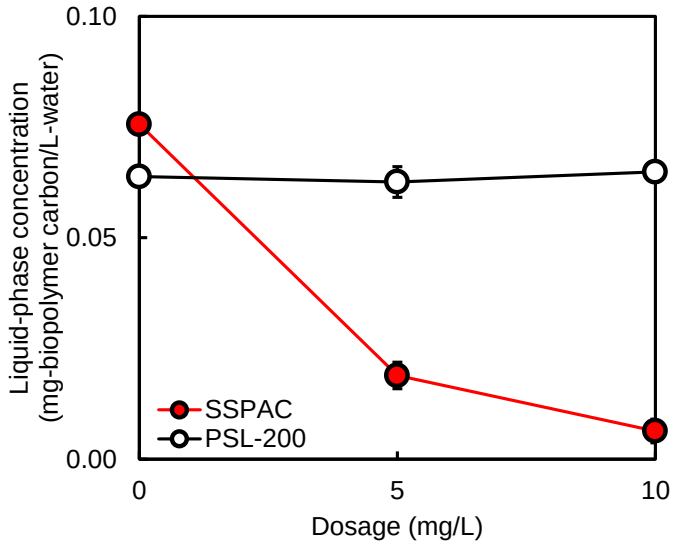

Fig. 2-16. Liquid-phase concentration of biopolymer versus SSPAC and PSL-200 dosages. Water-2 was used in this experiment. Error bars indicate standard deviations of measurements.

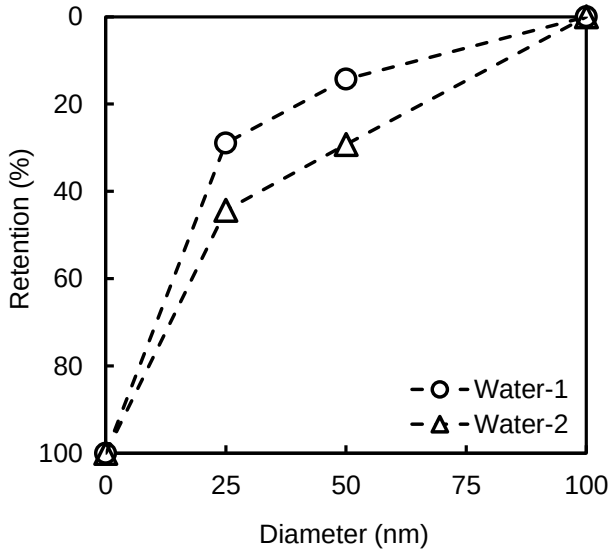

Fig. 2-17. Retention of biopolymer vs. membrane pore diameter.

2.3.3. Batch precoat repeated filtration on biopolymer removal

Batch precoat repeated filtration experiments were then conducted to further understand the straining effect on SPAC and SSPAC precoating layer on biopolymer removal. Fig. 2-18 shows the percentage of biopolymers remaining in the filtrates versus the filtration volume per membrane surface area. The low biopolymer concentration (high removal rate) at the beginning of the filtration can be explained as the high adsorption capacity of fresh ACs. As the filtration progressed, biopolymer concentration in the

filtrate increased while never reached the influent level, which indicates that there was a certain degree of removal that maintained by the straining effect even when the ACs adsorption capacity is saturated. This stable level of removal was higher with SSPAC precoating than with SPAC precoating, and the straining effect seemed to be strengthened when ACs suspensions were sonicated before precoating dosing. SPAC and SSPAC mildly agglomerate after milling (Pan et al., 2016), which explained why AC particles can be sufficiently dispersed by sonication and deposited densely on the membrane for a stronger straining effect.

Biopolymer is known as a membrane-fouling substance. The high biopolymer removal by precoated SSPAC layer owing to its high adsorption capacity and straining effect strongly suggests that precoating a membrane with SSPAC can mitigate the buildup of TMP during the operation of a membrane filtration system.

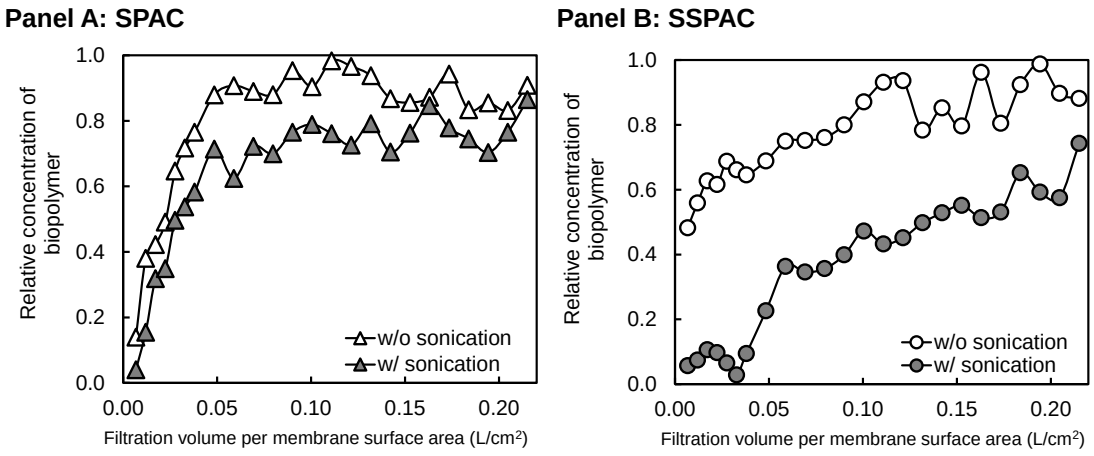

Fig. 2-18. Relative concentration of biopolymer versus filtration volume per membrane surface area of water samples. The amount of powdered activated carbon (PAC) deposited on the membrane for precoating was 0.38 mg/cm^2. Panel A: SPAC. Panel B: SSPAC. Water-1 was used in this experiment.

2.3.4. TMP changes during AC addition and membrane filtration

The changes of TMP during filtration with periodic backwashes was shown in Fig. 2-19. In experiments with Method A, AC was dosed after every backwash using a direct pulse dose and the suction force during the filtration will form a precoat layer of AC on the membrane automatically.

Among PAC/SPAC/SSPAC, SSPAC alleviated the buildup of TMP the most, followed by SPAC and PAC. TMP increased rapidly without AC pretreatment. However, TMP increased with time even with SSPAC, and the backwashes could not reset TMP increase back to the start level of filtration. This implicated that hydraulically irreversible membrane fouling cannot be stopped simply by precoating with SSPAC or SSPAC itself may also contribute to irreversible fouling.

In full-scale water treatment plants, the application of SPAC into membrane filtration has already been carried on (Kanaya et al., 2015). In that study, SPAC has been added continuously prior to coagulation pretreatment. A continuous SPAC addition followed by coagulation has successfully mitigated TMP increase better than coagulation pretreatment alone, which implies the important role of coagulation in controlling membrane fouling (Matsui et al., 2009). Coagulation process was then introduced into this study and Fig. 2-20 was shown as a comparison of TMP changes with and without coagulation. The fact that TMP increases at a much lower rate with coagulation than without coagulation indicates that coagulation pretreatment before AC dosing is necessary to mitigate membrane fouling.

It has been widely accepted that coagulation removes biopolymers and NOM to a certain extent and therefore mitigate TMP increase (Jung et al., 2006; Kimura et al., 2018; Wray and Andrews, 2014). NOMs are coagulated to form large flocs, which increases the permeability of the gel cake layer formed on the membrane surface and thereby mitigates the buildup of TMP. In Fig. 2-20, the depositions on the membrane were similar because the same water and AC dose were applied, although the fact that the rate of increase in the TMP during each filtration cycle was lower with coagulation than without coagulation suggests that the material deposited on the filters was more permeable in the former case. Membrane fouling always comes with an increase of TMP and is commonly divided into hydraulically reversible and irreversible fouling. Hydraulically reversible fouling can be physically removed (e.g., backwash) while hydraulically irreversible fouling can be removed only through chemical cleaning methods, which requires more efforts (Kimura et al., 2008; Peiris et al., 2013). Controlling hydraulically irreversible fouling is therefore essential to reduce the operational cost during the filtration. In Fig. 2-20, dotted lines were drawn to show the TMP increases by hydraulically irreversible fouling. Direct

pulse dosing of SPAC with coagulation mitigates irreversible fouling better than without coagulation. Fig. 2-21 shows photographs of the submerged tank during backwash (Fig. 2-22 shows the case of SSPAC). The membrane remained black because of AC accumulation in the system without coagulation pretreatment, whereas the membrane became white because of a detachment of the floc particles during the backwash with coagulation. A more severe hydraulically irreversible fouling that occurs without coagulation pretreatment may therefore be due to the AC along with NOM attachments on membrane. Coagulation alleviates such attachment because the hydrolysis of the aluminum polymer formed from the polyaluminum chloride coagulant may impede the strong attachment of AC to the membrane and can thereby facilitate such release.

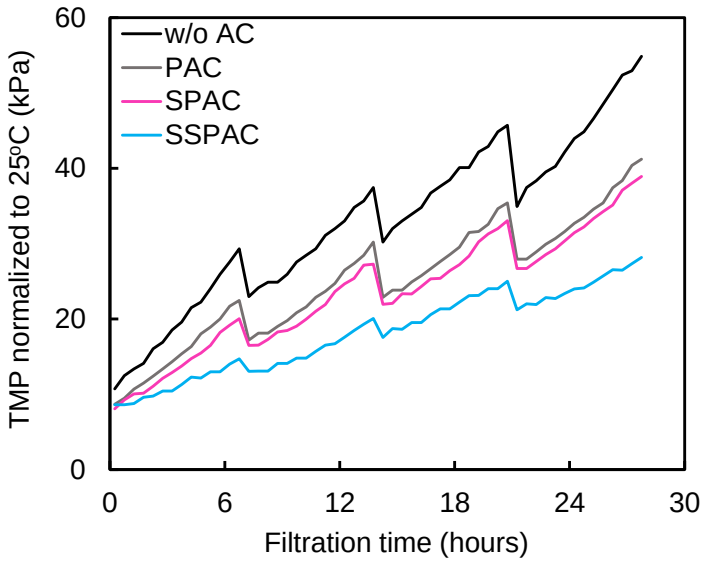

Fig. 2-19. TMP versus filtration time for powdered activated carbon (PAC), superfine PAC (SPAC) and submicron SPAC (SSPAC). The experiments were conducted by Method A, where direct pulse dose (explained in Figs. 2-3 and 2-6) was used. Backwash interval was 7 hours. Filtrate rate was 70.8 L m^{-2} h^{-1}. Water-2 was used in this experiment.

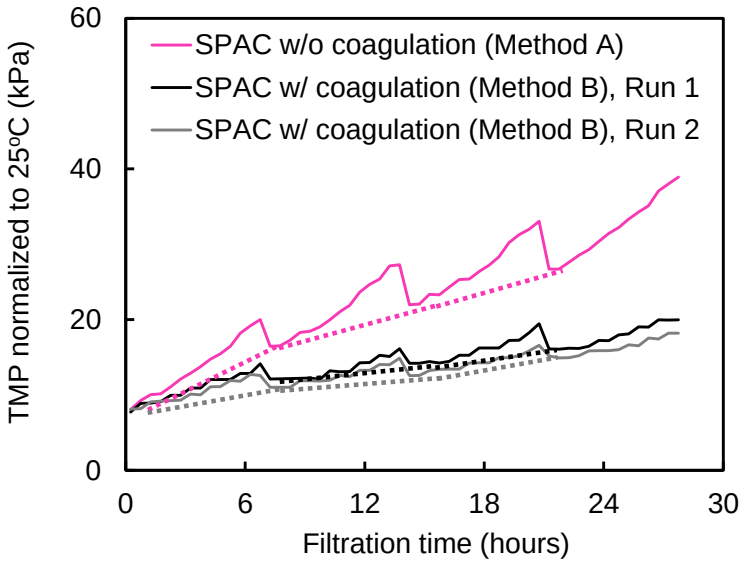

Fig. 2-20. TMP versus filtration time with/without coagulation. The experiments were conducted by Method A and B, where direct pulse dose (explained in Figs. 2-3, 2-4 and 2-6) of superfine powdered activated carbon (SPAC) was used. Dotted lines show TMP rise due to hydraulically irreversible fouling. Backwash interval was 7 hours. Filtrate rate was 70.8 L m^{-2} h^{-1}. Water-2 was used in this experiment.

Panel A: SPAC direct pulse dose w/o coagulation (Method A)

Panel B: SPAC direct pulse dose w/ coagulation (Method B)

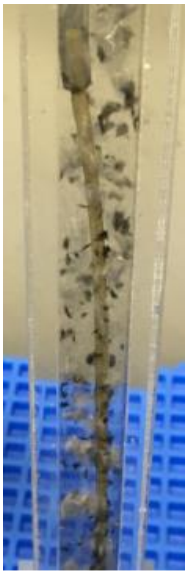

Fig. 2-21. Photographs of a membrane tank during backwash. Panel A is a picture of the system without coagulation pretreatment (Method A). Panel B is a picture of the system with coagulation pretreatment (Method B). Direct pulse dose (explained in Figs. 2-3, 2-4 and 2-6) was used in the experiments. Backwash pressure was 50 kPa. Filtration rate was 70.8 L m^{-2} h^{-1}). Water-2 was used in this experiment.

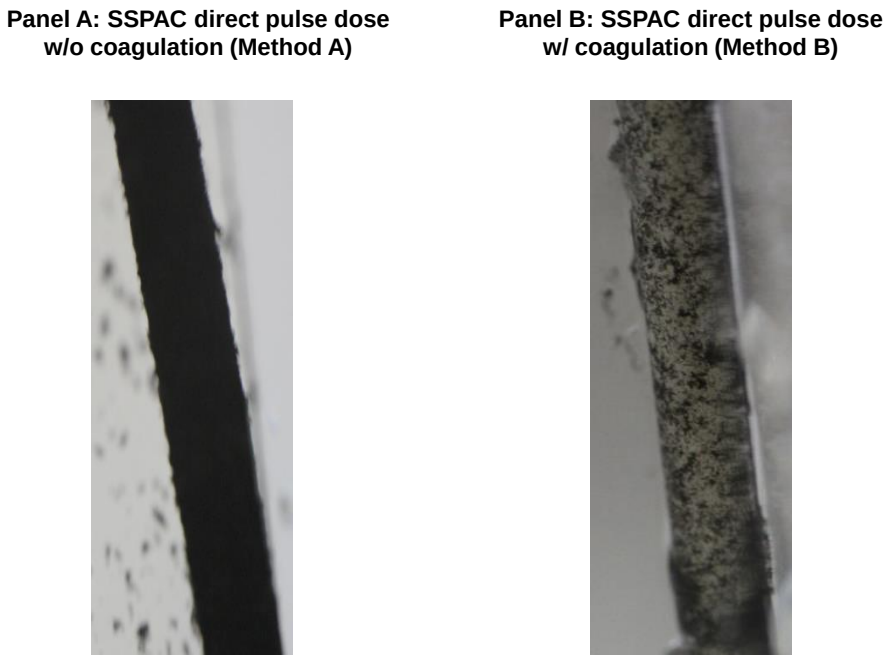

Fig. 2-22. Photographs of a membrane tank during backwash. Panel A is a picture of the system without coagulation pretreatment (Method A). Panel B is a picture of the system with coagulation pretreatment (Method B). Direct pulse dose (explained in Figs. 2-3, 2-4 and 2-6) of submicron SPAC (SSPAC) was used in the experiments. Backwash pressure was 50 kPa. Filtration rate was 70.8 L m^{-2} h^{-1}). Water-2 was used in this experiment.

Membrane filtration with continuous and pulse AC dosing were then conducted to compare the effectiveness of a precoating layer as a means of controlling the membrane fouling. In the pulse AC dose experiments, AC was dosed right after water filling stage to form a precoating layer after each backwash. In the continuous AC dose experiments, Method D doses AC before coagulation and Method E doses AC after coagulation treatment, which was identical to that used in Method B.

Fig.2-23 compares the changes of TMP between the systems with continuous or pulse AC dosing in the case of SPAC/SSPAC. For SSPAC, TMP increases at slower rates in both direct and indirect pulse dose rather than in continuous dose. The superiority of pulse dose for preventing TMP increase was confirmed during the experiments in which SSPAC was added as a pulse or continuous after coagulation. The amount of SSPAC used to precoat the membrane was higher for the pulse dose from the beginning of the filtration. The precoating prevented biopolymers from reaching to the membrane through the adsorptive removal of the biopolymers and base on the straining effect described in Sections 2.3.1 and

2.3.2. The superiority of the pulse dose method over than continuous does was clear for SSPAC while less apparent for SPAC. Precoating using AC to mitigate membrane fouling was therefore effective when the AC particles were within the submicron range. In the other words, continuous AC dosing, which is simpler than pulse dosing, is a reasonable dosing method if the AC particles are within the micron range.

Comparative plots of TMP versus the filtration time for direct and indirect pulse dose methods with coagulation treatment are shown in Fig. 2-24. Analogous comparisons between SPAC and SSPAC are shown in Fig. 2-25. The indirect pulse dosing method resulted in a more stable and lower TMP than the direct pulse dosing method for both SPAC and SSPAC. In the case of indirect pulse dosing, water was manually shaken vigorously after the injection of the AC. In the case of direct pulse dosing, the AC was injected into the tank and mixed with raw water by bubbling for 3 min. The TMP was therefore lower with indirect doing than with direct dosing because indirect pulse dosing produced a well-mixed AC suspension. The implication here is that complete dispersion of the AC before being deposited on the membrane is a key for a better precoating and therefore contributes to better mitigation of TMP increase.

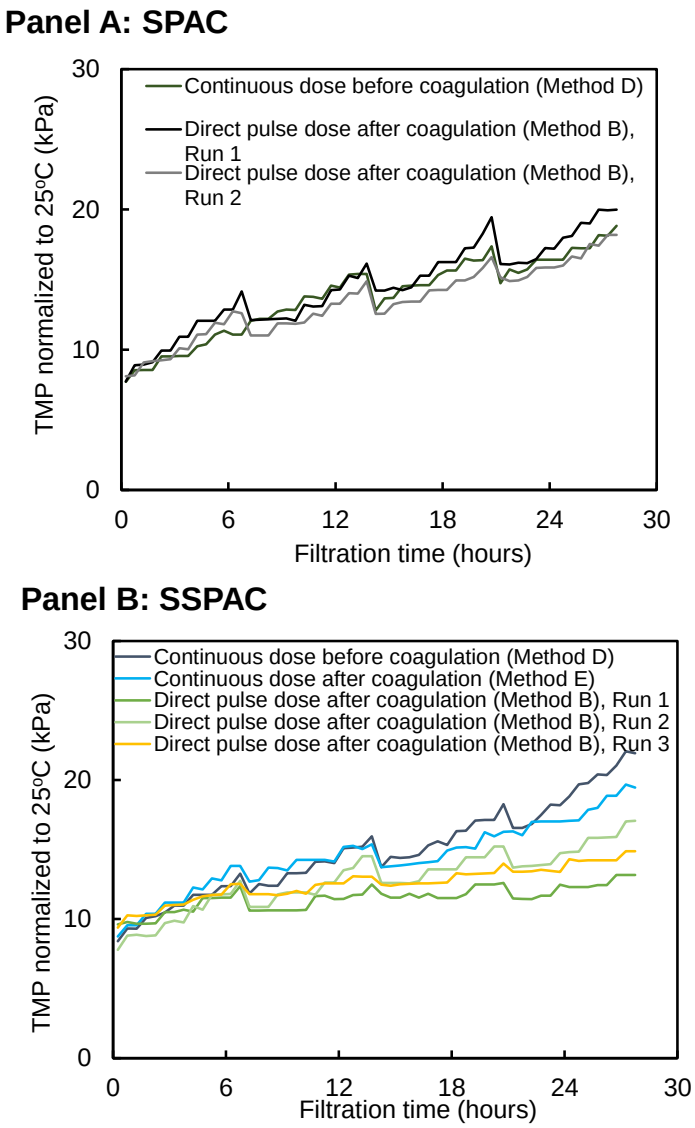

Fig. 2-23. TMP as a function of filtration time when membrane filtration was conducted after SPAC (Panel A) and SSPAC (Panel B) adsorption and coagulation pretreatment. The experiments were conducted by Methods B, D and E (explained in Figs. 2-4, 2-7 and 2-8, respectively) to compare direct pulse dose and continues dose. Backwash interval was 7 hours. Filtration rate was 70.8 L m^{-2} h^{-1}. Water-2 was used in this experiment.

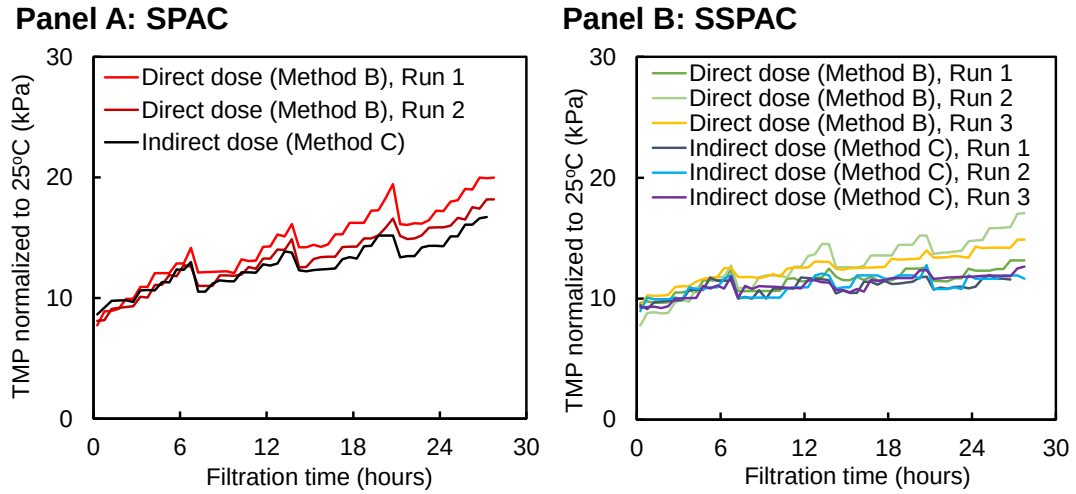

Fig. 2-24. TMP as a function of filtration time when membrane filtration was conducted after SPAC/SSPAC adsorption and coagulation pretreatment. SPAC (Panel A) and SSPAC (Panel B) with direct pulse dose and indirect pulse dose (Method B and C, respectively, as explained in Figs. 2-4 and 2-5) were used in this experiment. Backwash interval was 7 hours. Filtration rate was 70.8 L m^{-2} h^{-1}). Water-2 was used in this experiment.

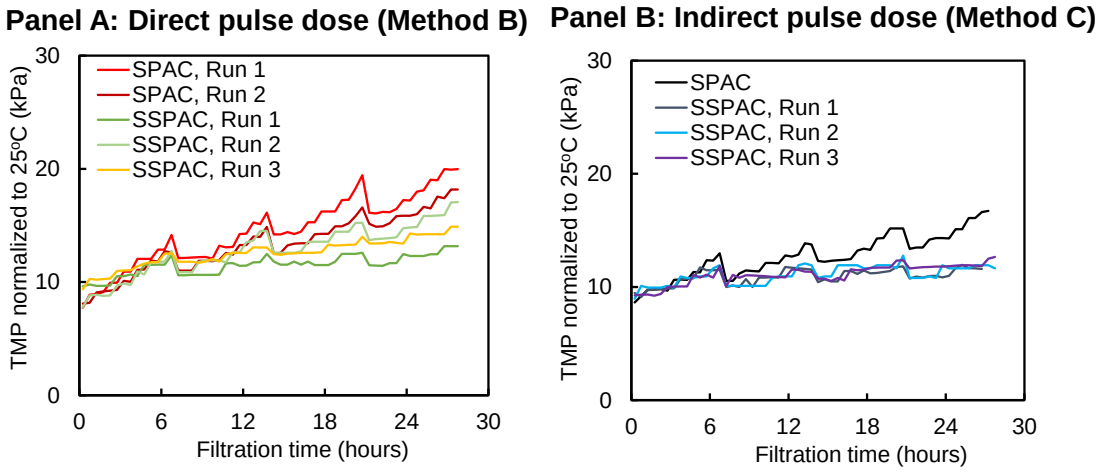

Fig. 2-25. TMP versus filtration time when membrane filtration was conducted after SPAC/SSPAC adsorption and coagulation pretreatment. Direct (Panel A) and indirect (Panel B) pulse dose (explained in Figs. 2-4, 2-5 and 2-6) were used in this experiment. Backwash interval was 7 hours. Filtration rate was 70.8 L m^{-2} h^{-1}). Water-2 was used in this experiment.

2.3.5. Removal of biopolymer and HS during membrane filtration

Filtrate samples were taken during the filtration and analyzed for biopolymer and HS concentrations as shown in Fig. 2-26. In the experiments with direct AC pulse dose without coagulation, the removal was mostly higher for biopolymers than for HS. Biopolymer removal was improved by reducing the AC particle size and through coagulation pretreatment and such effect is more apparent than for HS. The biopolymer concentration in the filtrate were reduced by precoating SSPAC > SPAC >PAC, such order was the same as that of TMP reduction in Fig. 2-19. During experiments with direct pulse dosing of SSPAC without coagulation, biopolymer removal reached 75%, which indicated that the biopolymers were removed primarily by the cake layer formed with SSPAC on membrane surface before the biopolymers could reach and foul the membrane. However, the quantitative contributions of the coagulation, adsorption and straining effects on biopolymer removal as well as TMP mitigation have yet to be investigated.

The fact that biopolymer removal was also higher with pulse dosing of SSPAC than with continuous dosing of SSPAC supports the merit of using a precoating to prevent membrane fouling. In direct pulse dosing of SSPAC, biopolymer removal was higher without coagulation than with coagulation. This result was unexpected but can be explained if a denser deposition of SSPAC on the membrane without coagulation than with coagulation leads to a higher biopolymer removal. It should be noted, however, that without coagulation, the membrane was severely fouled by the AC itself as explained in Section 2.3.4.

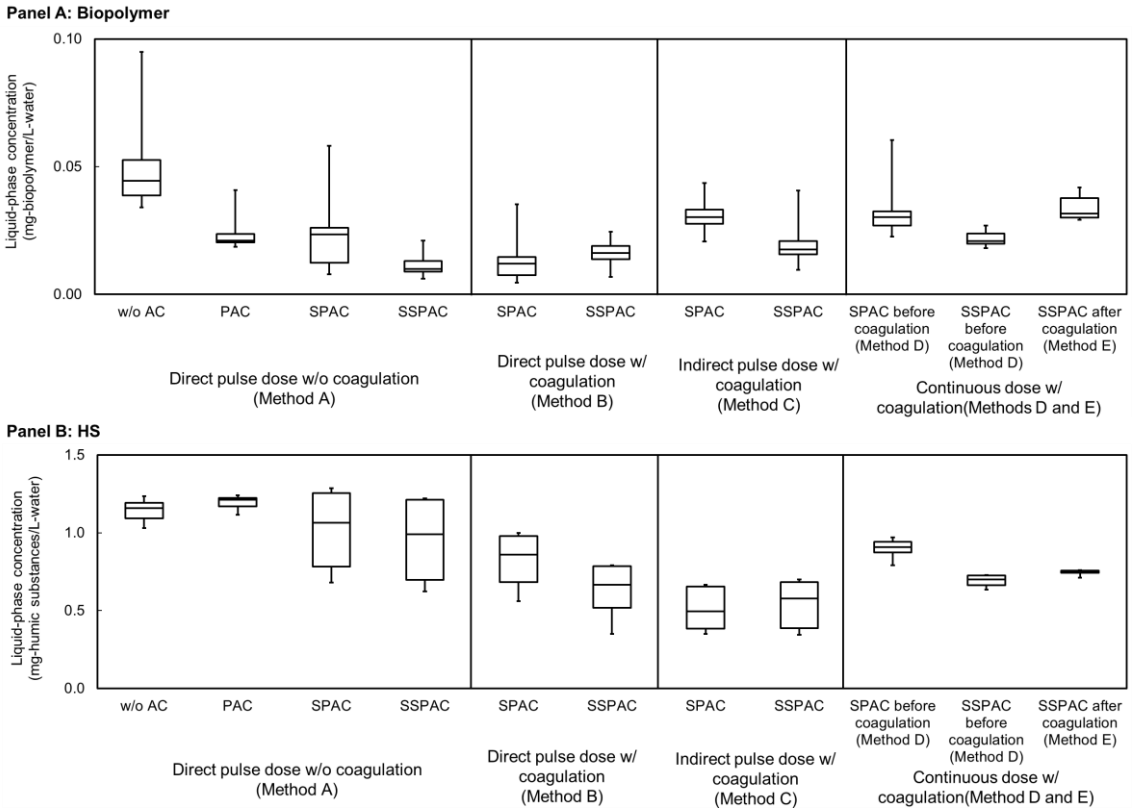

Fig. 2-26. Box and whisker plots of biopolymers and HS concentrations in filtrates for different combinations of coagulation and powdered activated carbon (PAC) treatment. Horizontal lines within boxes represent median values, the upper and lower lines of the boxes represent the 75th and 25th percentiles, respectively, and the upper and lower bars outside the boxes indicate the maximum and minimum values, respectively.

2.4. Chapter conclusions

1) The capacity of AC to adsorb biopolymers increases with a decrease in the AC particle size and hence follows the order as PAC < SPAC < SSPAC. SSPAC selectively adsorbs biopolymers form NOM compared with PAC and SPAC. The superiority of SSPAC for biopolymer adsorption suggests that it has potential application in the control of membrane fouling.
2) Biopolymers can be strained out by SPAC/SSPAC precoat layer on membrane surface. SSPAC precoating removes biopolymers with a stronger straining effect than SPAC precoating caused by the difference between AC particle sizes. Furthermore, sonication enables the dispersion of agglomerated SPAC/SSPAC so that a denser precoat layer can be formed and thus enhances the straining effect.
3) Coagulation is indispensable in AC precoat filtration process because coagulation removes biopolymers and facilitates the detachment of AC particles from the membrane during hydraulic backwashing, and in this way prevents hydraulically irreversible membrane fouling by AC itself.
4) Pulse dosing of SSPAC allows a precoat layer to form on the submerged membrane and shows superiority in mitigating the buildup of TMP owing to hydraulically irreversible membrane fouling versus continuous dosing. The fact that the indirect pulse dosing of SSPAC preceded by coagulation pretreatment achieves the best mitigation result on TMP increase in the study indicates that AC dispersion is important for precoating.

2.5. References

Ando, N., Matsui, Y., Matsushita, T., Ohno, K., 2011. Direct observation of solid-phase adsorbate concentration profile in powdered activated carbon particle to elucidate mechanism of high adsorption capacity on super-powdered activated carbon. Water Research 45, 761–767.

Bonvin, F., Jost, L., Randin, L., Bonvin, E., Kohn, T., 2016. Super-fine powdered activated carbon (SPAC) for efficient removal of micropollutants from wastewater treatment plant effluent. Water Research 90, 90–99.

Campinas, M., 2010. Assessing PAC contribution to the NOM fouling control in PAC/UF systems. Water Research 44, 1636–1644.

Crittenden, J.C., Trussell, R.R., Hand, D.W., Howe, K.J., Tchobanoglous, G., 2012. MWH's water treatment: principles and design.

Crozes, G., Anselme, C., Mallevialle, J., 1993. Effect of adsorption of organic matter on fouling of ultrafiltration membranes. Journal of Membrane Science 84, 61–77.

Heijman, S.G.J., Hamad, J.Z., Schippers, J., Amy, G., Kennedy, M.D., 2009. Submicron powdered activated carbon used as a pre-coat in ceramic micro-filtration. Desalination and Water Treatment 9, 86–91.

Huber, S.A., Balz, A., Abert, M., Pronk, W., 2011. Characterisation of aquatic humic and non-humic matter with size-exclusion chromatography - organic carbon detection - organic nitrogen detection (LC-OCD-OND). Water Research 45, 879–885.

Jung, C.W., Son, H.J., Kang, L.S., 2006. Effects of membrane material and pretreatment coagulation on membrane fouling: fouling mechanism and NOM removal. Desalination 197, 154–164.

Kanaya, S., Kawase, Y., Mima, S., Sugiura, K., Murase, K., Yonekawa, H., 2015. Drinking water treatment using superfine PAC (SPAC): Design and successful operation history in full-scale plant. American Water Works Association Salt Lake City, Utah, USA, pp. 624–631.

Kim, J., Cai, Z., Benjamin, M.M., 2008. Effects of adsorbents on membrane fouling by natural organic matter. Journal of Membrane Science 310, 356–364.

Kimura, K., Maeda, T., Yamamura, H., Watanabe, Y., 2008. Irreversible membrane fouling in microfiltration membranes filtering coagulated surface water. Journal of Membrane Science 320, 356–362.

Kimura, K., Shikato, K., Oki, Y., Kume, K., Huber, S.A., 2018. Surface water biopolymer fractionation for fouling mitigation in low-pressure membranes. Journal of Membrane Science 554, 83–89.

Kimura, K., Tanaka, K., Watanabe, Y., 2014. Microfiltration of different surface waters with/without coagulation: Clear correlations between membrane fouling and hydrophilic biopolymers. Water Research 49, 434–443.

Kweon, J.H., Hur, H.W., Seo, G.T., Jang, T.R., Park, J.H., Choi, K.Y., Kim, H.S., 2009. Evaluation of coagulation and PAC adsorption pretreatments on membrane filtration for a surface water in Korea: A pilot study. Desalination 249, 212–216.

Lin, C.F., Huang, Y.J., Hao, O.J., 1999. Ultrafiltration processes for removing humic substances: Effect of molecular weight fractions and PAC treatment. Water Research 33, 1252–1264.

Lin, C.F., Liu, S.H., Hao, O.J., 2001. Effect of functional groups of humic substances on UF performance. Water Research 35, 2395–2402.

Matsui, Y., Ando, N., Yoshida, T., Kurotobi, R., Matsushita, T., Ohno, K., 2011. Modeling high adsorption

capacity and kinetics of organic macromolecules on super-powdered activated carbon. Water Research 45, 1720–1728.

Matsui, Y., Hasegawa, H., Ohno, K., Matsushita, T., Mima, S., Kawase, Y., Aizawa, T., 2009. Effects of super-powdered activated carbon pretreatment on coagulation and trans-membrane pressure buildup during microfiltration. Water Research 43, 5160–5170.

Matsui, Y., Nakao, S., Taniguchi, T., Matsushita, T., 2013. Geosmin and 2-methylisoborneol removal using superfine powdered activated carbon: Shell adsorption and branched-pore kinetic model analysis and optimal particle size. Water Research 47, 2873–2880.

Matsui, Y., Sakamoto, A., Nakao, S., Taniguchi, T., Matsushita, T., Shirasaki, N., Sakamoto, N., Yurimoto, H., 2014. Isotope microscopy visualization of the adsorption profile of 2-methylisoborneol and geosmin in powdered activated carbon. Environmental Science and Technology 48, 10897–10903.

Matsui, Y., Sanogawa, T., Aoki, N., Mima, S., Matsushita, T., 2006. Evaluating submicron-sized activated carbon adsorption for microfiltration pretreatment. Water Science and Technology: Water Supply 6, 149–155.

Myat, D.T., Mergen, M., Zhao, O., Stewart, M.B., Orbell, J.D., Merle, T., Croué, J.P., Gray, S.R., 2014. Membrane fouling mechanism transition in relation to feed water composition. Journal of Membrane Science 471, 265–273.

Pan, L., Matsui, Y., Matsushita, T., Shirasaki, N., 2016. Superiority of wet-milled over dry-milled superfine powdered activated carbon for adsorptive 2-methylisoborneol removal. Water Research 102, 516–523.

Pan, L., Nishimura, Y., Takaesu, H., Matsui, Y., Matsushita, T., Shirasaki, N., 2017a. Effects of decreasing activated carbon particle diameter from 30 Mm to 140 nm on equilibrium adsorption capacity. Water Research 124, 425–434.

Pan, L., Takagi, Y., Matsui, Y., Matsushita, T., Shirasaki, N., 2017b. Micro-milling of spent granular activated carbon for its possible reuse as an adsorbent: Remaining capacity and characteristics. Water Research 114, 50–58.

Peiris, R.H., Jaklewicz, M., Budman, H., Legge, R.L., Moresoli, C., 2013. Assessing the role of feed water constituents in irreversible membrane fouling of pilot-scale ultrafiltration drinking water treatment systems. Water Research 47, 3364–3374.

Tian, J., Ernst, M., Cui, F., Jekel, M., 2013. Correlations of relevant membrane foulants with UF membrane fouling in different waters. Water Research 47, 1218–28.

Weiss, V.U., Golesne, M., Friedbacher, G., Alban, S., Szymanski, W.W., Marchetti-Deschmann, M., Allmaier, G., 2018. Size and molecular weight determination of polysaccharides by means of nano electrospray gas-phase electrophoretic mobility molecular analysis (nES GEMMA). Electrophoresis 39, 1142–1150.

Wray, H.E., Andrews, R.C., 2014. Optimization of coagulant dose for biopolymer removal: Impact on ultrafiltration fouling and retention of organic micropollutants. Journal of Water Process Engineering 1, 74–83.

Zheng, X., Ernst, M., Huck, P.M., Jekel, M., 2010. Biopolymer fouling in dead-end ultrafiltration of treated domestic wastewater. Water Research 44, 5212–5221.

Chapter 3. Pulse dosing of submicron super-fine powdered activated carbon: effects of filtration flux, coagulant types, and coagulant-dose timing

3.1. Chapter introduction

Coating membrane surface to mitigate membrane fouling has been widely studied in some areas of water treatment to alleviate the effect of membrane fouling on filtration process (Kim et al., 2010; Kochkodan and Hilal, 2015; Qiu et al., 2018; Zahid et al., 2018), but there have been few studies of coating with inexpensive materials applicable to drinking water treatment (Lee et al., 2021; Lohwacharin et al., 2010). In Chapter 2, submicron superfine powdered activated carbon (SSPAC) has been proved to adsorb NOM (especially biopolymer) with a higher level than PAC and SPAC, and when SSPAC is dosed in a pulse at the beginning of each filtration in a submerged membrane system, a precoating layer of SSPAC forms on the membrane surface as the filtration proceeds. This precoating layer protects the membrane by enhancing its adsorption capacity and straining ability versus ordinary PAC and thereby mitigating the membrane fouling (Heijman et al., 2009; Zhao et al., 2020). Furthermore, the introduction of a coagulant eliminates the concern that SSPAC itself may foul the membrane. In fact, the precoating layer can be easily peeled off by periodic hydraulic backwashing. However, this mitigation of membrane fouling by pulse dosing of SSPAC with a coagulant has been studied under only one condition: pulse dosing of SSPAC at the beginning right before the filtration process, continuous dosing of one type of polyaluminum-chloride (PACl) coagulant with a high basicity (70%) during the filtration period but not the water filling period, and under only one constant filtration flux with 70.8 L m-2 h-1. There are still lots of parameters remain to be investigated regarding to achieve the optimum TMP prevention by pulse dosing of SSPAC (e.g., the effects of the timing of coagulant addition and the filtration flux for precoating, etc.). Moreover, it is reasonable to infer that the type of coagulant would also influence the degree of mitigation of membrane fouling when coagulation pretreatment is combined with pulse dosing

of SSPAC because coagulation pretreatment is effective in mitigating membrane fouling, and the pretreatment efficiency is highly dependent on the types of coagulant (Hidayah and Cahyonugroho, 2019; Jarvis et al., 2012; Yu et al., 2013).

The goal of the study in this chapter was to investigate the optimum ways to add SSPAC and coagulant in order to mitigate membrane fouling and suppress TMP rise during filtration in a submerged membrane system. To achieve this goal, experiments that involved filtering river water with periodic backwashing was conducted, and how the flux during the precoating period, dose timing of PACl, and the basicity of the PACl influenced the rise of TMP were investigated.

3.2. Materials and methods

3.2.1. Waters

Water from Wanigawa River (Wanigawa Water Purification Plant, Ibaraki, Japan) was sampled in May and November of 2019 (Designated as Water-1 and Water-2, respectively) and 2020 (Water-3 and Water-4, respectively). Here the sampled water is from the same place, but different timeline compared to the water used in Chapter 2, so that the influence of water quality could be excluded during the investigation of operation process. The water was stored at a temperature of 4 °C and was returned to 20 °C only before the experiment and then was pre-filtered by a coated cellulose acetate membrane filter with the pore size of 10 μm.

Concentrations of DOC, biopolymer, HS, and UV260 were used to characterize the water quality of the filtrates and raw water (after being pre-filtered through a 0.45-μm PTFE membrane). The measurements and analysis equipment are the inconsistent with those in Chapter 2. Table 3-1 shows the water quality metrics.

Table 3-1
Water quality. Measurements other than pH were taken after membrane filtration (Water-1: 0.1-μm MCE membrane. Water-2, Water-3 and Water-4: 0.45-μm PTFE membrane).

	pH	DOC mg/L	UV260 cm^{-1}	Biopolymer mg/L	Alkalinity mg/L as $CaCO_3$	Na^+ mg/L
Water-1	7.62	2.66	0.060	0.0800	72.0	43.7
Water-2	7.91	3.45	0.070	0.340	68.0	41.6
Water-3	7.17	3.08	0.054	0.280	68.0	38.7
Water-4	7.96	3.69	0.070	0.360	71.0	43.8

	K^+ mg/L	Mg^{2+} mg/L	Ca^{2+} mg/L	Cl^- mg/L	NO_3^- mg/L	SO_4^{2-} mg/L
Water-1	5.84	9.18	18.0	54.0	13.8	22.3
Water-2	5.48	8.61	17.3	41.3	14.1	28.0
Water-3	4.83	8.39	16.0	41.2	n/a	19.8
Water-4	5.55	9.25	17.9	51.6	n/a	14.8

3.2.2. Activated carbons

Activated carbon was prepared by the same procedure used in a previous study to ensure consistency

of experimental conditions (Zhao et al., 2020). A wood-based PAC (Taiko-W, Futamura Chemical Co., Ltd., Nagoya, Japan) with a median diameter (D50) of 12 μm was mixed with pure water (Milli-Q water, Merck KGaA, Darmstadt, Germany) to make a PAC slurry with a PAC concentration of 15% (w/w). The slurry was milled in a closed chamber filled with alumina balls for 6 h to reduce the D50 to less than 4 μm. The resultant slurry was ground with a bead mill filled with 0.2-mm-diameter beads for 2 h (LMZ015, Ashizawa Finetech, Ltd., Chiba, Japan) to obtain SSPAC with a D50 of 200 nm.

The SSPACs were mixed with a dispersant (Triton X-100, Kanto Chemical Co., Inc., Tokyo, Japan) and sonicated, then their particle sizes were measured with a laser-light-scattering instrument (Microtrac MT3300EXII, Nikkiso Co., Inc., Tokyo, Japan) (Pan et al., 2016). Fig. 3-1 shows the size distributions of the SSPACs.

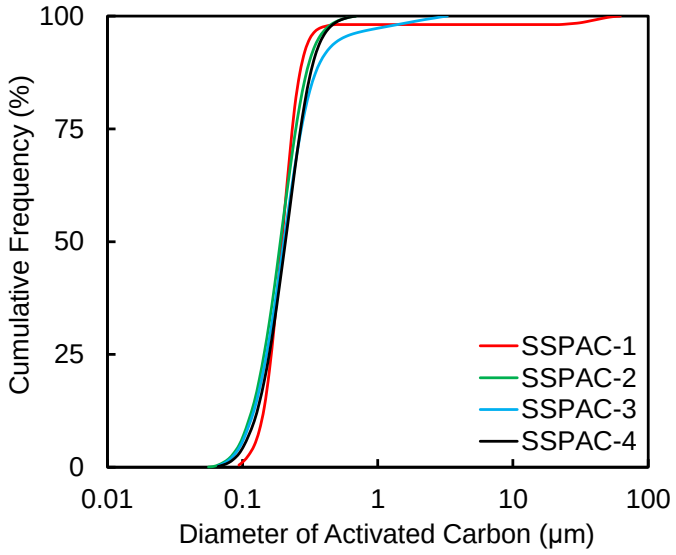

Fig. 3-1. Particle size distributions of SSPAC. Use of SSPAC-1 and SSPAC-4 are discussed in Section 3.3.1, use of SSPAC-2 in Section 3.3.2, and use of SSPAC-3 in Section 3.3.3.

3.2.3. Coagulants

Sulfated polyaluminum chloride (PACl) coagulants with a basicity of 50% and sulfate ion content of 3% w/w (designated as PACl-B50S) or basicity of 70% and sulfate ion content of 2% w/w (designated as PACl-B70S) were applied in this experiment (Taki Chemical Co., Hyogo, Japan). Non-sulfated

coagulants with basicities of 0%, 20%, 40%, 50%, and 70% (designated as PACl-B00, -B20, -B40, -B50, and -B70, respectively) were produced in the authors' laboratory by using basically the same method used to produce the PACl-B50S and B70S ($Al(OH)_3$ dissolution method) (Nakazawa et al., 2018). The AlCl3 H2O solution was mixed with $Al(OH)_3$ powder (Guaranteed Reagent, FUJIFILM Wako Pure Chemical Corporation, Osaka, Japan) and heated in a microwave labstation (ETHOS TC, Milestone S.r.l., Sorisole (BG), Italy) at 150 ºC for 3 h. The solution was then centrifuged at 3000 rpm (1140 g) for 10 min, and the supernatant was filtered through a 0.45-μm PTFE membrane filter (Toyo Roshi Kaisha, Ltd., Tokyo, Japan). The filtrate was transferred to a glass bottle that was placed on a hot plate/magnetic stirrer at a rotation rate of 600 rpm and heated to a temperature of 75 ºC. An amount of sodium carbonate (Guaranteed Reagent, FUJIFILM Wako Pure Chemical Corporation) calculated to produce the targeted basicity was dripped into the solution. The basicity was calculated with Eq. (1):

$$\text{Basicity}\ (\%) = \frac{[OH^-]}{3[Al]} \times 100 \qquad (1)$$

where [Al] is the aluminum concentration measured with an inductively coupled plasma mass spectrometer (ICPMS, 7700x, Agilent Technologies, Inc., Santa Clara, Ca, USA), OH^- is the concentration of hydroxyl groups calculated from the mass balance of Al(OH)3 and titrated sodium carbonate. Table 3-2 shows the conditions maintained during production of the coagulant.

In some experiments, floc particle-size measurements were conducted using a 1-L beaker (640 mL raw water) connected to a particle-size analyzer (Microtrac MT3300EXII, Nikkiso Co., Inc., Tokyo, Japan). After 1 min of rapid mixing, floc particle size measurements were begun and continued every 5 min. Measurements were taken in triplicate over a 20-second period, and the average value was recorded. Unlike typical measurements with a Microtrac particle-size analyzer, ultrasonication was turned off to avoid breakage of the floc particles. The beaker and particle-size analyzer were connected by a tube with a 7.9-mm inner diameter. A peristaltic pump circulated water to avoid floc breakage. A photograph of floc particles was taken with a digital, single-lens reflex camera (EOS 60D; Canon Ltd., Tokyo, Japan).

Table 3-2
Conditions during coagulant production. (Sodium carbonate was not added during the production of PACl-B00, B20, and B40 for basicity adjustment)

	Adjustment of basicity						
Name of coagulants	Temperature	Time	2M sodium carbonate	Al	Cl/Al	Na/Al	Basicity
	°C	min	mL	mol/L			%
PACl-B00				1.85	3.30		0
PACl-B20				2.35	2.29		20
PACl-B40				3.15	1.74		40
PACl-B50	75	50	1.47	3.62	1.68	0.183	50
PACl-B70	75	44	6.25	2.35	1.66	0.759	70

3.2.4. Experiment setup of submerged membrane filtration

Fig. 3-2 shows the experiment setup, which was unchanged from a previous study (Zhao et al., 2020). Water was fed by a peristaltic pump into a static mixer, and coagulants were fed through another line. The coagulant dosage was 2 mg-Al/L. After a dose of coagulant, NaOH was injected into the line to bring the pH to 7.5, and the water flowed into a submerged tank where a hollow fiber PVDF (polyvinylidene fluoride) membrane with a 0.1-μm pore size (Asahi Kasei Corp., Tokyo, Japan) was suspended. The membrane was sealed at one end so that suction pressure at the other end resulted in filtration. The suction pressure was recorded by a digital pressure meter (GC61, Nagano Keiki Products, Tokyo, Japan), and the water temperature was measured with a digital thermometer (LR5011, Hioki E.E. Corp., Nagano, Japan). Filtration was conducted at a constant flux of 70.8 L m−2 h−1 except for the initial period of filtration. Backwashing was conducted with pure water every 7 or 12 hours with a peristaltic pump at 50 kPa. After backwashing followed by drainage, the next round of filtration was begun. SSPAC was dosed in a pulse at the beginning of each filtration at a dosage of 5 mg/L. Dosage was equated to the mass of SSPAC divided by the volume of treated water. The experiments were conducted at a controlled temperature of 20 °C, and the filtrates were sampled with a fraction collector for water quality analysis.

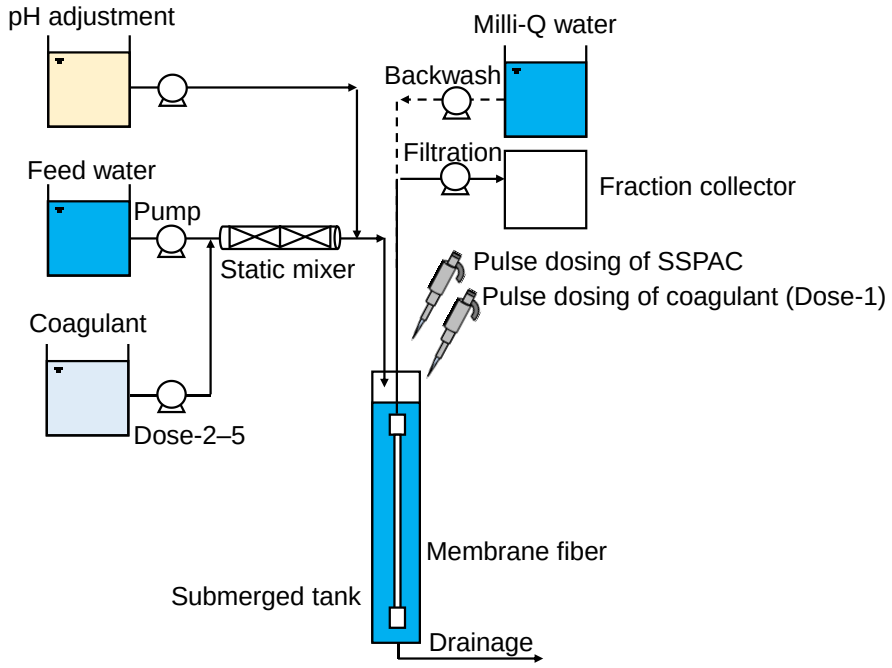

Fig. 3-2. Experiment setup for submerged filtration.

3.2.5. Filtration with changing precoat filtration flux

The filtration flux at the beginning of the filtration period (= precoat filtration flux in this study) and the filtration flux during the remainder of the filtration (main filtration flux) were considered separately. The duration of the precoat filtration (precoating period) was equated to the hydraulic retention time of the submerged tank, so that the precoating period was inversely proportional to the precoat filtration flux (Fig. 3-3). The precoat filtration flux was set to 50%, 100%, 200%, 300%, 400%, 500%, or 633% of the main filtration flux (70.8 L m^{-2} h^{-1}) (Fig. 3-4). These runs were designated as PF-50%, etc. In some experiments, a portion of the water in the submerged tank was sampled right after the SSPAC dose and before initiation of precoating. Another portion was sampled at the end of precoating. The turbidities of the water samples were measured after a one-min sonication. Precoating efficiency was defined as the SSPAC on the precoat divided by the total amount of dosed SSPAC and was estimated as 1.0 minus the ratio of turbidity after/before precoating. It was assumed that SSPAC was mainly responsible for the turbidity.

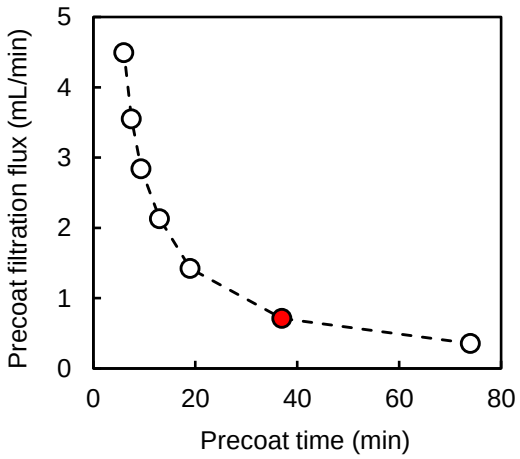

Fig. 3-3. Change of precoat filtration flux against precoat time. The red dot indicates the main filtration flux (70.8 L m^{-2} h^{-1} corresponds to 0.71 mL/min in this figure).

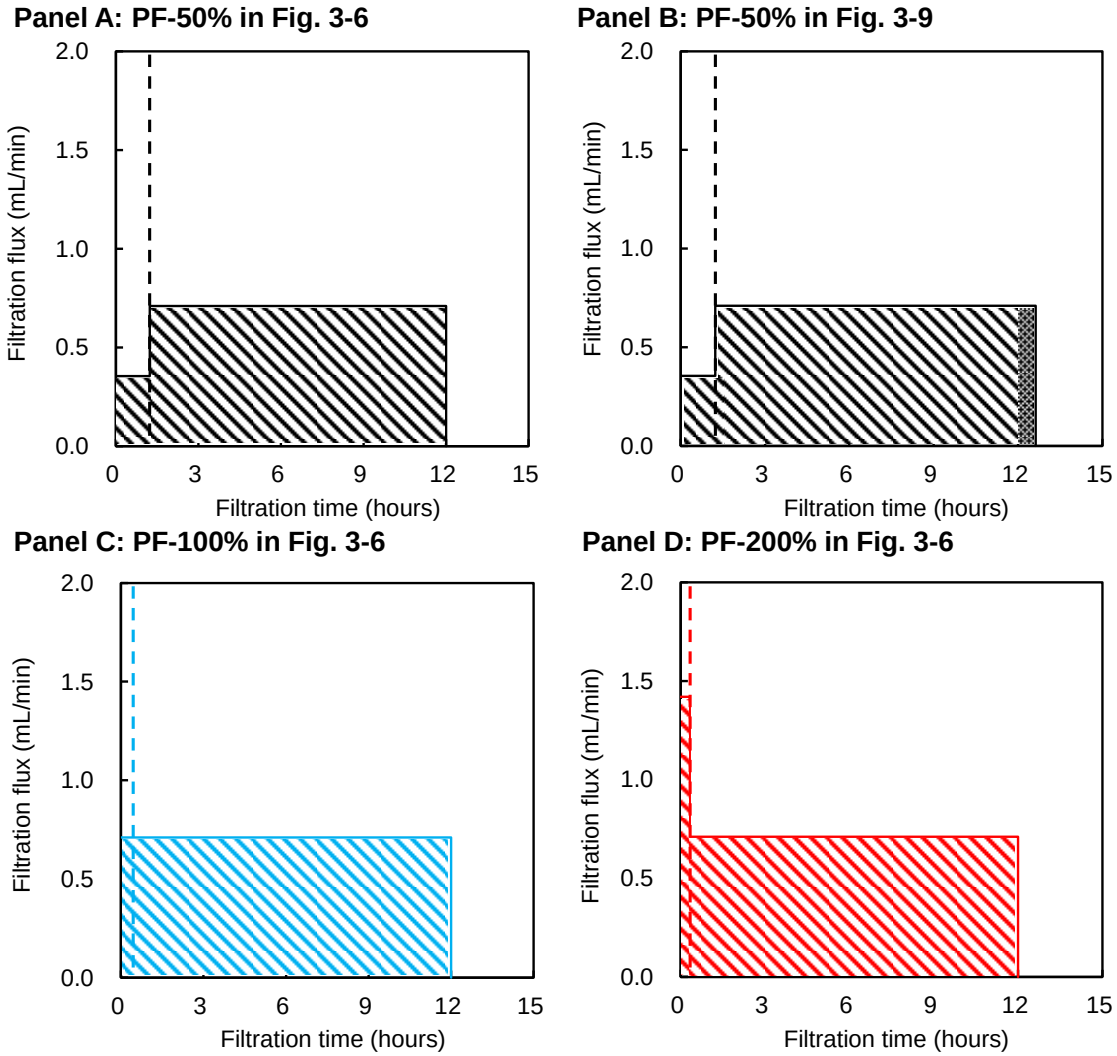

Fig. 3-4. Change of filtration flux against filtration time. Panels A, C, and D correspond to the experimental conditions of Fig. 3-6. Panel B corresponds to Fig. 3-9, where the filtration time has been slightly extended (dotted part) because the amount of filtered water was adjusted to be the same as in the case of PF-100%. The dashed line indicates the end of the precoat period and the start of main filtration.

3.2.6. Filtration with changing coagulant dose timing

The timing of the coagulant dose was changed in some experiments as follows:

Dose-1: pulse dosing of coagulant immediately after pulse dosing of SSPAC.

Dose-2: continuous dosing of coagulant during the time water was fed into the submerged tank and for 1 h after the start of filtration.

Dose-3: continuous dosing of coagulant for only 1 h after the start of filtration.

Dose-4: continuous dosing of coagulant during the time water was fed into the submerged tank and throughout the filtration period.

Dose-5: continuous dosing of coagulant during the filtration period only.

The dosage of coagulant was controlled so that the dose divided by the volume of treated water was constant and equal to 2 mg-Al/L. Fig. 3-5 illustrates the timing of the doses.

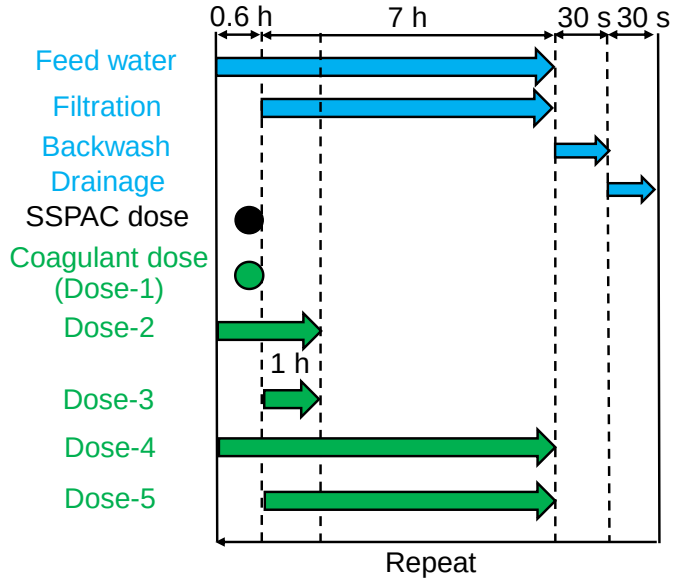

Fig. 3-5. Dose timing of coagulants.

3.3. Results and discussion

3.3.1. Effects of precoat filtration flux on TMP rise

Fig. 3-6 shows changes of TMP in the filtration experiments with a changing precoat filtration flux wherein the filtration flux was decreased/increased after pulse dosing of SSPAC and then restored to the original filtration flux. In the A series run (Panel A of Fig. 3-6: the dosages of SSPAC and coagulant were 5 mg/L and 2 mg-Al/L, respectively), the PF-50% resulted in the smallest TMP rise. PF-100% resulted in the second lowest TMP rise for the first 24 hours, but the PF-400% and 100% resulted in the second lowest TMP rise at 48-h. For comparison, panel A of Fig. 3-7 shows the TMP rise due to hydraulically irreversible fouling, i.e., the difference of the TMPs at the beginning of two consecutive batches of filtration with backwashing in between. The TMP rise due to hydraulically irreversible membrane fouling was the lowest in the experiment with the lowest initial filtration flux (PF-50%), followed by PF-100% and PF-400%. The TMP rises due to hydraulically irreversible membrane fouling were high in the four runs with precoat filtration fluxes that exceeded 100% (PF-200%, 300%, 500%, and 633%), except for PF-400%. In the B series of runs (Panel B of Fig. 3-6 and Panel B of Fig. 3-7: the dosages of SSPAC and coagulant were 1 mg/L and 1 mg-Al/L, respectively), the TMP rose more rapidly than in the A series because the lower dosages of SSPAC and coagulant more likely caused membrane fouling. Neither PF-50% nor 100% was found to be superior in suppressing TMP rise when compared with PF-200% and 300%. The data from all runs are shown in Fig. 3-8.

The slower and constant precoat filtration fluxes (PF-50% and 100%) seemed to be effective when the addition of SSPAC and coagulant was sufficient to basically mitigate membrane fouling. Then, additional experimental runs were conducted to compare PF-50% and 100%. In these experiments, the amounts of filtered water were adjusted so that they were the same by slightly (by 5.2%) prolonging the filtration time of the PF-50% run. The same filtration time would have resulted in slightly different filtration volumes between the low and high precoat filtration fluxes and might have caused different degrees of membrane fouling. Panel A of Fig. 3-9 shows that PF-50% suppressed TMP rise slightly

more than PF-100%, but the difference was small. There was almost no significant difference in the TMP rise due to hydraulically irreversible fouling between PF-50% and 100% (Panel B of Fig. 3-9).

Overall, the experimental results were not completely consistent, but they suggested that a high precoat filtration flux did not help to suppress a TMP rise. High precoat filtration fluxes have been thought to result in faster formation of a precoating layer that would protect the membrane from fouling, but the actual TMP rise was like or higher than the TMP rise with a lower precoat filtration flux. Unlike continuous dosing, pulse dosing of SSPAC created an overdose at the beginning of filtration so that more of the NOM that caused membrane fouling was adsorbed by the SSPAC. However, the mechanism that explains why a higher precoat filtration flux did not mitigate membrane fouling efficiently could be related to the portion of the precoat layer that was tightly attached to the membrane rather than to NOM fouling. Formation of a precoat layer that can be removed by backwashing is a key factor that suppresses TMP rise (Zhao et al., 2020). Another explanation might be related to the absence of a relationship between precoating efficiency and precoat filtration flux inferred from the fact that the precoating efficiencies of SSPAC in PF-100% and 300% were almost the same (~60%), as shown in Fig. 3-10. In addition, the fact that the entire amount of pulse dosed SSPAC was not applied for precoating might be related to the affinity of the SSPAC for the membrane. A slow precoat filtration flux may be effective in suppressing TMP rise, but it was not effective (e.g., when the SSPAC and coagulant dosages were low). Reducing the precoat filtration flux causes the precoat layer to not be very tightly bound to the membrane and thereby facilitates removal during backwashing. However, the longer time required for completion of precoating by SSPAC deposition increases the time during which the membrane is exposed to foulant. This problem is more likely to be troublesome when the SSPAC and coagulant dosages are low.

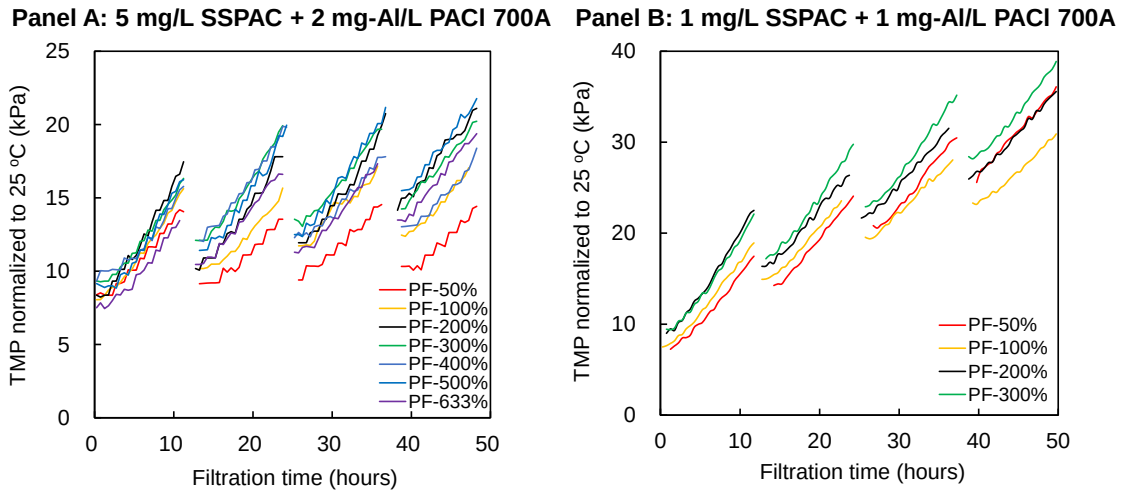

Fig. 3-6.TMP versus filtration time. SSPAC was dosed every 12 hours in a pulse at the beginning of each cycle of filtration after the backwash. After the pulse dose of SSPAC, filtration was conducted at the precoat filtration flux, and then the filtration flux was returned to the main filtration flux of 70.8 L m^{-2} h^{-1}. For example, in the PF-50% run, the precoat filtration flux was 50% of the main filtration flux. PACl-B70S coagulant was dosed continuously (Dose-4 in Fig. 3-5). SSPAC-1 and Water-2 were used in Panel A and SSPAC-2 and Water-3 were used in Panel B. The SSPAC and coagulant dosages were 5 mg/L and 2 mg-Al/L, respectively, in Panel A and 1 mg /L and 1 mg-Al/L, respectively, in Panel B. Panel A: experiments were conducted three times with PF-100% and twice with PF-300% and PF-633% for reproducibility. The average values were then calculated. Panel B: experiments were conducted two or three times for each condition, and the average values were then calculated (Fig. 3-8 shows all data).

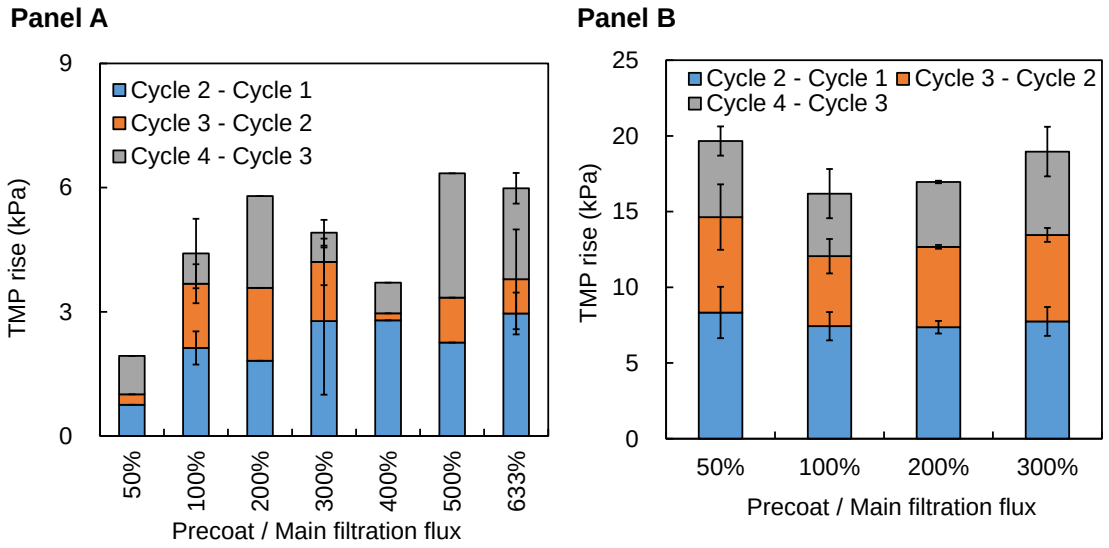

Fig. 3-7. TMP rise due to hydraulically-irreversible membrane fouling, which was determined as the differences of the initial TMPs of two consecutive batches of filtration process with backwashing in between. Panel A and Panel B in this figure correspond to Panel A and Panel B of Fig. 3-6, respectively. Error bars indicate standard deviation among different runs.

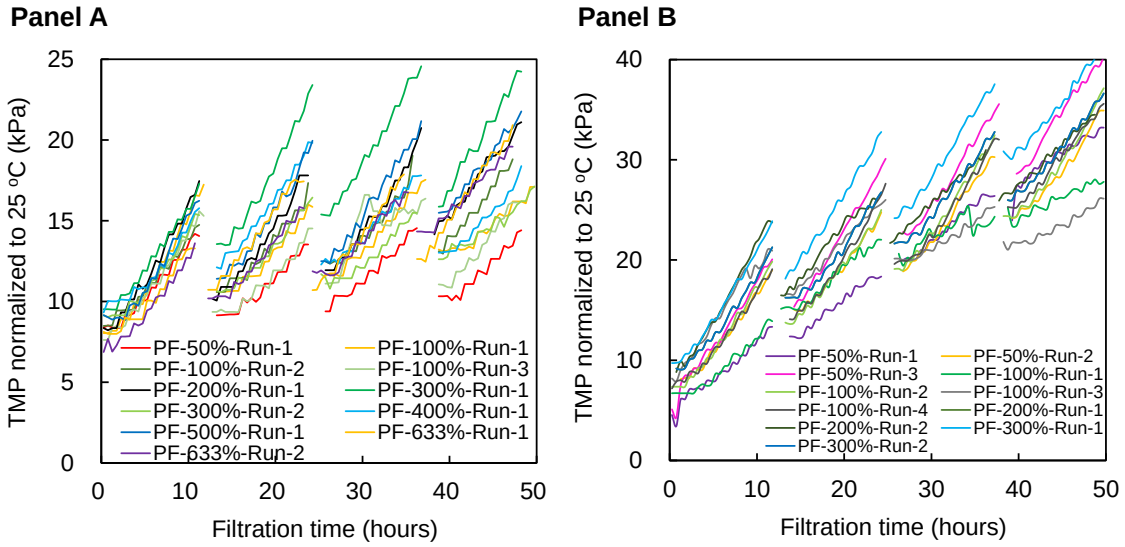

Fig. 3-8. TMP versus filtration time. SSPAC was dosed in a pulse at the beginning of each batch of filtration after a backwash every 12 hours. After the pulse dose of SSPAC, filtration was conducted at the precoat filtration flux, and then the filtration flux was returned to the main filtration flux of 70.8 L m^{-2} h^{-1}: for example, in the PF-50% run, the precoat filtration flux was 50% of the main filtration flux. The PACl-B70S coagulant was dosed continuously (Dose-4 in Fig. 3-5). SSPAC-1 and Water-2 were used in Panel A, and SSPAC-2 and Water-3 were used in Panel B. SSPAC and coagulant dosages were 5 mg/L and 2 mg-Al/L in Panel A and 1 mg /L and 1 mg-Al/L in Panel B, respectively.

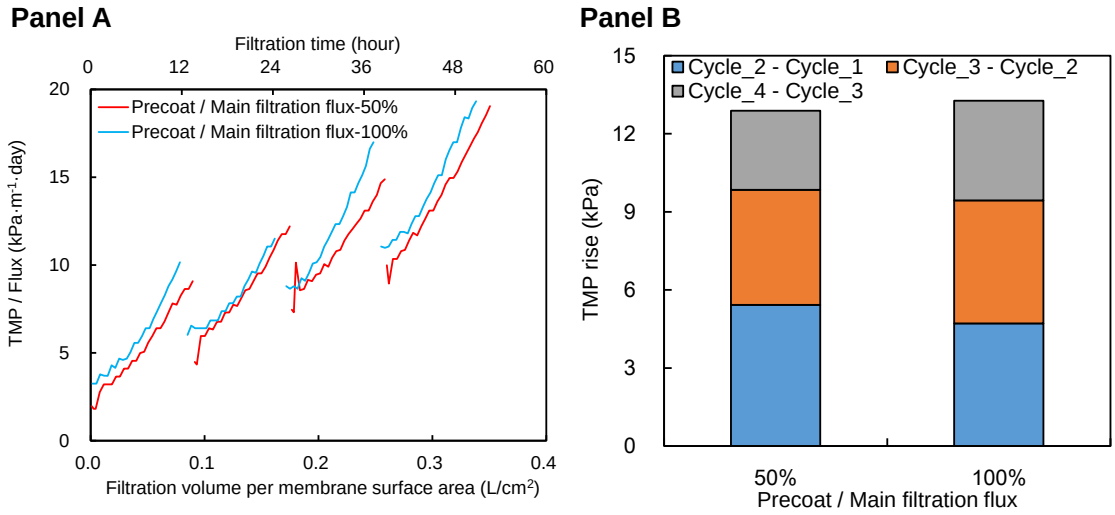

Fig. 3-9. Normalized (TMP/flux) versus filtration volume per membrane surface area (Panel A). TMP rise due to hydraulically irreversible membrane fouling, which was determined as the differences between the initial TMPs of two consecutive batches of filtration process with backwashing in between (Panel B). SSPAC was dosed at the beginning of each batch of filtration after a backwash every 12 hours. The experiments were conducted by using PACl-B70S with Dose-4 in Fig. 3-5. Filtration rate was 70.8 L m^{-2} h^{-1}. SSPAC-4 and Water-4 were used. Coagulant and SSPAC dosages were 2 mg-Al/L and 5 mg/L. In Panel B, no significant difference in TMP was found between PF-50% and 100% (p > 0.05 based on a Student's t-test).

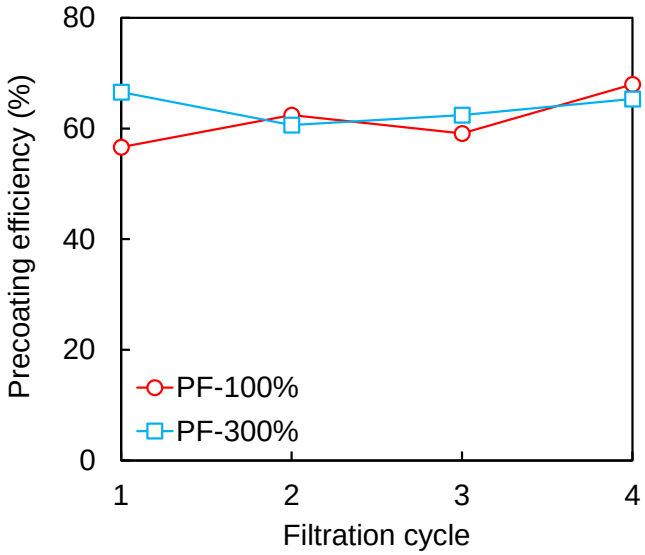

Fig. 3-10. Precoating efficiency: SSPAC attached to membrane expressed as percentage of dosed SSPAC. The experiments were conducted by using PACl-B70S with Dose-4 in Fig. 3-5. Filtration rate was 70.8 L m^{-2} h^{-1}). SSPAC-2 and Water-3 were used. Coagulant and SSPAC dosages were 1 mg-Al/L and 1 mg/L.

3.3.2. Effects of coagulant dose timing on TMP rise

Fig. 3-11 shows the rise of TMP with time in experiments at different coagulant doses. Experiments at each dose were conducted 2–4 times, and Fig. 3-11 shows the average values (Fig. 3-12 shows all the data). The TMP rise without SSPAC nor coagulant dosing reached 40 kPa after 28 hours (Control in Fig. 3-12). The TMP rose to 22 kPa after the same filtration time with pulse dosing of coagulant after pulse dosing of SSPAC (Dose-1 in Fig. 3-5). Continuous dosing of coagulant for only one hour from the start of filtration (Dose-3) resulted in a 10-kPa TMP rise. The rise of the TMP was only 5 kPa in the cases of (i) continuous, short-term dosing of coagulant when water was fed to the submerged tank for one hour after the start of filtration (Dose-2), (ii) continuous dosing of coagulant while water was fed to the submerged tank during the whole filtration period (Dose-4), and (iii) continuous dosing of coagulant during only the filtration period (Dose-5). Continuous dosing of coagulant while water was fed to the submerged tank throughout the whole filtration period (Dose-4) was the most effective way to constrain the TMP rise among all the dosing methods, although the improvements versus Dose-2 and Dose-4 were small.

Fig. 3-13 shows the concentrations of biopolymers and HS in the filtrates. Dose-4 achieved better

removal of biopolymers than any other method. In the case of HS, however, there were no significant differences among the dose methods. The success of Dose-2 (continuous, short-term dosing of coagulant) indicated that dosing of coagulant in the early stages of filtration (but not pulse dosing) was effective, and coagulant dosing could be omitted in the latter stages of filtration.

PACl is effective in removing hydrophobic matter composed of large molecules (Chow et al., 2009, 2008), and SSPAC has been reported to have a large capacity to adsorb onto DOC, especially biopolymers (Zhao et al., 2020). The combination of SSPAC along with coagulation is therefore expected to be effective in suppressing TMP rise due to multiple effects. After SSPAC is dosed in a pulse at the beginning of each filtration process, a precoating layer is formed on the membrane surface, and the precoating strains out a portion of foulants (Zhao et al., 2020). However, when the coagulant was dosed in a pulse as SSPAC, we observed deposition of many black floc particles at the bottom of the tank, as shown in the photograph of the submerged tank taken during filtration (Fig. 3-14). High concentrations of coagulant led to excessive coagulation of SSPAC, the settling of SSPAC to the bottom of the tank, and finally to the suppression of SSPAC from forming a precoat. The investigation of coagulant dose timing indicated that continuous dosing of coagulant during the feeding of water into the submerged tank and throughout the whole filtration period did the best job of suppressing the TMP rise. Another point to note here (Fig. 3-11) is that (i) the continuous dosing of coagulant during the feeding of water into the submerged tank and for one hour after the start of filtration and (ii) the continuous dosing of coagulant during only the filtration period were similarly effective in suppressing TMP rise. This result indicated that providing sufficient coagulant during the formation of the SSPAC precoating layer could help to eliminate the side effect of hydraulically irreversible fouling caused by the strong bonding between the SSPAC precoating layer and the membrane. Coagulation dosing during the period of water feeding (Dose-2 and Dose-4 in Fig. 3-5) was therefore necessary to ensure formation of a loose, porous precoating layer.

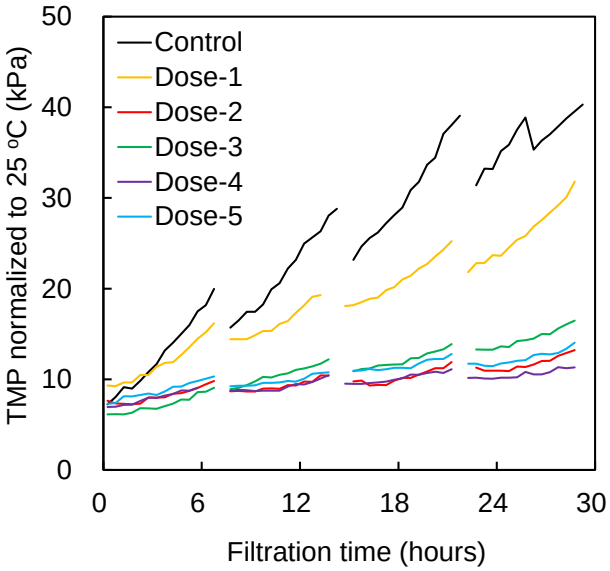

Fig. 3-11. TMP versus filtration time. SSPAC was dosed every 12 hours in a pulse at the beginning of each cycle of filtration after the backwash. The Control data indicate the results of the control experiment without dosing of SSPAC or coagulant. The dose methods are explained in Section 3.2.6 and Fig. 3-5. The filtration rate was 70.8 L m^{-2} h^{-1}. The reagents were PACl-B70S, SSPAC-1, and Water-1. The SSPAC and coagulant dosages were 5 mg/L and 2 mg-Al/L, respectively.

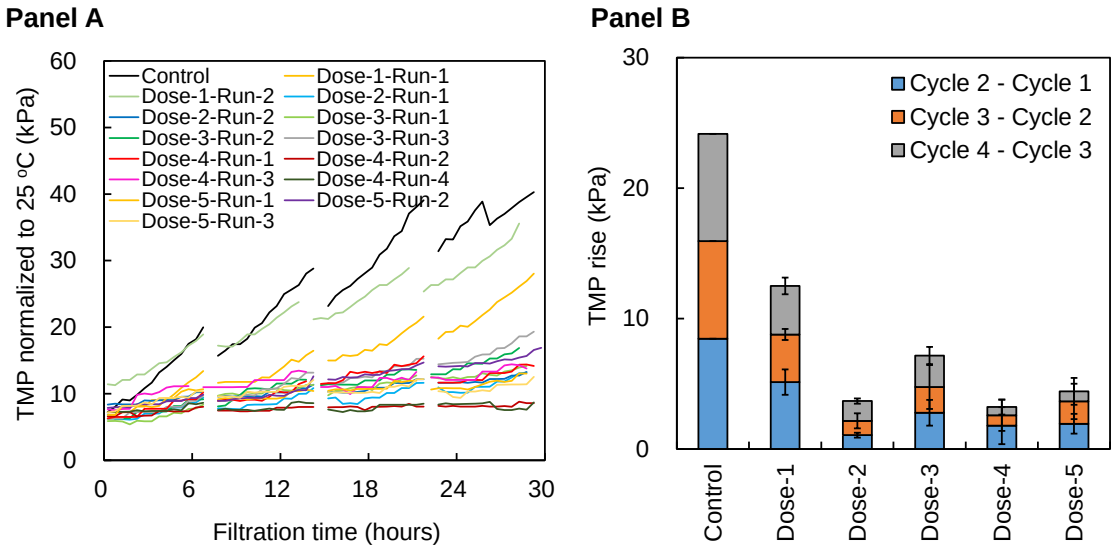

Fig. 3-12. TMP versus filtration time (Panel A). TMP rise due to hydraulically irreversible membrane fouling, which was determined as the differences between the initial TMPs of two consecutive batches of the filtration process with backwashing in between (Panel B). SSPAC was dosed in a pulse at the beginning of each batch of filtration after a backwash every 7 hours. The dose methods are explained in Section 3.2.6 and Fig. 3-5. Filtration rate was 70.8 L m^{-2} h^{-1}. PACl-B70S, SSPAC-1, and Water-1 were used. SSPAC and coagulant dosages were 5 mg/L and 2 mg-Al/L, respectively. Error bars indicate standard deviations among different runs.

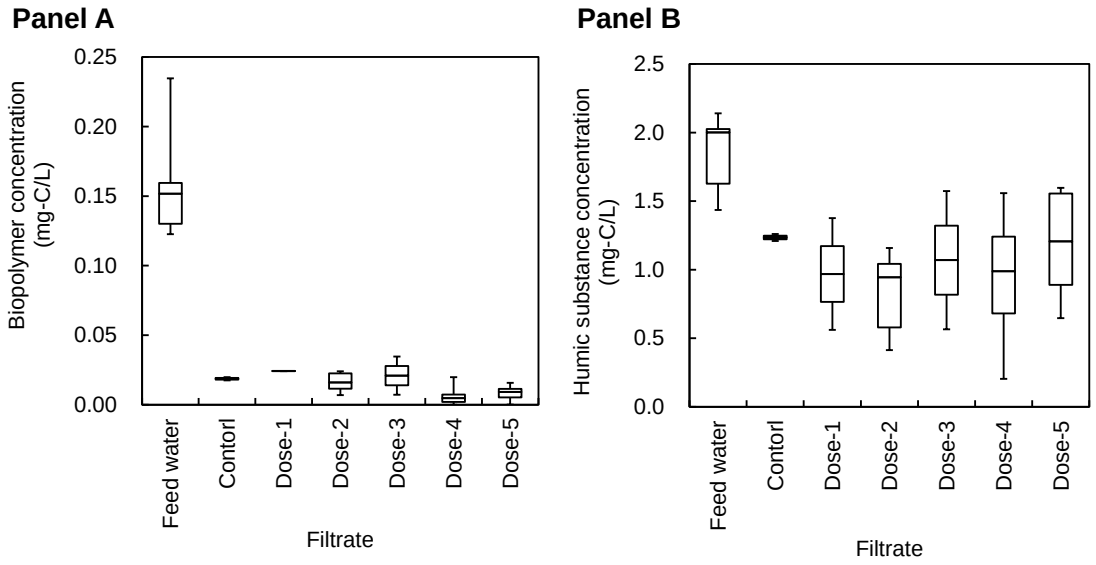

Fig. 3-13. Box-and-whisker plots of concentrations of biopolymer and HS in feedwater and filtrates. Dosing of SSPAC and coagulant were omitted in the Control experiment. SSPAC was dosed every 12 hours in a pulse at the beginning of each batch of filtration after the backwash. The reagents were PACl-B70S, SSPAC-1, and Water-1. The SSPAC and coagulant dosages were 5 mg/L and 2 mg-Al/L, respectively. The dose methods are explained in Section 3.2.6 and Fig. 3-5. Horizontal lines within boxes represent median values, the upper and lower horizontal lines in the boxes represent the 75th and 25th percentiles, respectively. The upper and lower bars outside the boxes indicate the maximum and minimum values, respectively.

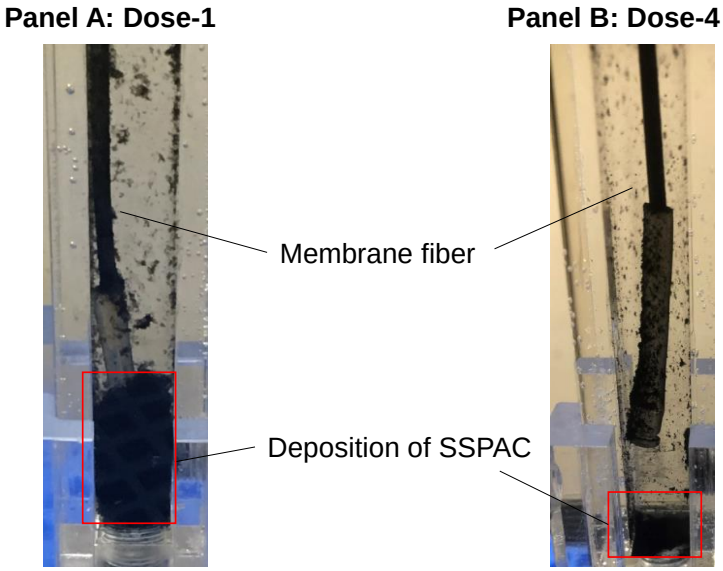

Fig. 3-14 Photographs of the submerged tank during filtration after the precoat period. The experiments were conducted by using PACl-B70S with Dose-1 for Panel A and Dose-4 for Panel B, as explained in Section 3.2.6 and Fig. 3-5. The filtration rate was 70.8 L m^{-2} h^{-1}. SSPAC-1 and Water-1 were used. Coagulant and SSPAC dosages were 2 mg-Al/L and 5 mg/L, respectively.

3.3.3. Effects of coagulant (PACl) types on TMP rise

Sulfated PACl (B50S and B70S) and non-sulfated PACl with a variety of basicities (B00, B20, B40,

B50, and B70) were used in the experiments with pulse dosing of SSPAC and continuous PACl dosing (Dose-4). Fig. 3-15 compares the TMP rises. PACl-B70S led to a 16-kPa rise of TMP during filtration, a rise that was much less than the 40-kPa rise when PACl-B50S was used. The implication is that the sulfated PACl with a higher basicity suppressed the rise of TMP much more effectively. This result is in accordance with a previous finding for ceramic filtration that high-basicity (71%) sulfated PACl performs better than normal basicity (51%) sulfated PACl in mitigating hydraulically irreversible fouling and suppressing TMP rise as well as in removing NOM because of its high charge neutralization capacity (Kimura et al., 2015).

The non-sulfated PACls suppressed a rise of TMP in the order B20 ≈ B40 > B50 > B00 > B70, though the differences were small compared with the much greater reduction of TMP rise achieved with the sulfated PACl. Higher basicity did not help to suppress a rise of TMP. Fig. 3-16 shows the concentrations of DOC, UV260, biopolymers, and HS. The removal rates of DOC, UV260, and HS were 30–40% between the feed water and filtrates for all the PACls. Differences of basicity between the in-house PACls did not result in any difference in the quality of these filtrates. The removal rates of biopolymers exceeded 90%, regardless of the basicity of the PACls, although biopolymer removal was slightly better with B20 than with the others. Because the differences of the TMPs were not large, the differences of water quality might have been difficult to compare.

A comparison of sulfated and non-sulfated PACls revealed that the sulfated, high-basicity PACl (PACl-B70S) was superior to the non-sulfated, high-basicity PACl (PACl-B70), but the sulfated, normal-basicity PACl (PACl-B50S) was inferior to the non-sulfated, normal-basicity PACl (PACl-B50). It has been reported that the non-sulfated, high-basicity PACl has a high charge-neutralization capacity but a low floc-formation ability because of its low rate of hydrolysis (Chen et al., 2020). It is therefore not surprising that the non-sulfated, high-basicity PACl (PACl-B70) was less effective in suppressing TMP rise than the sulfated, high-basicity PACl (PACl-B70S). However, the hydrolysis rate increases with decreasing basicity (Chen et al., 2020). Therefore, the non-sulfated, normal-basicity PACl suppressed TMP rise better than the non-sulfated, high-basicity PACl with decreasing basicity, although the charge

neutralization capacity decreases with decreasing basicity (Wang et al., 2002). The inferiority of the zero-basicity PACl (aluminum chloride solution) is probably due to its very low charge-neutralization capacity. The inferiority of the sulfated, normal-basicity PACl (PACl-B50S) compared to the non-sulfated, normal-basicity PACl (PACl-B50) could be explained by the fact that a sulfated PACl has a lower charge neutralization capacity than a non-sulfated PACl (Gao and Yue, 2005). The higher the basicity of the sulfated PACl, the greater the charge-neutralization effect (Ye et al., 2007), and thus the greater the suppression of TMP rise. Even though the charge neutralization effect of the non-sulfated PACl increased with increasing basicity, its rate of hydrolysis would become relatively low (Wang et al., 2002; Zhang et al., 2018). Among non-sulfated PACls, therefore, those with medium basicity would probably be most effective in suppressing TMP rise, but the difference in effectiveness would probably be small. To further investigate the effectiveness of different PACls, we conducted a batch experiment to reproduce conditions inside the submerged tank and measured floc particle sizes associated with different types of PACls. Fig. 3-17 and 3-18 show the results. The sizes of the floc particles associated with the PACls were not very different. Flocs that form rapidly and consist of large particles are considered to have a better coagulation effect (Chen et al., 2020) that might be related to better suppression of TMP rise. However, the floc particle measurements and observations during application of PACls with different basicities were not consistent with the increases of the TMP in the filtration experiments. Further studies are needed not only on the size of floc particles but also on membrane foulants and their removability as a function of coagulant properties.

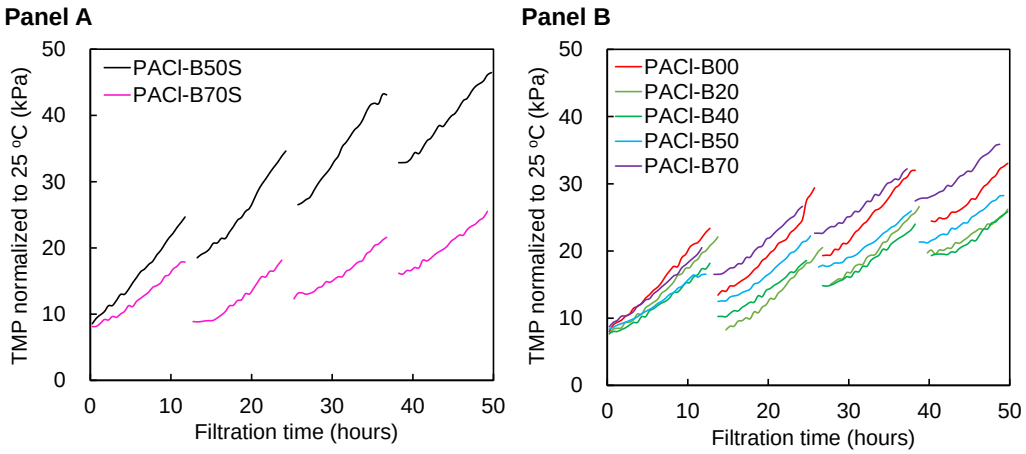

Fig. 3-15. TMP versus filtration time. SSPAC was dosed every 12 hours in a pulse. The experiments were conducted by using various coagulants (Section 3.2.3) by the Dose-4 method described in Section 3.2.6. Sulfated PACl (B50S and B70S) and non-sulfated PACl with a variety of basicities (B00, B20, B40, B50, and B70) were used. Filtration flux was 70.8 L m^{-2} h^{-1}. SSPAC-2 and Water-3 were used. SSPAC and coagulant dosages were 1 mg /L and 1 mg-Al/L, respectively.

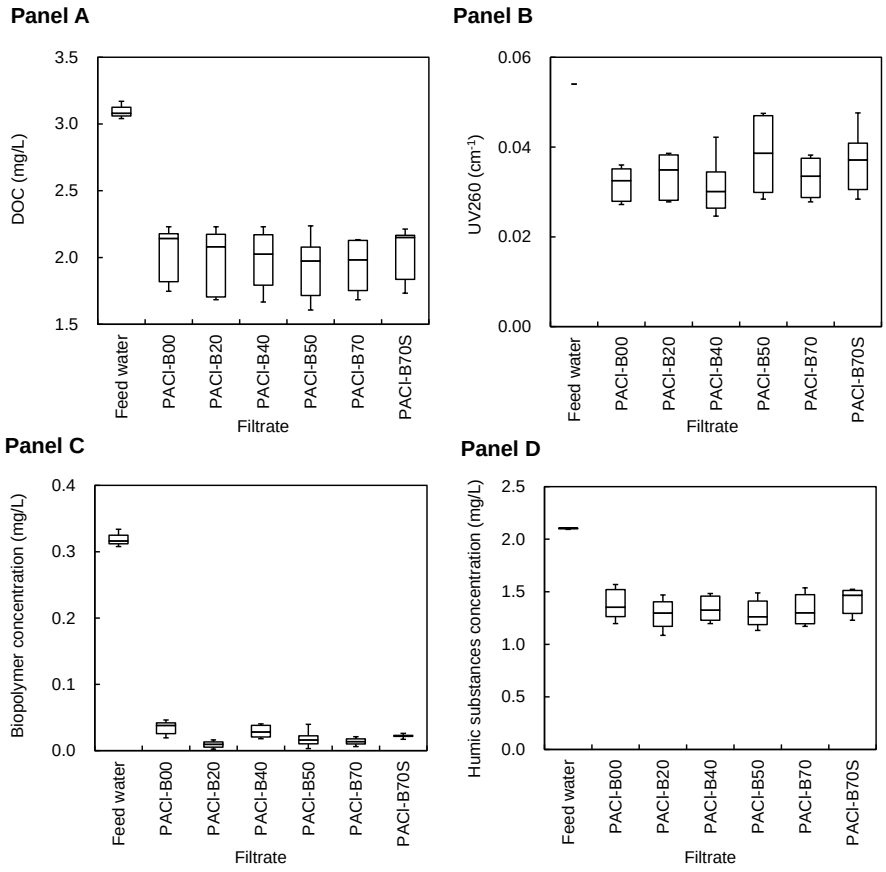

Fig. 3-16. Box-and-whisker plots of concentrations of DOC (Panel A), UV260 (Panel B), biopolymers (Panel C) and HS (Panel D) in feedwater and filtrates. No date for PACl-50S due to unavailability of samples. SSPAC was dosed every 12 hours in a pulse. SSPAC-2 and Water-3 were used. SSPAC and coagulant dosages were 1 mg /L and 1 mg-Al/L, respectively. Horizontal lines within boxes indicate median values, and the upper and lower horizontal lines in the boxes indicate the 75th and 25th percentiles, respectively. The upper and lower bars outside the boxes indicate the maximum and minimum values, respectively.

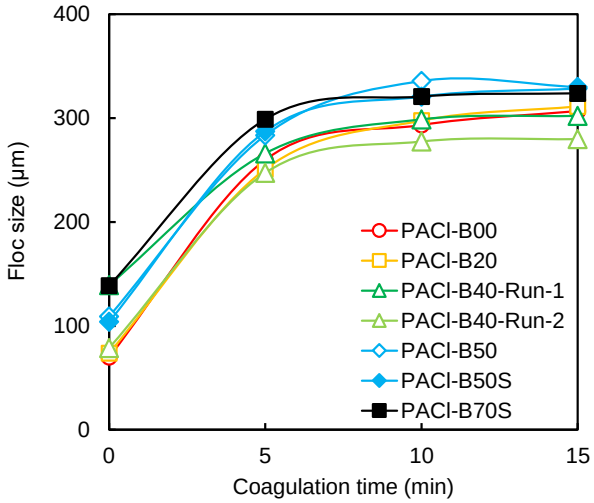

Fig. 3-17. Floc size versus coagulation time. SSPAC was pulse dosed into a beaker with the raw water and coagulants to reproduce the conditions inside the submerged tank in Section 3.2.4. After 1 min of rapid mixing, floc particle size was measured every 5 min. The samples were circulated during the experiment. PACls with basicity of 50% and 70% (PACl-B50S and 70S) and non-sulfated PACls with different basicities were used (PACl-B00, B20, B40, and B50). There are no data for PACl-B70 due to unavailability of samples. SSPAC-2 and Water-3 were used. SSPAC and coagulant dosages were 1 mg /L and 1 mg-Al/L, respectively.

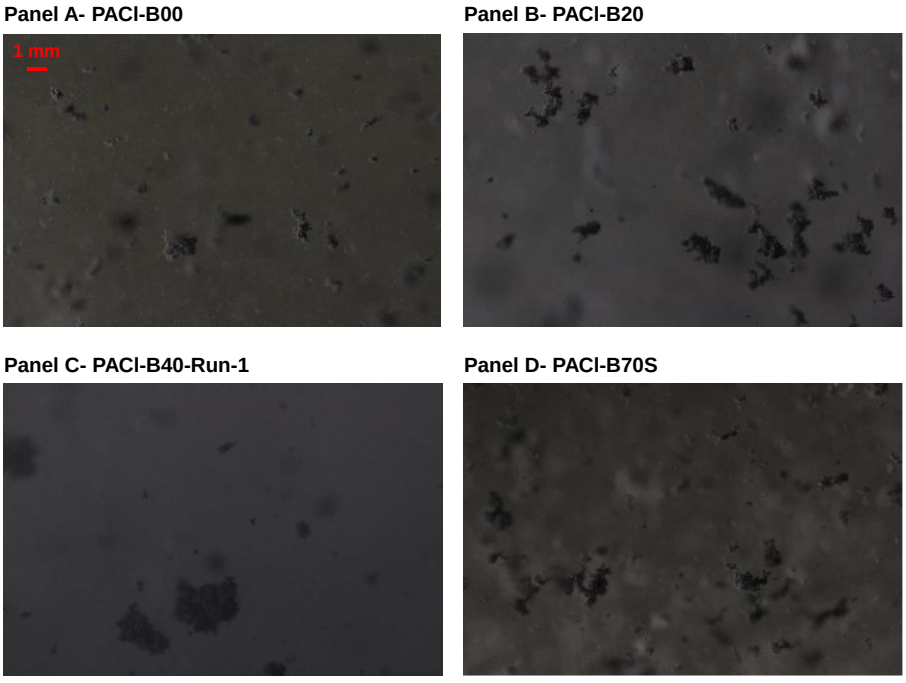

Fig. 3-18. Photographs of the floc particles after the 15-min coagulation described in Section 3.2.3. PACls with a basicity of 70% (PACl-B70S) and non-sulfated PACls with different basicities were used (PACl-B00, B20, and B40). No data for PACl-B50 and B70 due to unavailability of samples. The reagents were SSPAC-2 and Water-3. SSPAC and coagulant dosages were 1 mg /L and 1 mg-Al/L, respectively.

3.4. Chapter conclusions

1) Changing the precoat filtration flux after pulse dosing of SSPAC did not have a significant effect on suppression of TMP rise. However, a slow or constant flux rather than a high flux is recommended to suppress TMP rise because the formed precoat layer can be cleaned off by hydraulic backwashing more easily.
2) Dosing with PACl throughout the water feed and the whole filtration process was the most effective of the various dosing schedules of coagulant for suppressing TMP rise. Although pulse dosing of SSPAC was effective in suppressing TMP rise, pulse doing of PACl coagulant was not and resulted in excessively large floc particles that settled to the bottom of the membrane tank instead, where they influenced the formation of the precoat layer.
3) A sulfated PACl with high basicity (70%) seemed to be more effective in suppressing a rise of TMP than one with medium basicity (50%). However, for non-sulfated PACls, low-to-medium-basicity PACls (20% and 40%) effectively suppressed TMP rise rather than PACls with basicities of 0% and 70%.

3.5. References

Chen, Y., Nakazawa, Y., Matsui, Y., Shirasaki, N., Matsushita, T., 2020. Sulfate ion in raw water affects performance of high-basicity PACl coagulants produced by Al(OH)3 dissolution and base-titration: Removal of SPAC particles by coagulation-flocculation, sedimentation, and sand filtration. Water Research 183, 116093.

Chow, C.W.K., Fabris, R., Van Leeuwen, J., Wang, D., Drikas, M., 2008. Assessing natural organic matter treatability using high performance size exclusion chromatography. Environmental Science and Technology 42, 6683–6689.

Chow, C.W.K., van Leeuwen, J.A., Fabris, R., Drikas, M., 2009. Optimised coagulation using aluminium sulfate for the removal of dissolved organic carbon. Desalination 245, 120–134.

Gao, B., Yue, Q., 2005. Effect of SO42-/Al3+ ratio and O -/Al3+ value on the characterization of coagulant poly-aluminum-chloride-sulfate (PACS) and its coagulation performance in water treatment. Chemosphere 61, 579–584.

Heijman, S.G.J., Hamad, J.Z., Schippers, J., Amy, G., Kennedy, M.D., 2009. Submicron powdered activated carbon used as a pre-coat in ceramic micro-filtration. Desalination and Water Treatment 9, 86–91.

Hidayah, E.N., Cahyonugroho, O.H., 2019. Assessment of organic fraction based on its molecular weight and disinfection by-product formation through different coagulant. Journal of Ecological Engineering 20, 276–283.

Huber, S.A., Balz, A., Abert, M., Pronk, W., 2011. Characterisation of aquatic humic and non-humic matter with size-exclusion chromatography - organic carbon detection - organic nitrogen detection (LC-OCD-OND). Water Research 45, 879–885.

Jarvis, P., Sharp, E., Pidou, M., Molinder, R., Parsons, S.A., Jefferson, B., 2012. Comparison of coagulation performance and floc properties using a novel zirconium coagulant against traditional ferric and alum coagulants. Water Research 46, 4179–4187.

Kim, J., Cai, Z., Benjamin, M.M., 2010. NOM fouling mechanisms in a hybrid adsorption/membrane system. Journal of Membrane Science 349, 35–43.

Kimura, M., Matsui, Y., Saito, S., Takahashi, T., Nakagawa, M., Shirasaki, N., Matsushita, T., 2015. Hydraulically irreversible membrane fouling during coagulation-microfiltration and its control by using high-basicity polyaluminum chloride. Journal of Membrane Science 477, 115–122.

Kochkodan, V., Hilal, N., 2015. A comprehensive review on surface modified polymer membranes for biofouling mitigation. Desalination 356, 187–207.

Lee, H.J., Kim, S.J., Kim, Y., Park, H., Park, Y.I., Nam, S.E., 2021. Effect of coating and surface modification on water and organic solvent nanofiltration using ceramic hollow fiber membrane. Ceramics International 47, 34020–34027.

Lohwacharin, J., Oguma, K., Takizawa, S., 2010. Use of carbon black nanoparticles to mitigate membrane fouling in ultrafiltration of river water. Separation and Purification Technology 72, 61–69.

Nakazawa, Y., Matsui, Y., Hanamura, Y., Shinno, K., Shirasaki, N., Matsushita, T., 2018. Minimizing residual black particles in sand filtrate when applying super-fine powdered activated carbon: Coagulants and coagulation conditions. Water Research 147, 311 – 320.

Pan, L., Matsui, Y., Matsushita, T., Shirasaki, N., 2016. Superiority of wet-milled over dry-milled superfine powdered activated carbon for adsorptive 2-methylisoborneol removal. Water Research 102, 516–523.

Qiu, H., Peng, Y., Ge, L., Villacorta Hernandez, B., Zhu, Z., 2018. Pore channel surface modification for

enhancing anti-fouling membrane distillation. Applied Surface Science 443, 217–226.

Wang, D., Tang, H., Gregory, J., 2002. Relative importance of charge neutralization and precipitation on coagulation of kaolin with PACI: Effect of sulfate ion. Environmental Science and Technology 36, 1815–1820.

Ye, C., Wang, D., Shi, B., Yu, J., Qu, J., Edwards, M., Tang, H., 2007. Alkalinity effect of coagulation with polyaluminum chlorides: Role of electrostatic patch. Colloids and Surfaces A: Physicochemical and Engineering Aspects 294, 163–173.

Yu, W. zheng, Graham, N., Liu, H. juan, Qu, J. hui, 2013. Comparison of FeCl3 and alum pre-treatment on UF membrane fouling. Chemical Engineering Journal 234, 158–165.

Zahid, M., Rashid, A., Akram, S., Rehan, Z.A., Razzaq, W., 2018. A Comprehensive Review on Polymeric Nano-Composite Membranes for Water Treatment. Journal of Membrane Science & Technology 08.

Zhang, Z., Jing, R., He, S., Qian, J., Zhang, K., Ma, G., Chang, X., Zhang, M., Li, Y., 2018. Coagulation of low temperature and low turbidity water: Adjusting basicity of polyaluminum chloride (PAC) and using chitosan as coagulant aid. Separation and Purification Technology 206, 131–139.

Zhao, Y., Kitajima, R., Shirasaki, N., Matsui, Y., Matsushita, T., 2020. Precoating membranes with submicron super-fine powdered activated carbon after coagulation prevents transmembrane pressure rise: Straining and high adsorption capacity effects. Water Research 177, 115757.

Chapter 4. Pulse dosing of submicron super-fine powdered activated carbon in outside-in-type tubular and inside-out-type monolithic ceramic membranes

4.1. Chapter introduction

As the previous chapters introduced, among all applications of PAC on mitigating membrane fouling, SPAC (median diameter 1–2 μm) (Ando et al., 2010; Ellerie et al., 2013; Heijman et al., 2009; Matsui et al., 2006; Pan et al., 2017) has been considered to meet the requirement that takes efficiency and cost into consideration. Matsui et al., have reported the superiority of SPAC adsorption-coagulation over conventionally sized PAC (10-30 μm) adsorption-coagulation in terms of both mitigation of membrane fouling and filtrate water quality. Kanaya et al., have subsequently reported the application of SPAC in a full-scale drinking water treatment plant using ceramic membranes. The SPAC was produced by onsite PAC grinding, and the treatment cost was less than the cost of treatment with PAC. The reduction in the dosage of activated carbon (AC) led to the overall reduction in the treatment cost because the price of AC exceeds the grinding cost.

Although the smaller AC particles themselves foul the membrane and cause a greater decline of flux (Ando et al., 2010; Heijman et al., 2009; Matsui et al., 2006; Partlan, 2017), coagulation pretreatment after AC injection could cancel out this problem (Kanaya et al., 2015). In the previous chapters, submicron-sized SPAC (SSPAC, median diameter 200 nm) has recently been shown to successfully retard the hydraulically irreversible membrane fouling of a polymeric membrane (Zhao et al., 2020) because it has a higher capacity to adsorb biopolymers, which are identified as one of the predominant contributors to fouling (Huber et al., 2011; Kimura et al., 2018; Tian et al., 2013), than SPAC and cconventionally sized PAC. In addition, unlike the normal dosing operation that involves continuous dosing with SSPAC, dosing with the same amount of SSPAC in a pulse at the beginning of filtration in a submerged polymeric membrane system has been shown to largely retard the rise of membrane

pressure (Zhao et al., 2020). This phenomenon has been explained to result from the formation of a precoated layer of the pulse dosed SSPAC on the membrane, which would prevent foulants from contacting the membrane (Zhao et al., 2020). However, this previous study has applied SSPAC to only a submerged-type hollow-fiber polymeric (polyvinylidene difluoride [PVDF]) membrane.

The application of SSPAC to other types of membranes is of great interest because membranes of many different materials and geometries are used in water treatment. Ceramic membranes have recently been increasingly used because of their superiority over polymeric membranes in terms of their service lifespan due to their chemical and thermal stability, resistance, and robustness (Asif and Zhang, 2021; Murić et al., 2014; Samaei et al., 2018). Because of the high cost of ceramic membranes compared with polymeric membranes, mitigating membrane fouling and achieving high-flux filtration are important objectives for lowering capital and operational costs (Samaei et al., 2018). In addition, SSPAC itself may cause fouling on a ceramic membrane because PAC on a ceramic membrane has been shown to cause cake fouling (Zhao et al., 2005), and the particle size of SSPAC (D10, 0.11 μm; D50, 0.2 μm) is close to the pore size of ceramic membranes (0.1 μm). It is generally understood that the fouling characteristics of ceramic membranes differ from those of polymeric membranes, for example in ways that cause organic fouling to be lower for ceramic membranes than for polymeric membranes (Asif and Zhang, 2021; Samaei et al., 2018). It is therefore of great interest to determine how combinations of SSPAC, pulse dose, and ceramic membranes with different geometries affect TMP rise.

In this chapter, the study was conducted with the goal of understanding whether and how pulse dosing of SSPAC attenuates the fouling of ceramic membranes with tubular and monolithic geometries better than continuous dosing with SSPAC. To achieve this goal, experiments were conducted using two very different types of membrane filtration setups that treated diluted secondary-treated municipal wastewater and natural river water through repeated membrane filtrations and hydraulic backwashes. One setup involved a submerged-tubular membrane (hereafter submerged membrane) that enabled vacuum-driven outside-in filtration, whereas the other involved a monolithic membrane that enabled pressure-driven, inside-out filtration.

This chapter has already been published by Elsevier, and the information is described as follows:

Title: Effectiveness of pulse dosing of submicron super-fine powdered activated carbon in preventing transmembrane pressure rise in outside-in-type tubular and inside-out-type monolithic ceramic membrane microfiltrations

Author: Yuanjun Zhao, Yoshihiko Matsui, Shun Saito, Nobutaka Shirasaki, Taku Matsushita

Name of journal: Separation and Purification Technology

Year: 2022

Volume: 296

Pages: 121403

DOI: https://doi.org/10.1016/j.seppur.2022.121403

4.2. Materials and methods

4.2.1. Waters

Two kinds of water were sampled to prepare feed waters for the membrane filtration experiments. Wanigawa River water (same in Chapter 2 and Chapter 3) was sampled in November of 2020. The water was filtrated through a membrane with a 10-μm pore size (flat-sheet membrane, coated-cellulose-acetate, Y100A142A, Advantec Toyo Kaisha, Ltd., Tokyo, Japan) to prepare feed water (designated as Water-W-1 and -2) for the experiments with a submerged ceramic membrane system (Section 4.2.4. The last number in the designation (e.g., 2) indicates the dilution factor).

Due to the difficulty in obtaining large amount of the river water, another water was prepared by diluting secondary-treated sewage water to simulate contaminated surface water where wastewater flows in. The secondary-treated wastewater was sampled from a sedimentation tank following the activated sludge process at a municipal wastewater treatment plant (Soseigawa Water Reclamation Plaza, Sapporo, Japan) in September and December of 2020 and June of 2021. These waters were filtered through a 10-μm pore size membrane (same as Water-W) and diluted with pure water (Milli-Q Advantage, Merck KGaA, Darmstadt, Germany) to prepare the feed water for experiments with a submerged ceramic membrane or filtered through a 10-μm pore size membrane (a capsule cartridge membrane, polypropylene, CCP-10-E1H, Advantec Toyo Kaisha, Ltd.) and diluted with dechlorinated tap water were used to prepare a large volume of feed water for experiments with a monolithic ceramic membrane. The feed waters prepared from the water sampled in September 2020, December 2020, and June 2021 were designated Water-S-1-4, Water-S-2-4, and Water-S-3-2, respectively. The last number in the designation (e.g., 4) indicated the dilution factor.

Concentrations of DOC, biopolymer, HS, and UV260 were used to characterize the water quality of the filtrates and raw water (after being pre-filtered through a 0.45-μm PTFE membrane). The measurements and analysis equipment are the inconsistent with those in Chapter 2 and Chapter 3. As an additional note, the HS were treated as a group that also included the building blocks because the HS

and the building blocks partly overlapped each other. However, the HS were much larger in chromatograms, as shown in Fig. 4-1. Table 4-1 shows the characteristics of the feed water.

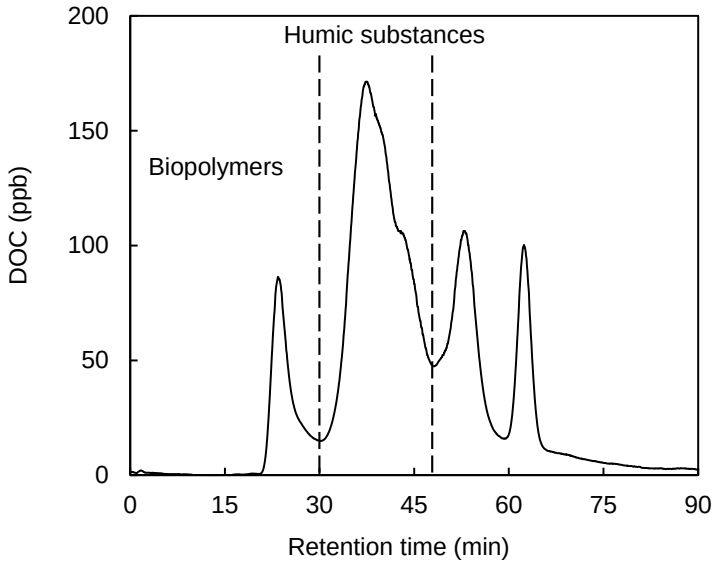

Fig. 4-1. Chromatograms by size-exclusion chromatography–organic carbon detection system. Water-S-2-1 was used.

Table 4-1
Feed water quality.

	pH	DOC mg/L	UV abs. at 260 nm cm^{-1}	Biopolymer mg/L	Humic substances mg/L	Alkalinity mg/L as $CaCO_3$	Na^+ mg/L
Water-W-1	7.96	3.69	0.070	0.31	2.55	71	43.8
Water-S-1-4	7.39	1.65	0.031	0.11	1.01	19	24.5
Water-S-2-1	6.56	4.31	0.099	0.33	3.12	16	51.1
Water-S-3-1	7.00	5.19	0.100	0.67	2.14	31	42.2

	K^+ mg/L	Mg^{2+} mg/L	Ca^{2+} mg/L	Cl^- mg/L	NO_3^- mg/L	SO_4^{2-} mg/L
Water-W-1	5.55	9.25	17.9	51.6	n/a	14.8
Water-S-1-4	4.56	2.55	13.1	36.3	9.22	20.7
Water-S-2-1	10.5	4.55	17.8	58.7	41.2	25.4
Water-S-3-1	9.77	3.97	17.4	49.0	29.7	23.2

4.2.2. Activated carbons and coagulants

SSPAC was prepared by the same procedure previously described (Pan et al., 2017). A wood-based, commercially available PAC with a volume median diameter (D50) of 12.7 μm (Taiko-W, Futamura

Chemical Co., Ltd., Nagoya, Japan) was dosed into pure water to make a PAC slurry. The PAC slurry was ground in a rotating grinding pot to obtain ACs with D50s of 3.5 μm. The ground AC slurry was then milled in a bead mill to obtain SSPAC with a D50 of 200 nm. The size distribution of the AC particles was measured with a laser diffraction analyzer (Microtrac MT3300EXII, Nikkiso Co., Inc., Tokyo, Japan) after the AC slurries had been supplemented with a dispersant (Triton X-100, Kanto Chemical Co., Tokyo, Japan; final concentration, 0.08% w/v) and then ultra-sonicated (Pan et al., 2016). Fig. 4-2 shows the size distributions of the AC particles. Poly-aluminum chloride with a basicity of 70% (PACl-70s) and sulfate ion (2% w/w) (Taki Chemical Co., Hyogo, Japan), which is used in actual water treatment plants, was used as the coagulant in this chapter.

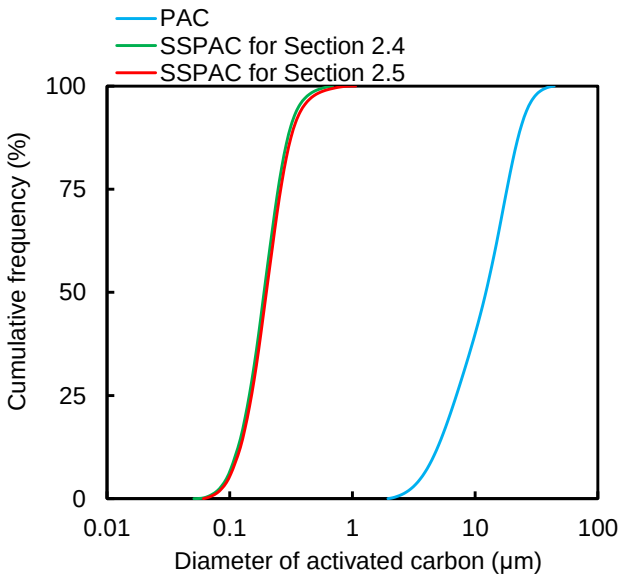

Fig. 4-2. Size distributions of PAC and SSPAC.

4.2.3. Ceramic membranes

A tubular ceramic membrane for practical use (nominal pore size 0.1 μm, inner diameter 0.9 cm, outer diameter 1.3 cm, length of 80 cm, Kubota Corp., Tokyo, Japan) was cut to obtain a piece of membrane with a length of 1.5 cm. One end of the membrane piece was covered with a polyvinyl chloride plate, whereas the other end was covered with a plate with an outlet port, which enabled outside-in filtration by vacuum. The resulting membrane element had a filtration area of 5.3 cm^2 (after considering the

adhesion area between the membrane and the plate), which was like that of a polymeric membrane (6 cm^2) applied in previous chapter (Zhao et al., 2020). All membrane elements were tested for their pure-water permeability and integrity, and membranes with the same permeability were used in the experiments (Fig. 4-3).

A monolithic ceramic membrane element (nominal pore size 0.1 μm, length 10 cm, diameter 3 cm, channel diameter 1.5 mm, Metawater Co., Tokyo, Japan) was used after sealing some of the membrane channels to reduce the number of channels from 55 to 22 or 7 to reduce feed water consumption in the membrane filtration experiments. Filtration areas were 172 and 54.7 cm^2 for the 22-channel and 7-channel membranes, respectively. Fig. 4-4 includes pictures that show the geometries of the membranes.

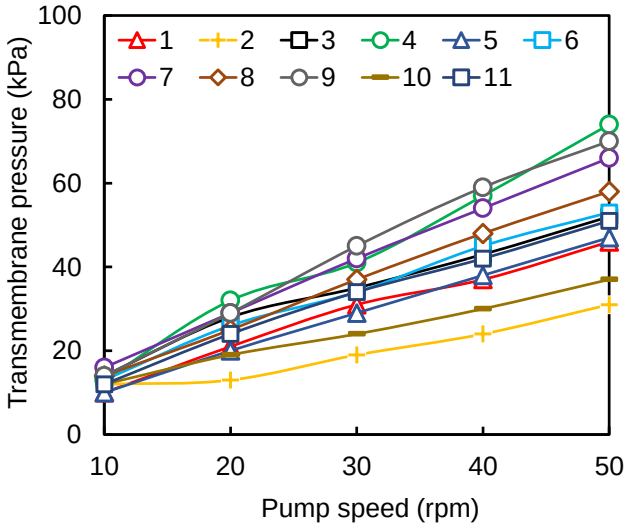

Fig. 4-3. Permeability test for cut pieces of submerged tubular ceramic membranes. The pair of membrane pieces 1 and 5 and the pair of membrane pieces 3 and 11 were used in the experimental comparisons.

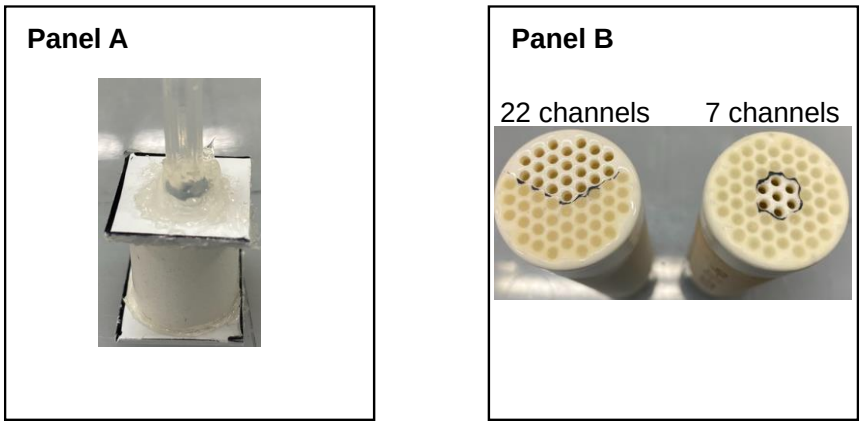

Fig. 4-4. Pictures of the geometries of a submerged membrane element (Panel A) and monolithic membrane elements (Panel B).

4.2.4. Submerged ceramic membrane filtration system

Panel A of Fig. 4-5 shows the system setup. The treatment flow except for SSPAC injection was basically the same as that commercialized by Kubota Corp. A rectangular container (2 × 2 × 10 cm height) was used as a submerged-membrane tank, in which a ceramic membrane element was placed beneath the water. The coagulant was injected in the feed line and mixed with the feed water by a static mixer to produce a dosage of 2 mg-Al/L, which is the same dosage that was applied in previous experiments with a PVDF membrane. The coagulated water was then fed into the submerged tank after being supplemented with NaOH to bring the pH of the treated water to ~7.5.

In the experiment with the continuous dose of SSPAC, the SSPAC suspension was dosed in the feed line at a dosage of 5 mg/L. In the experiment that involved pulse dosing of SSPAC, the SSPAC was manually dosed in a pulse to the submerged-membrane tank at the beginning of every filtration cycle. This pulse dosing was followed by 30 s of bubbling with an air pump in the tank for mixing. The pulse dosage was equated to the mass of SSPAC calculated from the rate of injection and the concentration of the continuously dosed SSPAC suspension. The overall dosages were therefore the same in the continuous-dosing and pulse-dosing experiments.

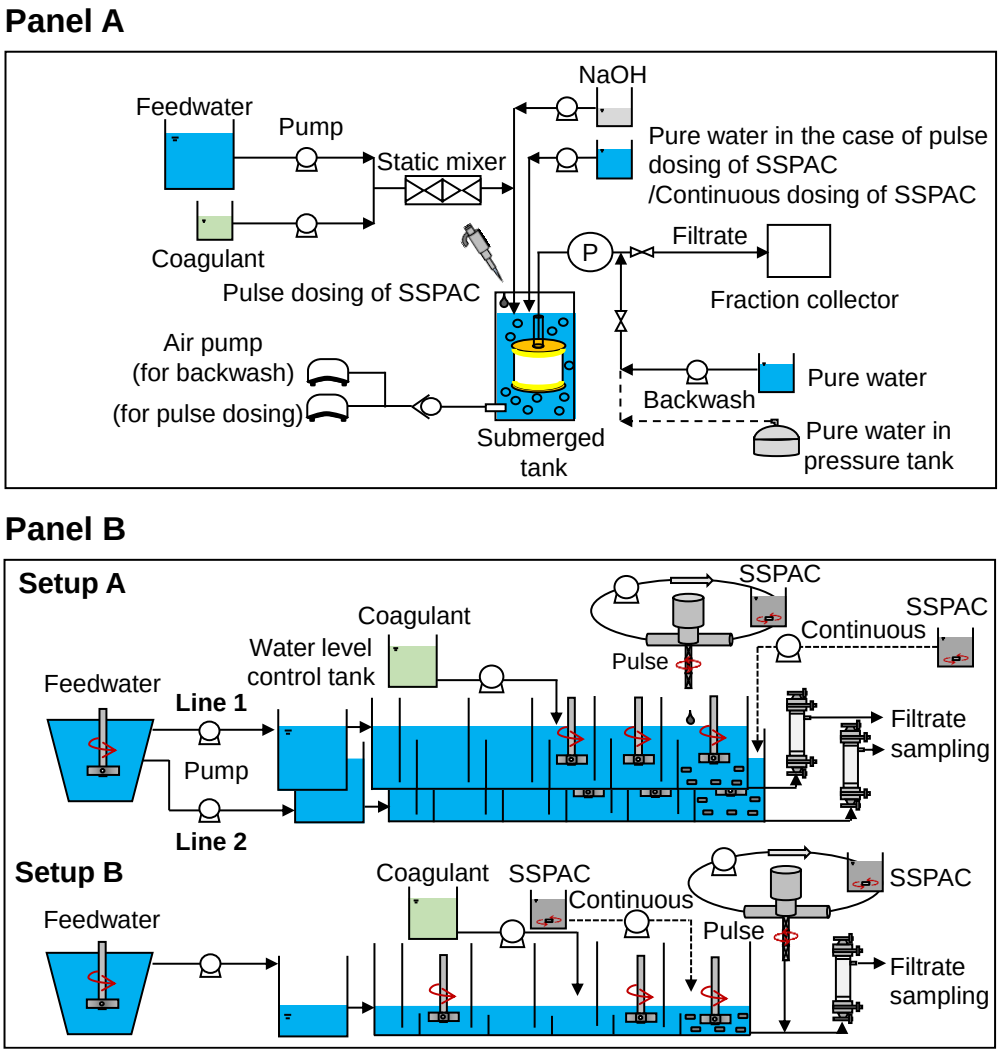

Fig. 4-5. System setups for submerged membrane (Panel A) and monolithic membrane (Panel B) with pulse and continuous dosing with SSPAC. Setup A of the monolithic membrane had two treatment lines with the same configuration and were operated in parallel, whereas Setup B had a single treatment line.

Membrane filtration was conducted in an outside-in mode with the flux of 80.4 L m^{-2} h^{-1}, which is slightly higher than those applied in actual full-scale plants to clarify membrane fouling in a shorter time but is similar to the previous SSPAC-precoating study, unless otherwise noted, using vacuum provided by a peristaltic pump. The membrane was hydraulically backwashed for 30 s every 7 h by pumping pure water in an inside-out direction at a rate of 351 L m^{-2} h^{-1}. In additional runs, hydraulic backwashing was conducted by using pure water from a tank under a pressure of 50 or 100 kPa. During the backwash, air-bubbling was conducted in the membrane tank. The water in the submerged-membrane tank was drained after each backwash, and the filtration was then restarted after the tank had filled with feed water.

The membrane filtrate was collected three times throughout one batch of filtration between backwash cycles. Vacuum pressure was recorded with a pressure meter. The experiments were conducted in a room controlled at a nearly constant temperature of 20 °C, but a digital thermometer was placed in the feed water tank to monitor the water temperature.

4.2.5. Monolithic ceramic membrane filtration system

Panel B of Fig. 4-5 shows the system setup. The treatment flow, except for SSPAC injection, was basically the same as that commercialized by Metawater Co. It consisted of tanks-in-series, including those for coagulation and flocculation, a membrane module, and a hydraulic backwash unit. Two kinds of setups with different configurations were constructed. Setup A was used for a membrane element with 22 channels, whereas Setup B was used for a membrane element with 7 channels.

For Setup A, two treatment lines were set in place and operated in parallel. Feed water was fed to the first tank, and the coagulant was fed to the fourth tank, where rapid mixing was performed. Slow mixing was performed in the fifth and the sixth tanks, and SSPAC was injected either continuously or in pulses to the sixth tank, from which the water was transferred to the membrane module. In Setup B, coagulant was fed to the fifth tank, where rapid mixing was performed for coagulation. Slow mixing for flocculation was performed in the sixth tank, and SSPAC was injected either continuously to the sixth tank or injected in pulses to the line to the membrane module. The same equipment was used for Setups A and B, but characteristics such as water levels were changed. The pH of the feed water was adjusted to 7.0 at the beginning, and no other adjustment was conducted during the experiment. The recording data indicated that coagulation pH was 7.5.

In both Setups A and B, pulse dosing of SSPAC was performed automatically at predetermined times. To prevent deposition of SSPAC in the injection pipe during the injection shutdown period, the injection pump was operated constantly, and the SSPAC suspension was circulated within a loop of pipe. The pulse injection was therefore not truly a pulse in the strict sense of the word, because it took 5 min to inject a suspension of SSPAC. However, 5 min was much shorter than the times of 2 h (Setup A) and

0.63 h (Setup B) for one batch filtration. It was therefore essentially a pulse injection. Coagulant and SSPAC dosages were 1 mg-Al/L and 2 mg/L, respectively, unless otherwise noted. Table 4-2 shows other configurations.

The membrane filtration was operated in an inside-out mode at a constant flux determined by positive pressure with a periodic hydraulic backwash from the filtrate side at a pressure of 500 kPa unless otherwise noted. The flux was 208 L m^{-2} h^{-1} for Setup A and 438 L m^{-2} h^{-1} for Setup B: the latter flux was clearly higher than those applied in actual full-scale plants in order to create fouling-prone conditions (Kimura et al., 2015). TMP and water quality were measured in the same way as they were measured in the submerged ceramic membrane filtration system.

Table 4-2
Operating conditions of submerged tubular and monolithic membrane systems.

Membrane	Channel number	Pore size µm	Filtration area cm^2	Flux m/d	L m^{-2} h^{-1}	Backwash interval h	Backwash time s	Backwash pressure kPa
Submerged tubular	1	0.1	5.30	1.93	80.4	7.0	30	50
Monolith (Setup A)	22	0.1	172	5.00	208	2.0	10	500
Monolith (Setup B)	7	0.1	54.7	10.5	438	0.63	10	500
Monolith (Setup B)	22	0.1	172	1.67	69.8	7.0	10	50

Membrane system	Channels	Mixing intensity (G value)			Detention time		
		Rapid mixing s^{-1}	Slow mixing 1 s^{-1}	Slow mixing 2 s^{-1}	Rapid mixing min	Slow mixing 1 min	Slow mixing 2 min
Submerged tubular	1	609			3.72		
Monolith (Setup A)	22	41.8	8.1	4.0	11.9	11.9	20.4
Monolith (Setup B)	7	71.8	9.4		7.70	13.2	
Monolith (Setup B)	22	110.6	17.9		15.9	27.3	

4.2.6. Membrane surface observation

Photographs of the surface of a tubular membrane were taken with a digital microscope (VHX-2000, Keyence, Osaka, Japan). A rigid industrial fiber microscope (MK012-009-000-45, Olympus, Tokyo, Japan), which reached inside the channels in the monolithic membrane, was used to take photographs of the surface of the monolithic membrane. The membrane surfaces before filtration, before backwash, and right after backwash were observed.

4.3. Results

4.3.1. Changes of TMP in submerged ceramic membrane systems with pulse and continuous dosing of SSPAC

Sixteen runs of membrane filtration were conducted with pulse or continuous dosing of SSPAC using three feed waters that contained various concentrations of NOM, including biopolymers (Table 4-1) that have been thought to cause severe, irreversible membrane fouling (Chen et al., 2014; Huber et al., 2011; Kimura and Oki, 2017).

Runs with continuous dosing of SSPAC were carried out eight times for Water-W-2 (Panel A of Fig. 4-6), Water-S-2-2, and Water-S-2-4 (Panels B and C of Fig. 4-6). The TMP rose almost continuously over the duration of the experiment and finally reached ~60 kPa. Among the 8 runs, the TMP rise was not as rapid in only one run (Run 2), but it was still higher than the TMP rise observed in the comparative runs with a pulse dose. The membrane was backwashed every 7 h to clean the membrane and decrease the elevated TMP, but the TMP decreased only marginally after each backwash, and it continued to rise throughout the entire experimental period.

Unlike the runs with continuous dosing of SSPAC, the TMP did not rise as much in the runs that involved pulse dosing of SSPAC. In all eight runs with pulse dosing, the TMP remained low because the backwash worked effectively. Specifically, the increase of the TMP during each 7-h batch filtration was like the increase observed during the runs that involved continuous dosing of SSPAC. However, backwashing reduced the TMP to the level that had been observed 7 h earlier, namely at the start of each batch filtration. As a result, pulse dosing was superior to continuous dosing for all runs in terms of attenuating the rise of TMP.

The filtration experiments were conducted again for 14 h, and during those experiments the backwash pressure was controlled at 100 kPa or 50 kPa: the use of a pressure tank instead of a peristaltic pump to apply the backwash pressure made it possible to apply a constant backwash pressure more quickly to the membrane. As shown in Fig. 4-7, the TMP increased rapidly probably due to the high DOC of the feed water, and the increase could be reduced only marginally by backwashing if the SSPAC was dosed

continuously, but the increase of the TMP was largely reversed by backwashing in the case of pulse dosing of SSPAC.

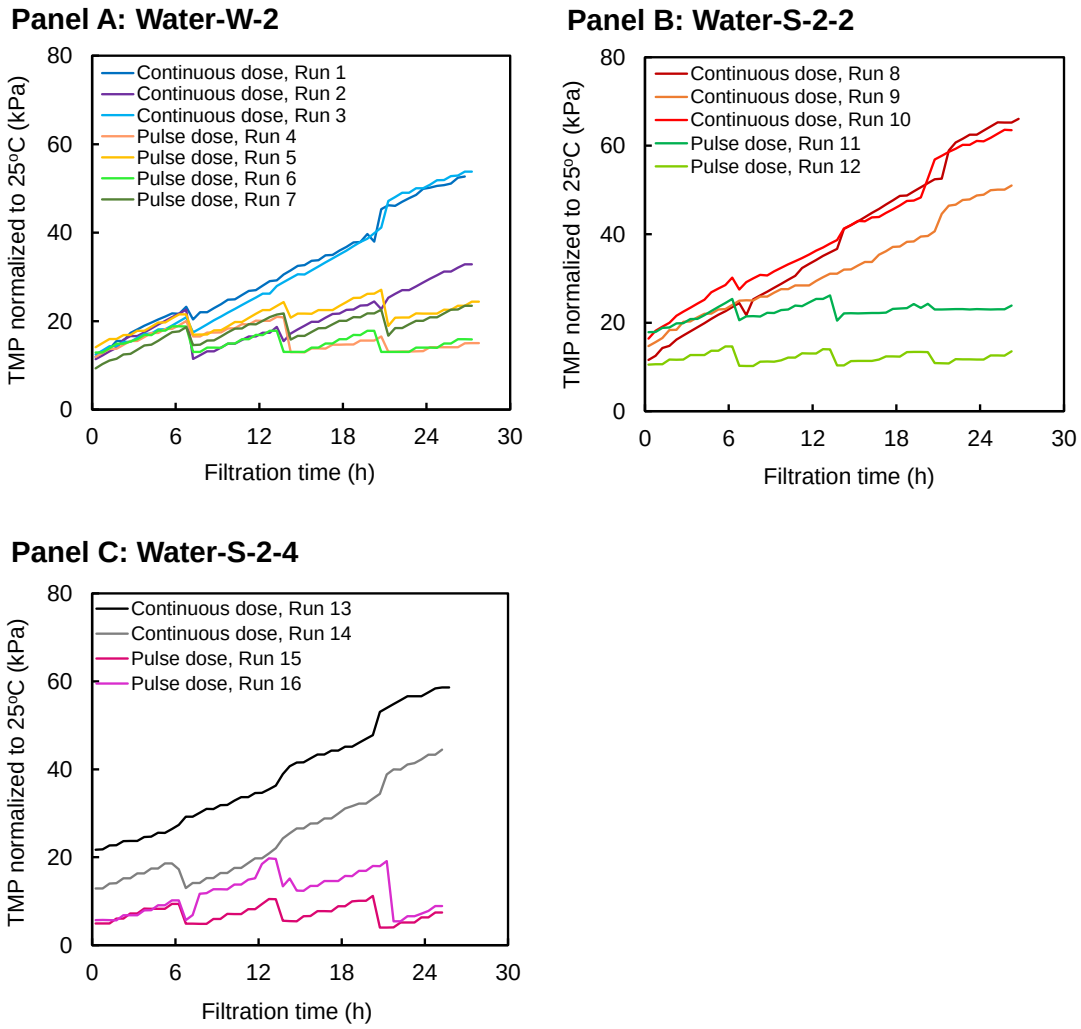

Fig. 4-6. TMP as a function of filtration time. Filtration was conducted in a submerged ceramic membrane tank fed with water pretreated by SSPAC adsorption and coagulation. SSPAC was dosed continuously or in a pulse after each backwash. The backwash interval was 7 h. The filtration flux was 80.4 L m^{-2} h^{-1}. Water-W-2 (Panel A), Water-S-2-2 (Panel B) and Water-S-2-4 (Panel C) were used.

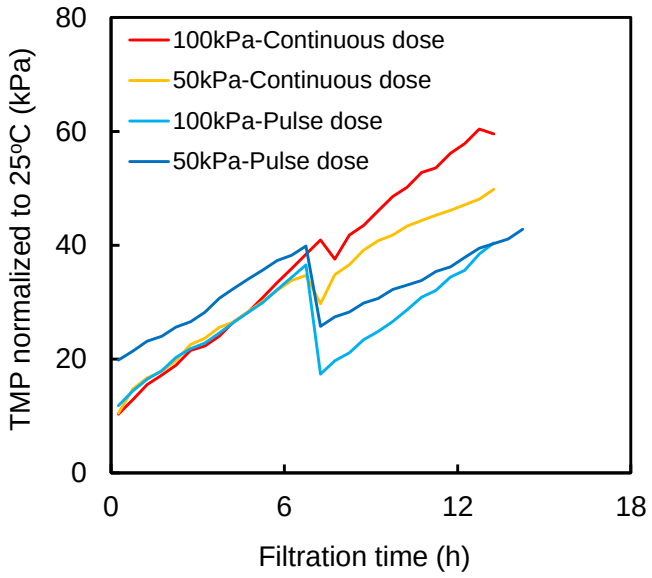

Fig. 4-7. TMP as a function of filtration time. Filtration was conducted in a submerged tubular ceramic membrane tank fed with water pretreated by SSPAC adsorption and coagulation. The SSPAC was dosed continuously or in pulses. Backwash interval was 7 h. Filtration flux was 80.4 L m^{-2} h^{-1}). Backwash pressure was applied from a pressure tank at 100 kPa or 50 kPa. Water-S-3-2 was used.

4.3.2. Changes of TMP in a monolithic ceramic membrane system with pulse and continuous dosing of SSPAC

The inside-out, pressure-driven monolithic ceramic membrane was tested to compare results with pulse and continuous dosing of SSPAC. In Setup A of the monolithic ceramic membrane, two filtration runs were conducted in parallel; one run employed pulse dosing, and the other run employed continuous dosing. Because the membranes were backwashed every 2 h, the TMP increased for 2 h, decreased because of backwashing, and then increased again. This cycle was repeated, but overall, the TMP gradually increased over the entire time of the system operation. As shown in Panel A of Fig. 4-8, during the first five-day operation, the TMP rise was somewhat lower in the system with continuous dosing of SSPAC than in the system with pulse dosing of SSPAC, but the difference of the TMP rise between the two systems was not as large as the difference observed in the submerged ceramic membrane systems (Section 4.3.1). After five days of operation, each membrane was replaced with a new one, and the two systems were restarted. However, the applications of pulse/continuous dosing to the two systems were inverted (the pulse dosing was applied to Line 1 during days 0–5 and to Line 2 during days 5–9, whereas the continuous dosing was applied to Line 2 during days 0–5 and to Line 1 from days 5–9). After the

restart, the TMP rose at a somewhat slower pace in the system with continuous dosing of SSPAC than in the system with pulse dosing, but the difference of the TMP rise between the two systems was again small. Hydraulically reversible rises of TMP (most of the TMP rose in each batch filtration every 2 h was restored by the backwash) were also similar between pulse and continuous dosing (Fig. 4-9).

We conducted other runs by using Setup B in which SSPAC was either not dosed, was dosed continuously, or was dosed in pulses directly into the lines to the ceramic membrane. The flux was doubled, and the backwash was repeated more frequently (every 0.63 h) compared with Setup A. The goal of this configuration was to compare pulse and continuous dosing under conditions that were more likely to cause membrane fouling. As shown in Panel B of Fig. 4-8, the increases of the TMP were lower with pulse and continuous dosing of SSPAC than without SSPAC dosing, but the difference of the TMP rise between the two dosing methods was again small. The superiority of pulse over continuous dosing of SSPAC in attenuating the TMP rise was marginal. The small difference between the two dosing was also observed in the filtration operation with a lower backwash pressure of 50 kPa, which was the same as the backwash pressure applied in the submerged membrane system. TMP rose rapidly due to the low backwash pressure (Fig. 4-10), but the rate of TMP buildup was not very different between pulse and continuous SSPAC dosing. Even when the backwash pressure was the same, 50 kPa, the rate of TMP rise was slower in the monolithic membrane system than in the submerged membrane system (Fig. 4-5), but this difference was caused by the higher backwash frequency in the monolithic membrane system. When the backwash pressure was increased from 50 kPa to 500 kPa during the pulse dose run, the TMP rise was much slower (Fig. 4-10).

Furthermore, no significant differences in the TMP rise between the systems with pulse and continuous dosing of SSPAC were observed, even when the monolithic membrane system was operated under the same conditions as the submerged membranes (Table 4-2). Specifically, we ran the Setup B system at a similar filtration flux of 69.8 L m^{-2} h^{-1}, backwash frequency 7 h, pressure of 50 kPa, coagulant dosage 2 mg-Al/L, and SSPAC dosage of 5 mg/L. The changes of TMP were almost the same for pulse and continuous dosing of SSPAC (Fig. 4-11).

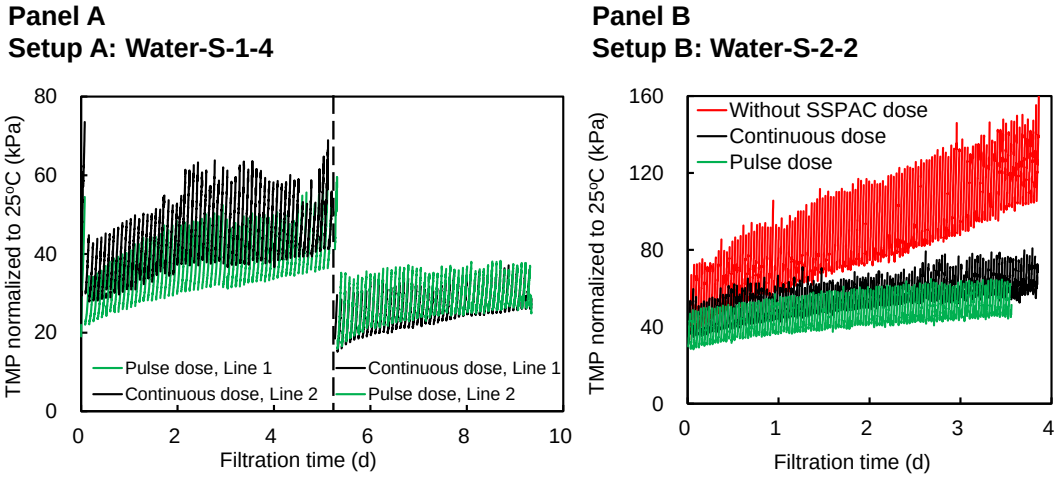

Fig. 4-8. TMP as a function of filtration time. Filtration was conducted in a monolithic ceramic membrane system after SSPAC adsorption and coagulation pretreatment. SSPAC was dosed continuously or in pulses. The filtration flux and backwash interval were 208 L m^{-2} h^{-1} and 2 h for Panel A and 438 L m^{-2} h^{-1} and 0.63 h for Panel B. Water S-1-4 (Panel A) and Water-S-2-2 (Panel B) were used. For Panel A experiment, coagulant and SSPAC dosages were controlled at 1 mg-Al/L and 2 mg/L during operation days 0-5 and 0.5 mg-Al/L and 1 mg/L during operation days 5-9, respectively. For the Panel B experiment, coagulant and SSPAC dosages were controlled at 1 mg-Al/L and 2 mg/L, respectively.

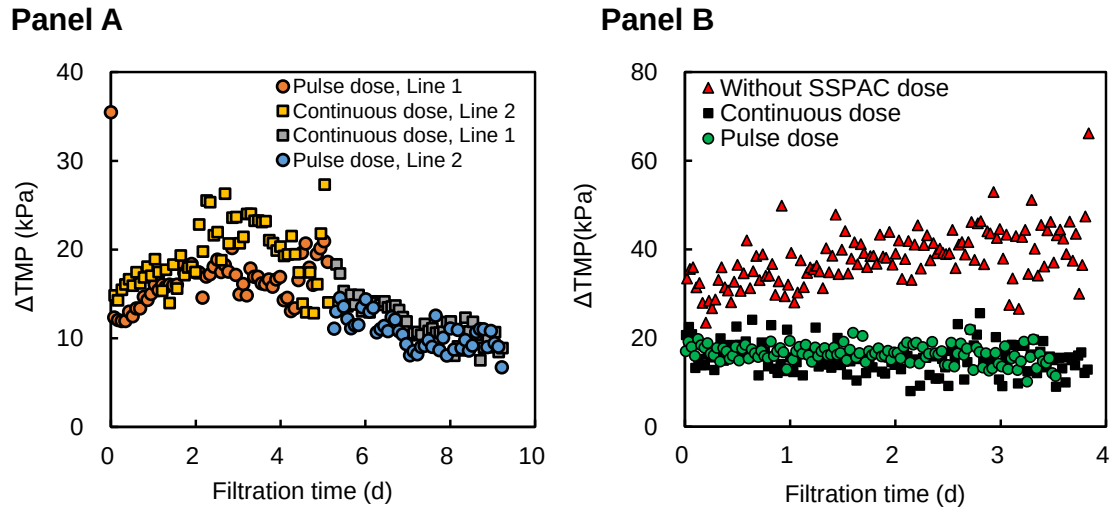

Fig. 4-9. ΔTMP (increase of TMP during one batch of filtration after backwash) as a function of filtration time. Filtration was conducted in a monolithic ceramic membrane system after SSPAC adsorption and coagulation pretreatment. SSPAC was dosed continuously or in pulses. The filtration flux and backwash interval were 208 L m^{-2} h^{-1} and 2 h for Panel A and 438 L m^{-2} h^{-1} and 0.63 h for Panel B. Water-S-1-4 (Panel A) and Water-S-2-2 (Panel B) were used. For panel A, coagulant and SSPAC dosages were controlled at 1 mg-Al/L and 2 mg/L during operation days 0–5, and 0.5 mg-Al/L and 1 mg/L during operation days 5–9, respectively. For panel B, coagulant and SSPAC dosages were controlled at 1 mg-Al/L and 2 mg/L.

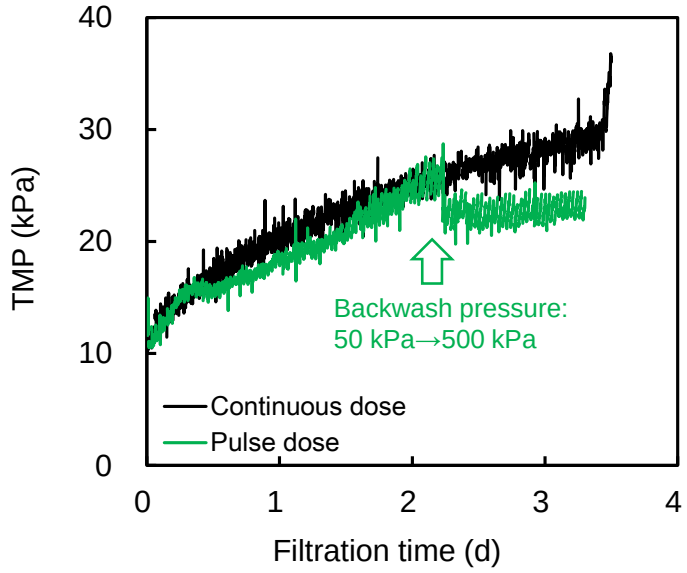

Fig. 4-10. TMP as a function of filtration time. SSPAC adsorption and coagulation pretreatment, filtration was conducted in the monolithic ceramic membrane system of Setup B. SSPAC was dosed continuously or in pulses. Backwash interval was 0.63 h. Filtration flux was 139 L m^{-2} h^{-1}. Water-S-3-2 was used in this experiment. Backwash pressure of the pulse dosing run was changed from 50 to 500 kPa at 2.2 days, whereas that of the continuous dosing run was kept at 50 MPa.

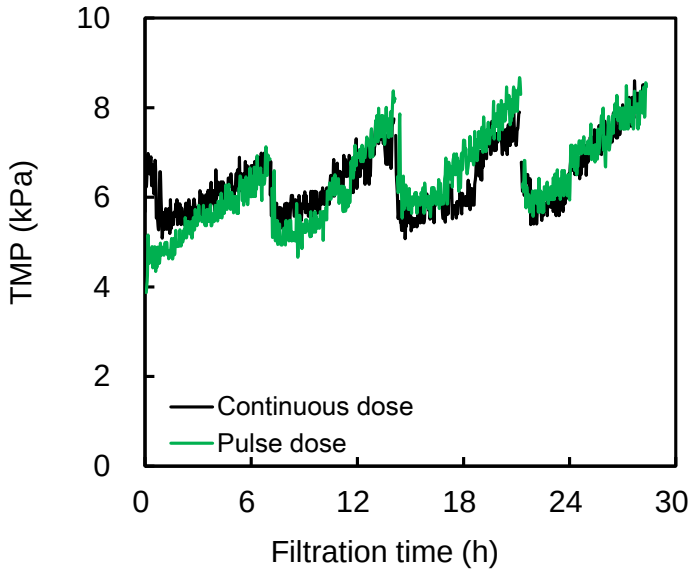

Fig. 4-11. TMP as a function of filtration time when filtration was conducted after SSPAC adsorption and coagulation pretreatment in a monolithic ceramic membrane system. The experiments were conducted by pulse dosing of SSPAC using Setup B (Fig. 4-5) but with 22-channel membranes. Backwash interval was 7 h, and the pressure was controlled at 50 kPa. Filtration flux was 69.8 L m^{-2} h^{-1}. Water-S-3-2 was used.

4.3.3. Filtrate qualities between pulse and continuous dosing of SSPAC in submerged and monolithic ceramic membrane systems

Feed water and filtrate were sampled in the membrane filtration experiments, and the DOC and UV260 were assessed to evaluate water quality. For the submerged ceramic membrane filtration system, continuous dosing of SSPAC achieved DOC removals of 10–20% and UV260 removal of 30–40%, whereas pulse dosing of SSPAC achieved 40–50% removal of DOC and 60–70% removal of UV260 (Fig. 4-12). The difference in the removal percentages of these two dosing methods was observed for all three feed waters tested. Pulse dosing of SSPAC removed HS more than continuous dosing of SSPAC. The superiority of pulse dosing was not observed for biopolymers because biopolymers were almost completely removed by both pulse and continuous dosing of SSPAC.

In the case of the monolithic ceramic membrane system, continuous dosing of SSPAC resulted in slightly higher removals of DOC and HS from Water-S-2-2 but not from Water S-1-4 (Fig. 4-13). Removal rates of DOC and E260 were overall 40–50%, no matter what dosing methods were used. The removal of biopolymer slightly exceeded 60%. Except for the concentrations of DOC and HS in Water-S-2-2, pulse and continuous dosing of SSPAC did not appear to result in significant differences in the qualities of filtrates based on DOC (including biopolymers and HS) and UV260.

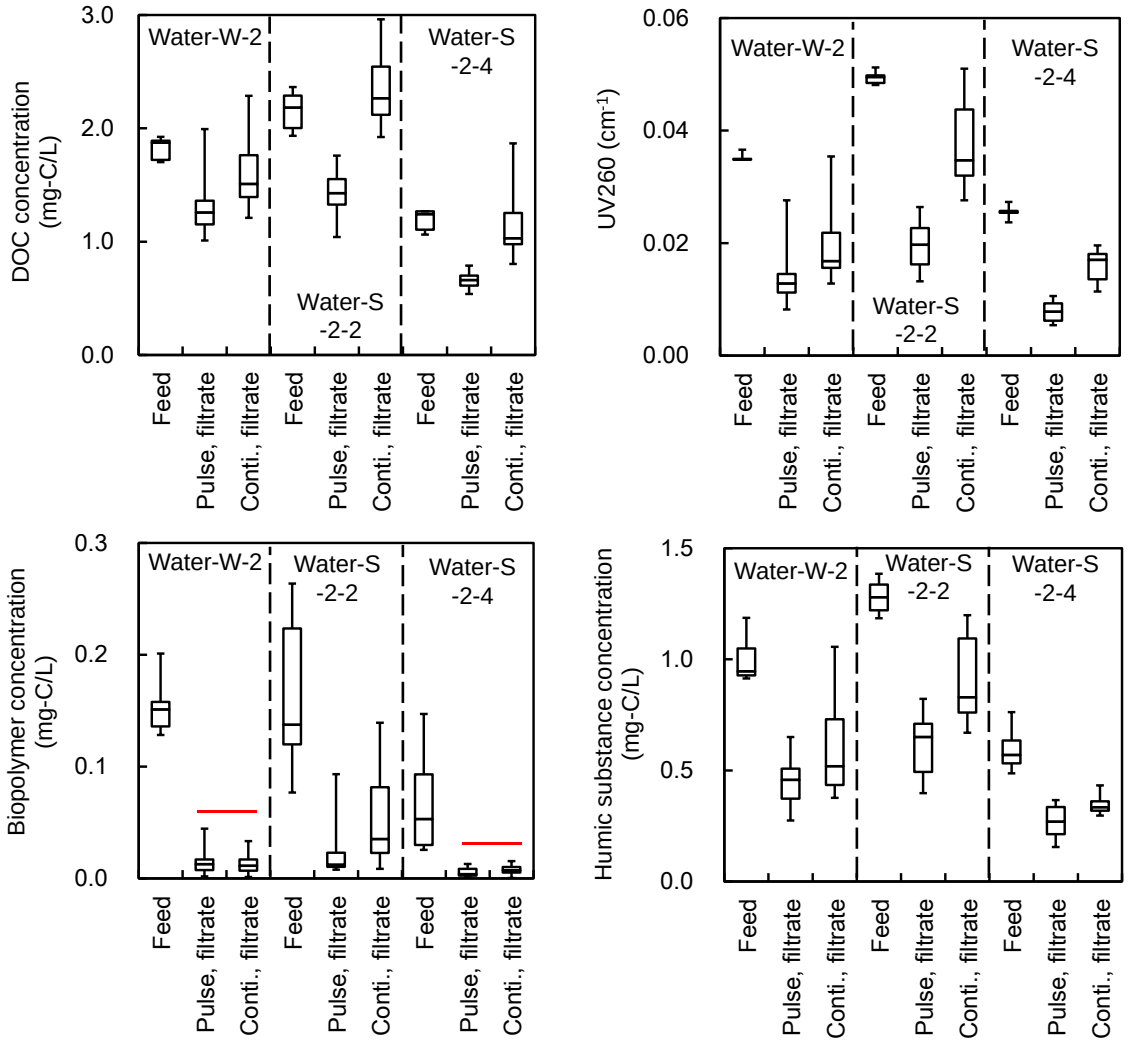

Fig. 4-12. Box and whisker plots of DOC, UV260, biopolymers and HS in feed water and filtrates after pulse and continuous dosing of SSPAC in the case of a submerged membrane (designated as Feed, Pulse and Conti., respectively). Horizontal lines within boxes represent median values, the upper and lower lines of the boxes represent the 75th and 25th percentiles, respectively, and the upper and lower bars outside the boxes indicate the maximum and minimum values, respectively. The red bars over boxes indicate no significant differences ($p > 0.05$) based on a Student's *t*-test.

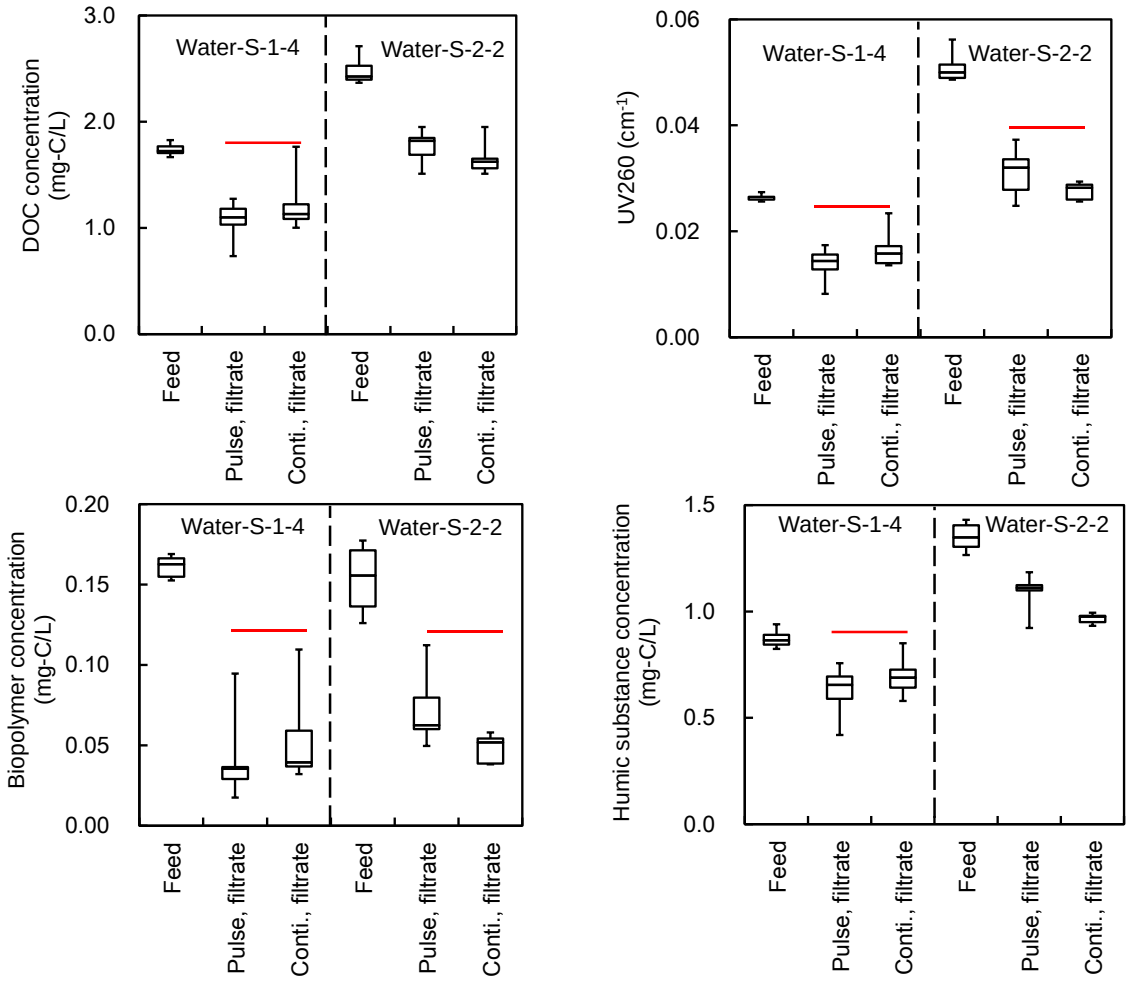

Fig. 4-13. Box-and-whisker plots of concentrations of DOC, UV260, biopolymers and HS in feed water and filtrates after pulse and continuous dosing of SSPAC in the case of monolithic membrane filters (designated as Feed, Pulse and Conti., respectively). Horizontal lines within boxes represent median values, the upper and lower lines of the boxes represent the 75th and 25th percentiles, respectively. The upper and lower bars outside the boxes indicate the maximum and minimum values, respectively. Red bars over boxes indicate no significant differences ($p > 0.05$) based on a Student's *t*-test.

4.3.4. Surface observations of submerged and monolithic ceramic membranes

The surfaces of submerged membranes were observed by taking photographs (Panels A-D in Fig. 4-14 and Fig. 4-15. The surface of the membrane was initially white, but after 30 min, which was the hydraulic retention time of the submerged membrane tank, part of the membrane surface remained white, but most of it had turned black. The black area was larger in the pulse dosing than in the continuous dosing of SSPAC. After a 7-h filtration, the membrane surface appeared to be covered with a layer of suspended solids, including SSPAC. After backwashing, the surface of the membrane was white with

many black spots in the case of pulse dosing. In the case of continuous dosing, the black layer remained and covered most of the membrane.

The surfaces of a monolithic membrane were observed with a fiber microscope, which was inserted into the membrane channels. The photographs (Observation 1) were first taken in the middle part of a channel of a blank membrane, a membrane after a 5-min filtration, a membrane after a 0.63-h filtration, and a membrane immediately after backwashing (Panels A–D in Fig. 4-16, respectively). The inside of the membrane channel (middle part of channel no. 1 in Fig. 4-17) became black 5 min after a pulse dose of SSPAC, but it did not after a continuous dose of SSPAC. After filtration for 0.63 h, which took place immediately before backwashing, the channels of the membrane had become black for both systems with a pulse and a continuous dose of SSPAC. Their color returned to white after backwashing, but a few black particles were observed for the system with a continuous dose but not the system with a pulse dose.

To further understand the accumulation of SSPAC in channels after a pulse dose of SSPAC, we observed all the channels of a membrane element after a 5-min filtration run. The SSPAC dosage was increased from 2 mg/L to 5 mg/L to observe the accumulation of SSPAC more clearly, and the experiments were conducted six times. In Fig. 4-18 (Observation 2), we observed that the no. 1 channel, which was in the middle of the membrane, was blacker than the other channels. The indication was that the distribution of SSPAC was uneven between channels. In Observation 3 (Fig. 4-19), which involved the same membrane element as Observation 2, the black area seemed to have become more even than in Observation 2, but a non-uniformity of the black area between channels was still observed at the inlet (lower part) of channels 2, 4, 5, and 6. Such non-uniformity was also apparent in some channels during Observation 2 (Fig. 4-18). The uneven distribution of SSPAC particles between channels and the non-uniformity of the black area in a channel were also observed in Observations 4 and 5 (Figs. 4-20, 4-21), where the membrane elements differed from those used in Observations 2 and 3.

Based on the above results, observation experiments to compare a pulse and a continuous dose were conducted again, but floc particles that had grown large were present in the slow mixing tank

(Observations 6 and 7). As shown in Fig. 4-22 and Fig. 4-23, black particles were found mostly in the lower part of the channels and were distributed unevenly. They were seldom observed in the middle and upper parts of channels.

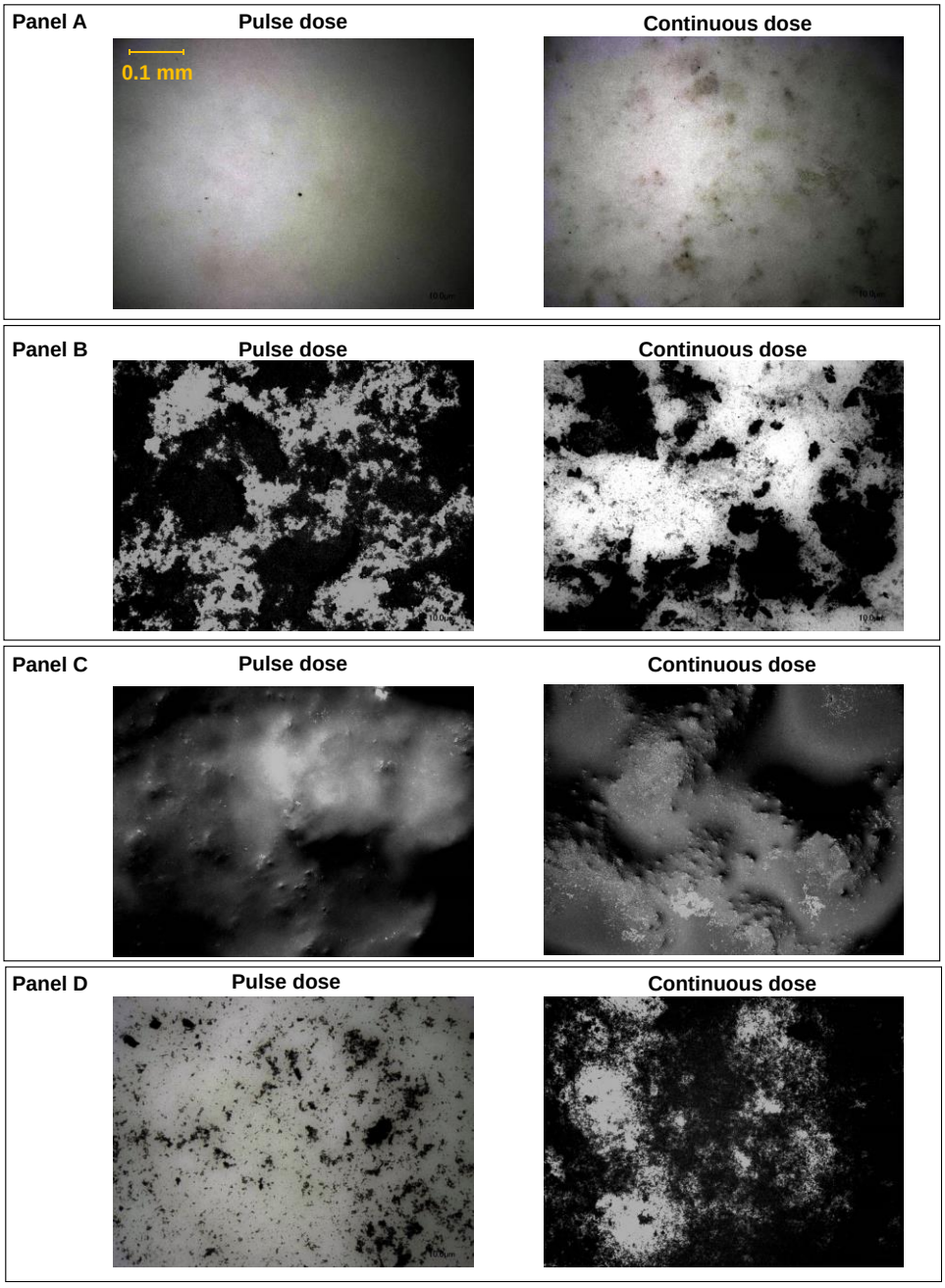

Fig. 4-14. Photographs of the surface of the submerged ceramic membrane (500-fold magnification). Panel A shows pictures of membranes before filtration. Panel B shows pictures of membranes after a 30-min filtration. Panel C shows pictures of membranes after a 7-h filtration, which took place immediately before the backwash. Panel D shows pictures of membranes immediately after backwashing. SSPAC was dosed in a pulse or dosed in a continuous. The backwash was conducted at 50 kPa for 30 s. The filtration flux was 80.4 L m^{-2} h^{-1}. Water-S-2-4 was used in this experiment.

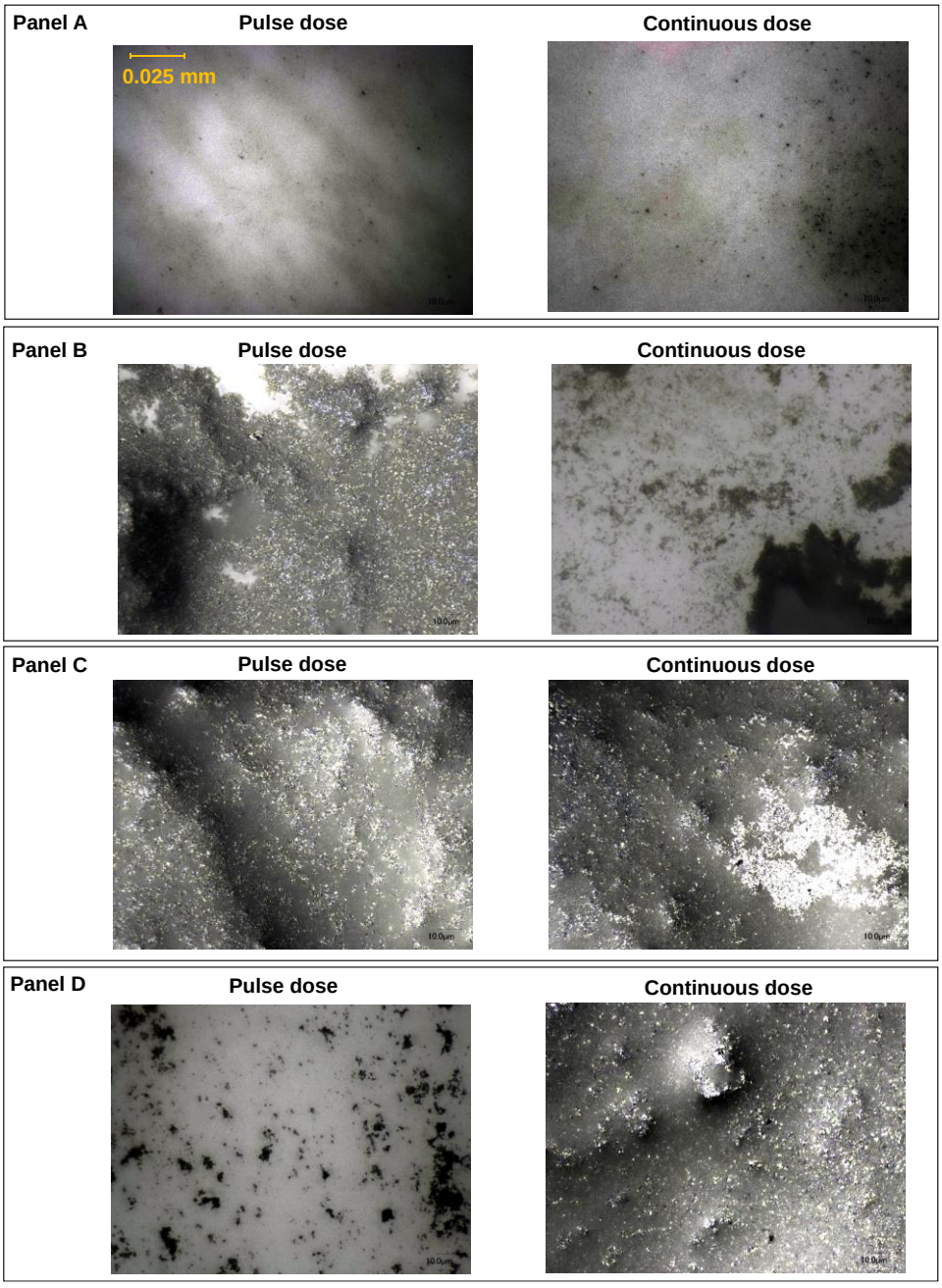

Fig. 4-15. Photomicrographs of the surface of submerged-tubular ceramic membrane (magnification by 2000×). Panel A shows pictures of membranes before filtration. Panel B shows pictures of membranes after a 30-min filtration. Panel C shows pictures of membranes after a 7-h filtration, which was right before hydraulic backwashing. Panel D shows the membranes right after hydraulic backwashing. SSPAC was dosed in a pulse or dosed in a continuous. Hydraulic backwash was conducted at 50 kPa for 30 s. The filtration flux was 80.4 L m^{-2} h^{-1}. Water-S-2-4 was used in this experiment.

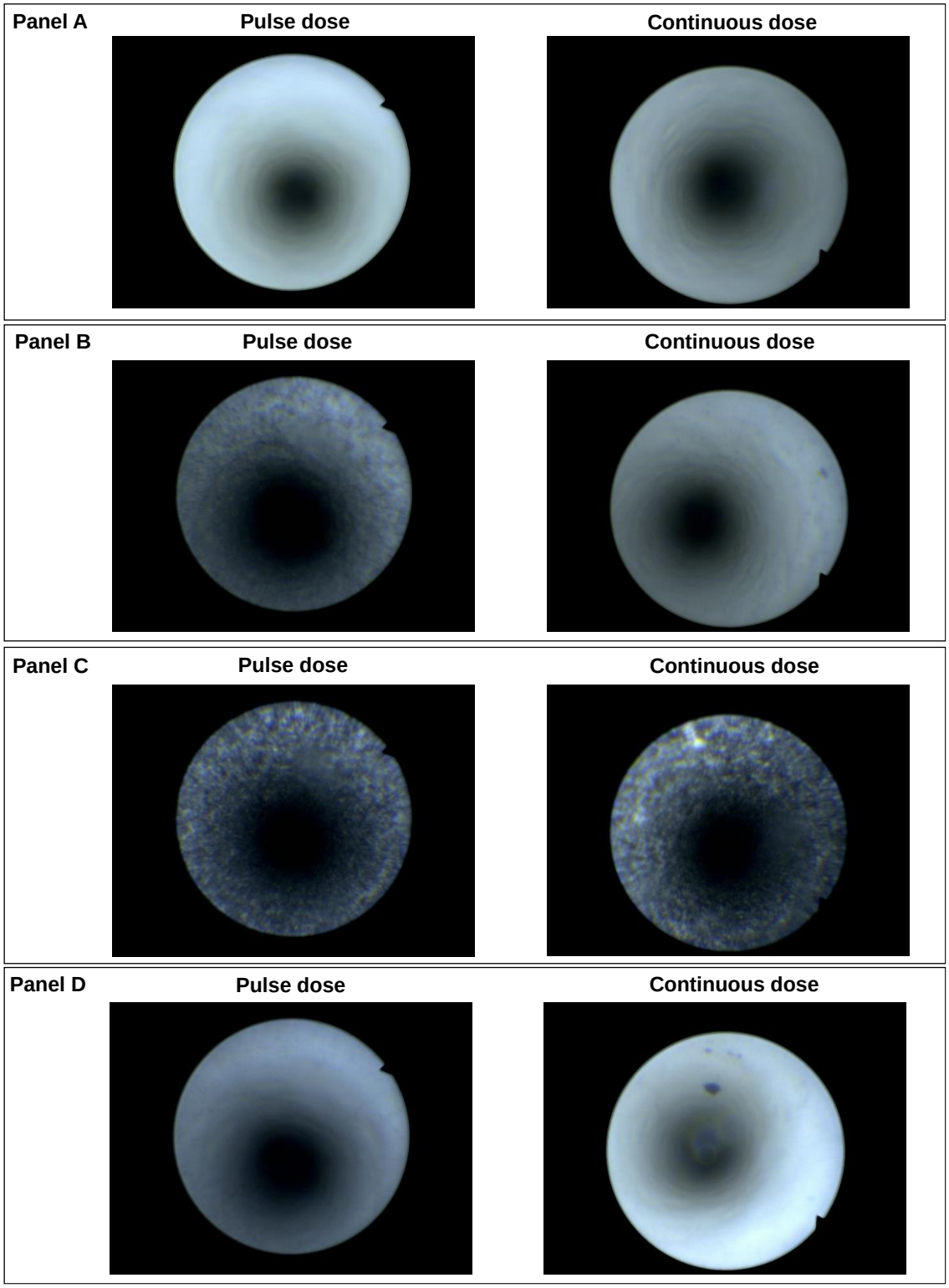

Fig. 4-16. Photographs (Observation 1) of the inside of channels in a monolithic ceramic membrane taken under a fiber microscope. Panel A shows the membranes before filtration. Panel B shows the membranes after a 5-min filtration. Panel C shows the membranes after a 0.63-h filtration, which was right before hydraulic backwashing. Panel D shows the membranes right after hydraulic backwashing. The middle part of channel no. 1 of the membrane element (see Fig. 4-17) in Setup B was observed. SSPAC was dosed in a pulse or dosed in a continuous. Hydraulic backwashing was conducted at 500 kPa for 10 s. Filtration flux was 438 L m^{-2} h^{-1}. Water-S-2-2 was used.

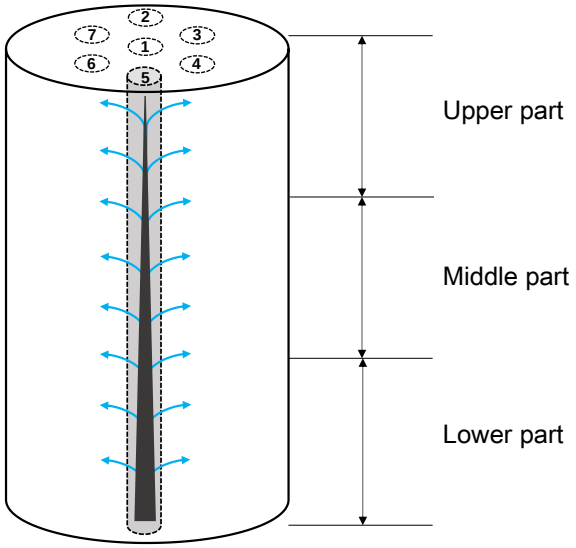

Fig. 4-17. Schematic of monolithic membrane indicating filtration direction and channels. The numbers indicate channel locations. Blue arrows indicate the direction of water flow in a membrane element.

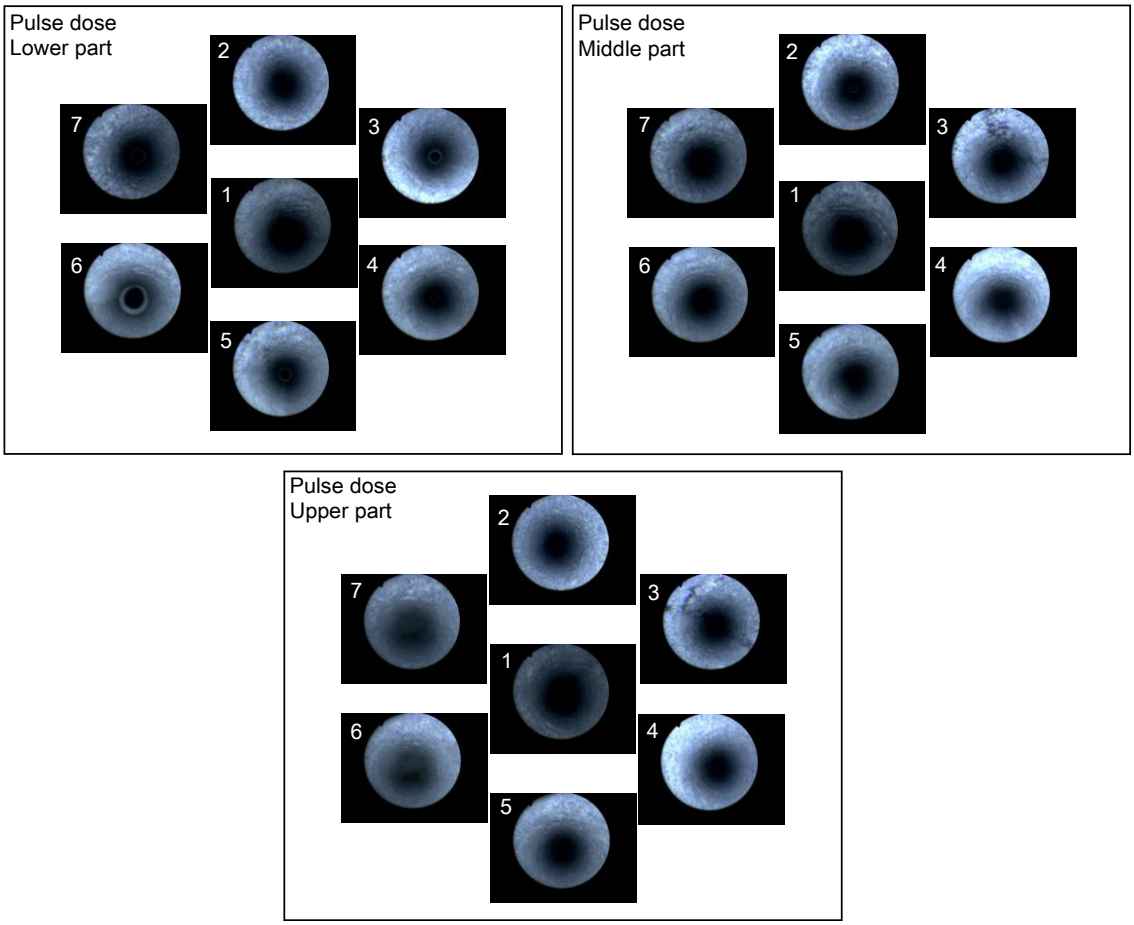

Fig. 4-18. Photographs of the inside of channels in a monolithic ceramic membrane (Observation-2). The membrane (Membrane-1) was removed at a filtration time of 5 min after a pulse dose of SSPAC. The locations of the channel areas (lower part, middle part and upper part) and numbers that identify the channel locations are presented in Fig. 4-17. The filtration flux was 438 L m^{-2} h^{-1}. Water-S-3-2 was used.

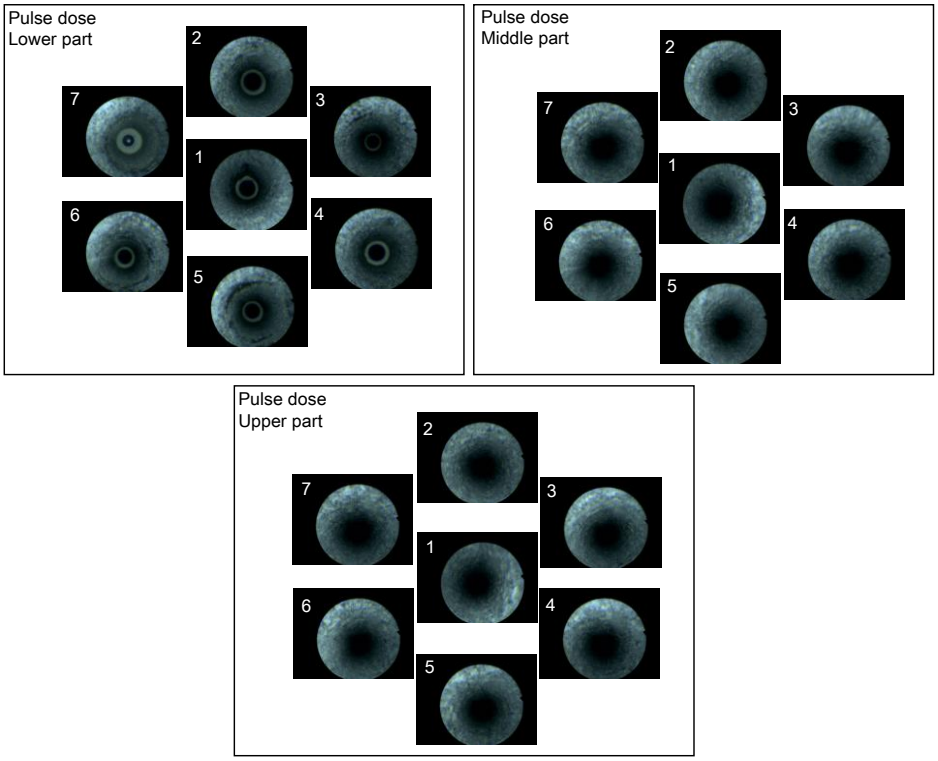

Fig. 4-19. Photographs of the insides of channels in a monolithic ceramic membrane. Observation-3 corresponds to the membrane's (Membrane-1) being taken out after a filtration of 5 min after a pulse dose of SSPAC. The locations are shown in Fig. 4-17. Filtration flux was 438 L m^{-2} h^{-1}. Water-S-3-2 was used.

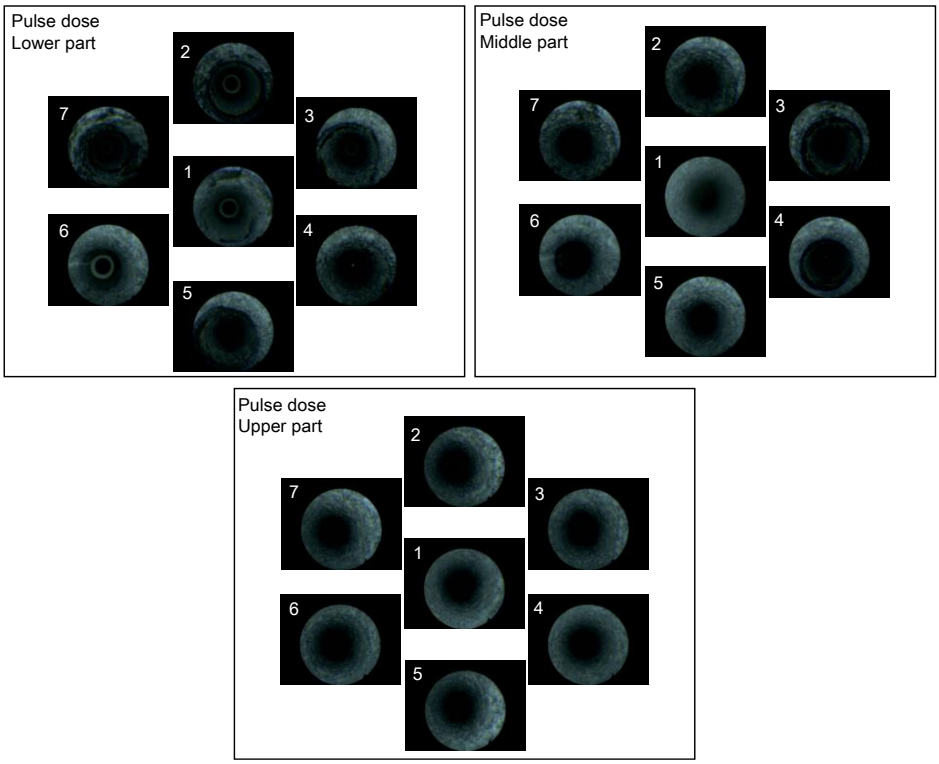

Fig. 4-20. Photographs of the insides of channels in a monolithic ceramic membrane. Observation-4 corresponds to the membrane's (Membrane-2) being taken out after a filtration of 5 min after a pulse dose of SSPAC. The locations are presented in Fig. 4-17. Filtration flux was 438 L m^{-2} h^{-1}). Water-S-3-2 was used.

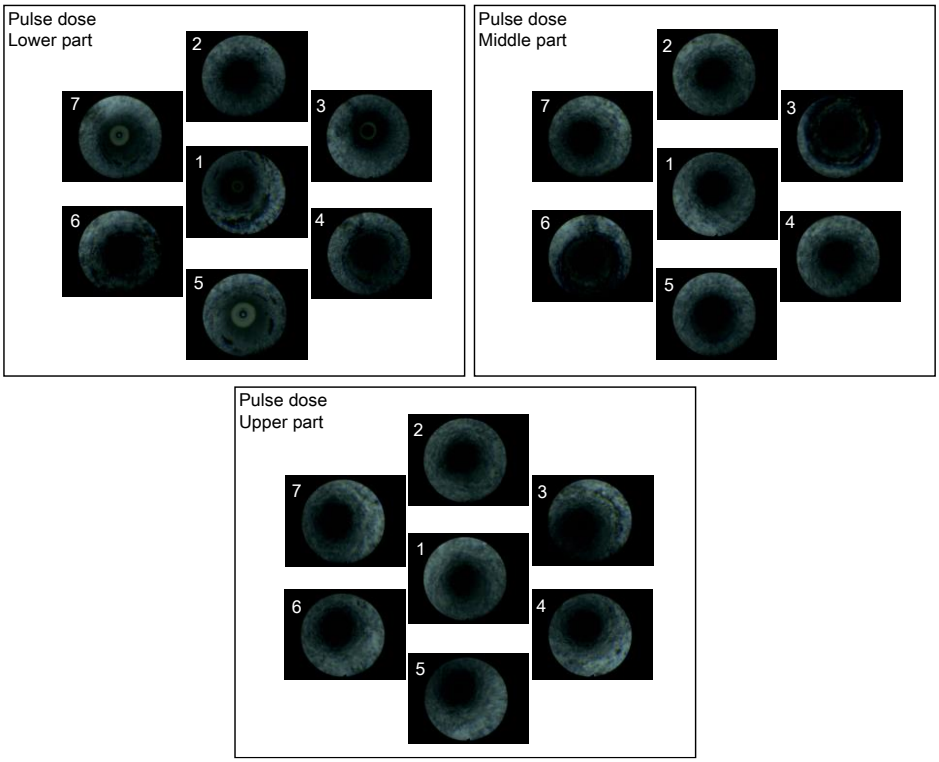

Fig. 4-21. Photographs of the insides of channels in a monolithic ceramic membrane. Observation-5 corresponds to the membrane's (Membrane-3) being taken out after a filtration of 5 min after a pulse dose of SSPAC. The locations are shown in Fig. 4-17. Filtration flux was 438 L m^{-2} h^{-1}. Water-S-3-2 was used.

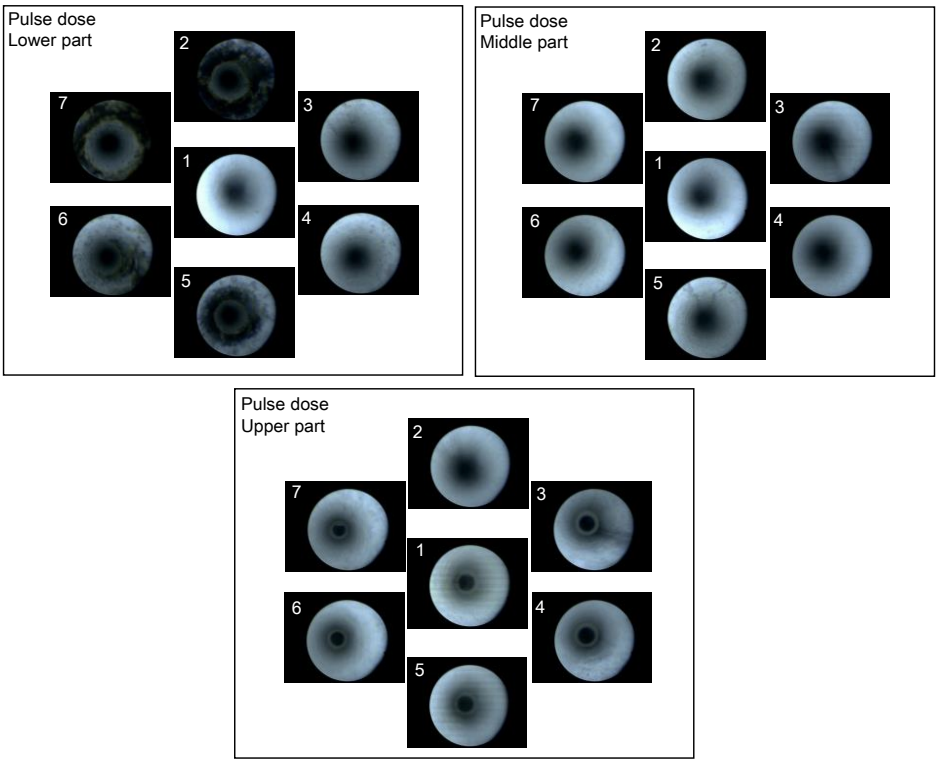

Fig. 4-22. Photographs of the insides of channels in a monolithic ceramic membrane (Observation-6). The membrane (Membrane-4) was taken out after a 5-min filtration after a pulse dose of SSPAC. The locations are shown in Fig. 4-17. Filtration flux was 438 L m^{-2} h^{-1}. Water-S-3-2 was used.

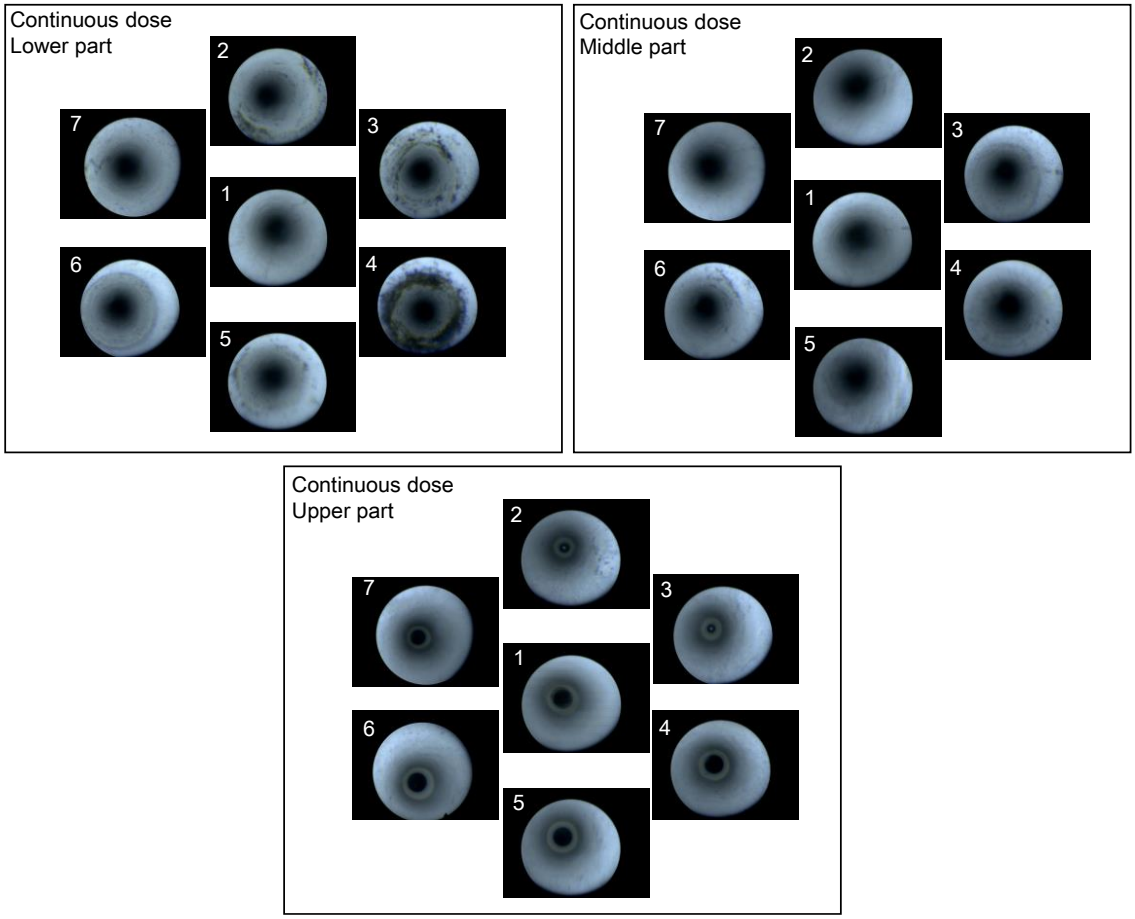

Fig. 4-23. Photographs of the insides of channels in a monolithic ceramic membrane taken under a fiber microscope. Observation-7 corresponds to the membrane's (Membrane-5) being taken out after a filtration time of 5 min in the experiments with a continuous dose of SSPAC. The locations of the channel areas (lower part, middle part and upper part) and numbers are presented in Fig. 4-17. Filtration flux was 438 L m^{-2} h^{-1}. Water-S-3-2 was used.

4.4. Discussion

4.4.1. Effectiveness of pulse dosing of SSPAC for mitigating hydraulically irreversible membrane fouling

In previous chapter, we have recently shown that pulse dosing of SSPAC to a submerged polymeric membrane filtration system can suppress the increase of TMP during filtration better than continuous dosing of SSPAC. However, this result was obtained with one type of polymeric membrane system: an outside-in, vacuum-driven, submerged type. In this chapter, the pulse dosing of SSPAC was shown to be effective for the ceramic inorganic membrane of an outside-in, vacuum-driven, submerged membrane, but it was not effective for an inside-out, pressure-driven, monolithic membrane. As described in Section 4.3.1, when SSPAC was dosed in pulses in the tank where the membrane had been submerged after the membrane was backwashed, the TMP did not increase Table 4S, SI).

We applied a model to quantify the change of TMP as a function of time (Kovalsky et al., 2008).

$$P_L = \alpha\mu c_s \frac{Q^2}{A^2} t + \mu R_c \frac{Q}{A} \qquad (1S)$$

where P_L is transmembrane pressure (Pa), α is specific cake resistance (m/kg, constant in the case of incompressible cake layer) and c_s is solid volume fraction of the suspension being filtrated (kg/m^3), Q is volumetric flow rate (m^3/s), A is filter cross-sectional area (m^2), t is time (s), μ is fluid viscosity (Pa·s) and R_c is cake resistance (m^{-1}).

For submerged tubular ceramic membrane, data from Panel B in Fig. 4-6 was used for calculating the slope and intercept. For monolithic ceramic membrane, data from Panel B in Fig. 4-8 was used and the calculated parameter is shown in Table 4-3. Pulse dosing of SSPAC achieves much smaller slope and intercept than continuous dosing of SSPAC in the case of tubular ceramic membrane, indicating a smaller cake resistance. On the other hand, pulse dosing of SSPAC achieves a similar slope and relatively smaller intercept than continuous dosing of SSPAC in the case of monolithic membrane, indicating that at the point of t=0, the initial TMP of pulse dosing of SSPAC is slightly smaller while no significant differences during the filtration than continuous dosing of SSPAC, which can be explained as the pulse dosing of SSPAC provides sufficient SSPAC for foulants removal.

Table 4-3

Parameter values of the model fitted to equation (1S). The data from Panel B in Fig. 4-5 was used for submerged tubular ceramic membrane, while the data from Panel B in Fig. 4-6 was used for monolithic ceramic membrane.

	Tubular membrane		Monolithic membrane	
	αc_s	R_c	αc_s	R_c
	10^6 m^{-2}	10^6 m^{-1}	10^6 m^{-2}	10^6 m^{-1}
Continuous dosing of SSPAC	0.89±0.20	1.42±0.68	0.54±0.11	0.39±0.06
Pulse dosing of SSPAC	0.34±0.19	0.68±0.25	0.58±0.04	0.31±0.04

The attenuation of TMP buildup by the pulse-dosed SSPAC can be explained by 1) higher adsorption capacity of SSPAC than SPAC and PAC on NOM especially for biopolymers (Zhao et al., 2020), which is regarded as the dominant contributor to irreversible fouling (Ayache et al., 2013; Huang et al., 2017; Kimura et al., 2014; Tian et al., 2013); and 2) formation of a precoat SSPAC layer on the membrane surface in the initial stage of every batch filtration by a pulse dose of SSPAC. In this chapter, we conducted the adsorption isotherm experiments by using PAC, SPAC, and SSPAC. As shown in Fig. 4-24, SSPAC adsorbed foulants (especially biopolymers) better than PAC and SPAC at low dosages. The precoat SSPAC effectively removes NOM, in particular biopolymer, by straining as well as by adsorption. In our previous study (Zhao et al., 2020), the straining effect of the SSPAC precoat layer is investigated by using an analytical MCE (mixed cellulose esters) flat-sheet membrane. In the present study, we conducted a batch experiment by using precoat layer of non-adsorbent, submicron polystyrene latex (PSL) particles (particle diameter; 200 nm) on top of a flat sheet ceramic membrane (Table 4-4). The results shown in Fig. 4-25 indicate that the precoat layer composed of submicron particles strains a portion of biopolymers out. On the surface of the ceramic membrane submerged in water, the formation of the precoat layer was observed (Section 4.3.4). Therefore, mechanism 2) as well as mechanism 1) are applicable to the submerged ceramic membrane with vacuum-driven, outside-in filtration. Better removal by pulse dosing of SSPAC than continuous dosing of SSPAC was observed for HS. We had expected higher biopolymer removal by pulse dosing of SSPAC. In fact, the rate of biopolymer removal by pulse dosed SSPAC was high, as described in Section 4.3.3. However, the biopolymer removal by

continuously dosed SSPAC was also high probably due to high dose of SSPAC and/or coagulant, so the difference in biopolymer removal between the two dosing methods was unclear. The high removal of NOM in conjunction with the membrane surface observations (Section 4.3.4) suggests that pulse dosing of SSPAC can form a better precoat layer than continuous dosing of SSPAC and the precoat layer of SSPAC removed HS as well as biopolymers and resulted in the high mitigation of membrane fouling.

In contrast, it is likely that SSPAC itself causes membrane fouling because activated carbon tends to adhere firmly to the surface of ceramic membranes (Zhao et al., 2005). Moreover, the particle size of SSPAC (D10, 0.11 μm; D50, 0.2 μm) is close to the pore size of ceramic membranes (nominal size of 0.1 μm). Therefore, it is very likely that SSPAC itself is a strong membrane foulant. However, as described in Section 4.3.4, the SSPAC on the surface of the membrane was cleared after a backwash because of coagulation pretreatment. This is in accordance with the fact that ceramic membrane filtration is often operated with coagulation pretreatment (Alansari et al., 2015; Lee and Kim, 2015; Zhu et al., 2012). Fouling of ceramic membranes by particulate matter is likely to occur without coagulation pretreatment. Moreover, the SSPAC was cleared at a lesser extent when the SSPAC was dosed in a continuous than when the SSPAC was dosed in a pulse. This difference is related to the difference in the TMP increase between pulse and continuous dosing.

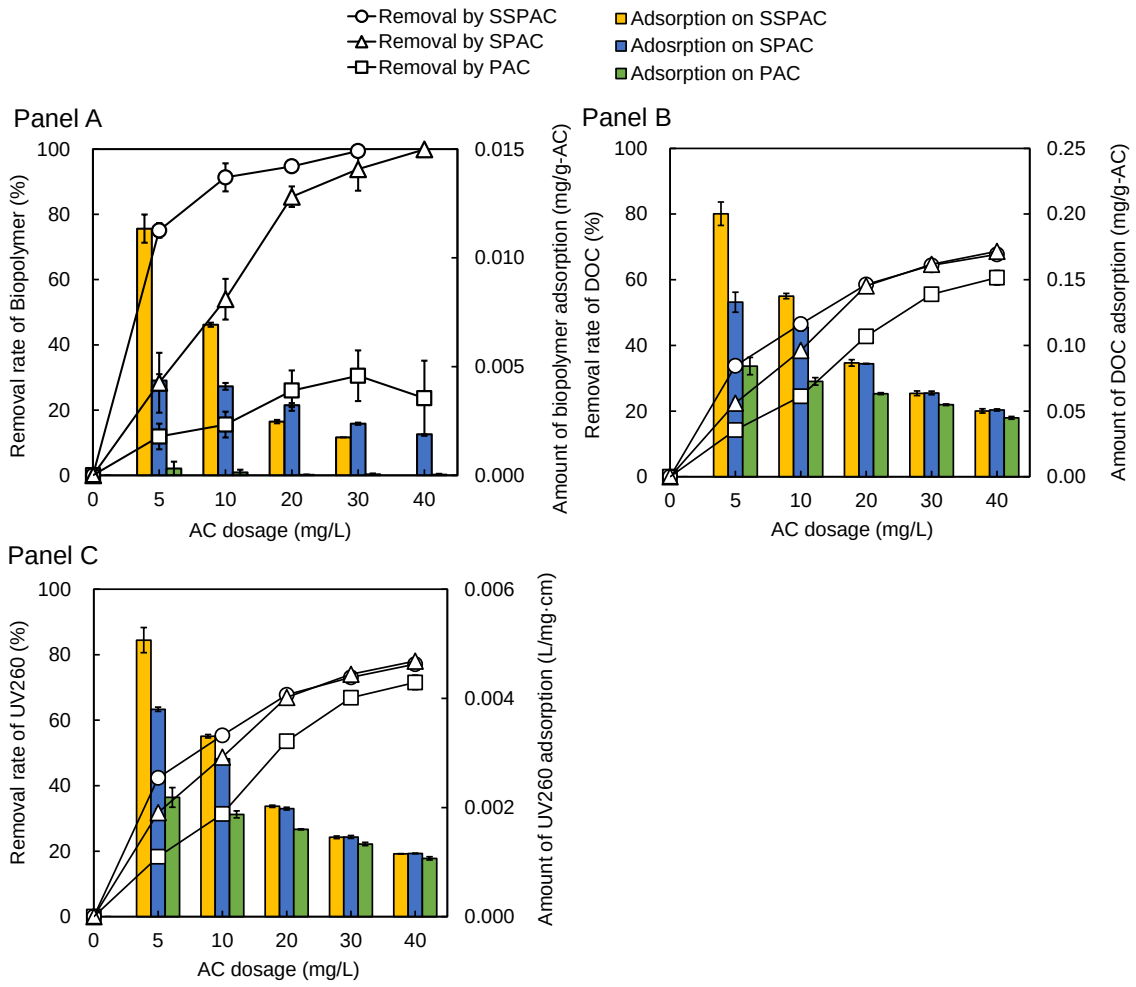

Fig. 4-24. Removal rate and adsorption amount of Biopolymer (Panel A), DOC (Panel B) and UV260 (Panel C) as a function of AC dosage. Adsorption isotherm experiment was conducted at room temperature (20°C) for one week. Data from Section 2.3.1 were used.

Table 4-4
Specifications of the tubular ceramic membrane and the monolithic ceramic membrane from the catalogs of the manufacturers.

Membrane type	Tubular	Monolithic	Flat sheet
Maker	Kubota Corp.	Metawater Co. Ltd.	Metawater Co. Ltd.
Material	Ceramics	Ceramics	Ceramics
Nominal pore size	0.1 μm	0.1 μm	0.1 μm
Filtration direction	Outside-in	Inside-out	Upstream-downstream
Filtration pressure	Negative pressure	Positive pressure	Positive pressure
Setting	Submerged in a tank	Housed in a casing	Housed in a casing

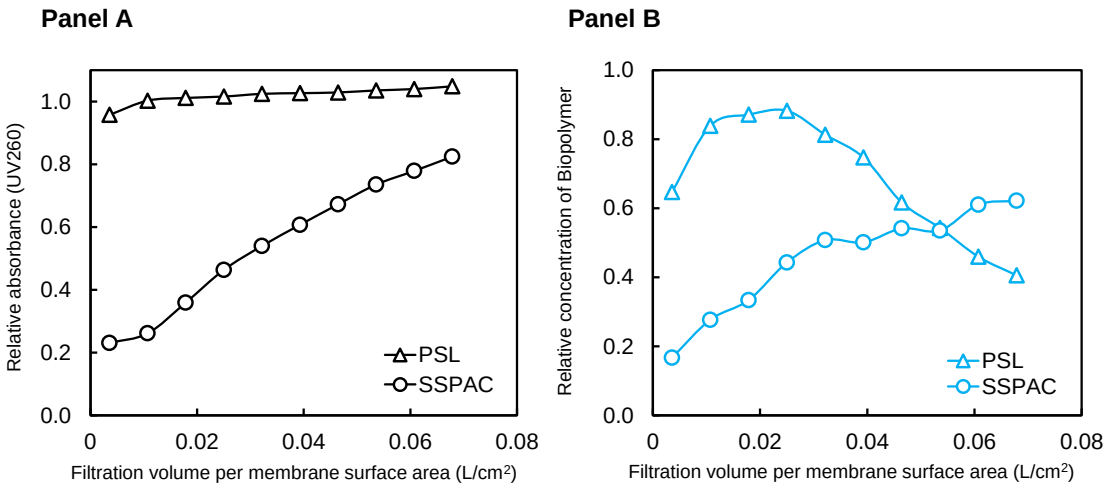

Fig. 4-25. Relative absorbance (UV260, Panel A) and relative concentration of biopolymer (Panel B) as a function of filtration volume per membrane surface area. Filtration experiments were conducted by a flat sheet ceramic membrane (Table 4-4) with positive pressure. Polystrene latex (PSL) with particle size of 200 nm and SSPAC were used as coating materials. Water-S-3-1 was used in this experiment.

4.4.2. Importance of precoat layer formation

In the inside-out monolithic ceramic membrane system, pulse dosing of SSPAC did not appear markedly superior to continuous dosing of SSPAC: the increases of the TMP were similar (Section 4.3.2). In the case of filtrate quality such as DOC, there was no consistent trend: neither pulse nor continuous dosing was consistently better, as described in Section 4.3.3. In other words, the effectiveness of the pulse dosing of SSPAC differed for the two ceramic membranes: the monolithic ceramic membrane and the submerged ceramic membrane. The nominal pore sizes of the two ceramic membranes are the same (Table 4-4), but the structure of the membranes is very different (inside-out monolithic vs. outside-in tubular).

Another major difference between the two ceramic membrane systems is the operating pressure. Monolithic ceramic membrane systems are usually operated at a high flux because the filtration was pressurized, and the pressure during backwashing is also high (Asif and Zhang, 2021; City of Yokohama, 2018). In contrast, submerged ceramic membranes are filtered by suction pressure, so the available TMP is smaller than in the case of monolithic ceramic membrane systems (Dong et al., 2014; Nagahoro Water Supply Authority, 2006). In most of the experiments, we applied a higher filtration flux with a higher

backwash pressure to the monolithic membrane than to the submerged membrane. This operation is in accordance with the practice of full-scale, drinking water treatment plants. However, when the backwash pressure in the submerged membrane was doubled and was applied from a pressure tank (as it was in the monolithic system), the superiority of the pulse dosing of SSPAC over the continuous dosing of SSPAC dose was maintained, as described in Section 4.3.1. In contrast, even when the filtration flux and backwash pressure in the monolithic membrane were decreased to the same levels as in the submerged membrane, the performances of the pulse dosing of SSPAC and the continuous dosing of SSPAC were still the same, as described in Section 4.3.2. The differences in the effectiveness of the pulse dosing of SSPAC on the two ceramic membranes were thus unrelated to the backwash pressure and its method of application.

In addition, the TMP was much lower in the monolithic membrane than in the submerged membrane, even when the backwash interval, filtration flux, and chemical dosages were the same in the two systems. The implication is that the coagulation-flocculation process in the mixing tanks of the monolithic membrane system achieved better performance than the static mixer in the submerged ceramic membrane system. Although it is recognized that further research is needed to determine the optimum mixing conditions for SSPAC pre-coating, this study was not able to go that far.

Coagulation plays an important role in preventing membrane fouling due to SSPAC particles themselves (Zhao et al., 2020). On the other hand, it is reported that synergetic fouling exists between PAC and organic foulants such as humic acid (Shao et al., 2016). Biopolymers are well removed by the precoating of SSPAC, but the TMP during the filtration becomes high without coagulation pretreatment (Heijman et al., 2009). Our previous study also revealed that when SSPAC is pulse-dosed to form precoating without coagulation pretreatment, the rise of TMP was canceled only partially by hydraulic backwash, indicating that SSPAC itself contributes to irreversible fouling (Zhao et al., 2020). However, when the coagulant was added before filtration, the effectiveness of the hydraulic backwash was remarkably enhanced. It can be explained such that the coagulant loosens the bonding between the membrane and SSPAC layer, and thus the irreversible fouling due to SSPAC is prevented (Zhao et al.,

2020). Further elucidation of the phenomenon requires experimental analysis, such as quantifying the organic foulants at different depths of the SSPAC layer. In order to conduct such a study, however, further challenges would be necessary for not only slice sampling but also the separation of activated carbon and organic foulant (Aschermann et al., 2019; Pelekani and Snoeyink, 1999).

The important difference between the two ceramic membranes was the formation of the precoat layer on the membrane surface. In the submerged membrane system, we observed that the membrane surface became black with SSPAC at a higher rate when SSPAC was applied in a pulse dose than a continuous dose (Section 4.3.4). This result indicates that the formation of a precoat layer of SSPAC is rapid in the case of pulse dosing compared to continuous dosing. Moreover, the SSPAC precoat layer was cleared by the backwash more efficiently. In contrast, in the monolithic membrane system, we observed the accumulation of SSPAC, but it was unevenly distributed. Some channels were loaded more with SSPAC than other channels (Section 4.3.4). Heijman et al., 2009 have mentioned the possibility of an uneven distribution of precoated SPAC, but they do not include any data relevant to this possibility. In this study, we observed an uneven distribution of pulse dosed SSPAC, which we had expected to form a uniform precoat. The non-uniform distribution was clearly apparent when large floc particles along with SSPAC were introduced into the membrane.

Moreover, the degree of non-uniformity of the distribution differed somewhat between the two filtration experiments (Observations 2 and 3 in Section 4.3.4), although the same membrane element was used. This difference suggests that the non-uniform coating was caused not only by the effects of non-uniform flow distribution at the inlet of an element and any differences in factors such as local permeability but also by stochastic factors. In a full-scale membrane element, there are 2000 channels in one membrane element, and the length of the membrane is much longer: it is 1.5 m. Therefore, it would be more difficult to suppress the non-uniformity of the distribution of the pulse dosed SSPAC and to precoat the membrane surface evenly with SSPAC in a full-scale plant than in a laboratory experimental setup like this study.

In the case of a submerged membranes system, when the scale of the system reaches full scale with

many tubes of membranes elements, it is also necessary to provide a method to uniformly precoat all the membrane tubes with pulse dosed SSPAC. The tank of a full-scale, submerged ceramic membrane filtration system is aerated with bubbles to reduce membrane fouling, but this aeration of the tank may also be effective in forming a uniform precoating. We cut tubular ceramic membranes 0.8 m in length to make small membrane elements for the experiment in this study, but we observed that the pure water permeabilities of the small membrane elements differed (Fig. 4-3). These differences indicated that the permeabilities of the membrane elements varied locally from place to place along the tube length. The filtration rate, namely the precoating rate, was therefore affected not only by local variation in hydraulic conditions but also by local variations of membrane permeability. This study enabled us to consider the possibility that there were local differences in the permeation rate of the membrane, and those differences may have affected the success or failure of the precoating method. This possibility is important to consider when apply pulse dosing of SSPAC to a full-scale membrane filtration system.

4.5. Chapter conclusions

Pulse and continuous dosing of SSPAC, which can efficiently remove NOM because of its high adsorption capacity, were applied as pretreatments for two different types of ceramic membrane filters (an outside-in vacuum-driven submerged membrane and an inside-out pressure-driven monolithic membrane) to try to attenuate increases of TMP due to the irreversible membrane fouling during filtration with periodic hydraulic backwashing. Major findings of the study were as follows:

1) Pulse dosing of SSPAC prevented TMP rise more than continuous dosing of SSPAC in the submerged membrane filtration system with a ceramic membrane. A precoating layer composed of SSPAC formed evenly on the ceramic membrane surface and was peeled off cleanly by hydraulic backwashing in the case of the pulse dosing of SSPAC. High removal of NOM (including biopolymer and HS) and a uniform layer of SSPAC, which prevented attachment of NOM to the membrane surface at the beginning of filtration, was thought to be the cause.
2) In monolithic ceramic membrane systems, pulse dosing of SSPAC did not alleviate TMP rise better than continuous dosing of SSPAC and did not remove NOM better. The uneven distribution of pulse dosed SSPAC in the membrane channels was thought to be a cause of the lack of any difference between the efficacy of the pulse dosing of SSPAC over the continuous dosing. The higher backwash pressure in the monolithic ceramic membrane system versus the submerged membrane filtration was not the cause of the absence of a treatment effect.

4.6. References

Alansari, A., Selbes, M., Karanfil, T., Amburgey, J., 2015. Optimization of coagulation pretreatment conditions in a ceramic membrane system. Journal – American Water Works Association 107, E693–E701.

Ando, N., Matsui, Y., Kurotobi, R., Nakano, Y., Matsushita, T., Ohno, K., 2010. Comparison of natural organic matter adsorption capacities of super-powdered activated carbon and powdered activated Carbon. Water Research 44, 4127–4136.

Aschermann, G., Neubert, L., Zietzschmann, F., Jekel, M., 2019. Impact of different DOM size fractions on the desorption of organic micropollutants from activated carbon. Water Research 161, 161–170.

Asif, M.B., Zhang, Z., 2021. Ceramic membrane technology for water and wastewater treatment: A critical review of performance, full-scale applications, membrane fouling and prospects. Chemical Engineering Journal 418, 129481.

Ayache, C., Pidou, M., Croué, J.P., Labanowski, J., Poussade, Y., Tazi-Pain, A., Keller, J., Gernjak, W., 2013. Impact of effluent organic matter on low-pressure membrane fouling in tertiary treatment. Water Research 47, 2633–2642.

Chen, F., Peldszus, S., Peiris, R.H., Ruhl, A.S., Mehrez, R., Jekel, M., Legge, R.L., Huck, P.M., 2014. Pilot-scale investigation of drinking water ultrafiltration membrane fouling rates using advanced data analysis techniques. Water Research 48, 508–518.

City of Yokohama, 2018. Kawai Purification Plant, Kanagawa, Japan. https://www.city.yokohama.lg.jp/kurashi/sumai-kurashi/suido-gesui/suido/suishitsu/josuijo/kawai/gaiyou.html (accessed 2.1.22).

Dong, S., Kim, E.S., Alpatova, A., Noguchi, H., Liu, Y., Gamal El-Din, M., 2014. Treatment of oil sands process-affected water by submerged ceramic membrane microfiltration system. Separation and Purification Technology 138, 198–209.

Ellerie, J.R., Apul, O.G., Karanfil, T., Ladner, D.A., 2013. Comparing graphene, carbon nanotubes, and superfine powdered activated carbon as adsorptive coating materials for microfiltration membranes. Journal of Hazardous Materials 261, 91–98.

Heijman, S.G.J., Hamad, J.Z., Schippers, J., Amy, G., Kennedy, M.D., 2009. Submicron powdered activated carbon used as a pre-coat in ceramic micro-filtration. Desalination and Water Treatment 9, 86–91.

Huang, B.C., Guan, Y.F., Chen, W., Yu, H.Q., 2017. Membrane fouling characteristics and mitigation in a coagulation-assisted microfiltration process for municipal wastewater pretreatment. Water Research 123, 216–223.

Huber, S.A., Balz, A., Abert, M., Pronk, W., 2011. Characterisation of aquatic humic and non-humic matter with size-exclusion chromatography - organic carbon detection - organic nitrogen detection (LC-OCD-OND). Water Research 45, 879–885.

Kanaya, S., Kawase, Y., Mima, S., Sugiura, K., Murase, K., Yonekawa, H., 2015. Drinking water treatment using superfine PAC (SPAC): Design and successful operation history in full-scale plant. American Water Works Association Salt Lake City, Utah, USA, pp. 624–631.

Kimura, K., Oki, Y., 2017. Efficient control of membrane fouling in MF by removal of biopolymers: Comparison of various pretreatments. Water Research 115, 172–179.

Kimura, K., Shikato, K., Oki, Y., Kume, K., Huber, S.A., 2018. Surface water biopolymer fractionation for fouling mitigation in low-pressure membranes. Journal of Membrane Science 554, 83–89.

Kimura, K., Tanaka, K., Watanabe, Y., 2014. Microfiltration of different surface waters with/without coagulation: Clear correlations between membrane fouling and hydrophilic biopolymers. Water Research 49, 434–443.

Kimura, M., Matsui, Y., Saito, S., Takahashi, T., Nakagawa, M., Shirasaki, N., Matsushita, T., 2015. Hydraulically irreversible membrane fouling during coagulation-microfiltration and its control by using high-basicity polyaluminum chloride. Journal of Membrane Science 477, 115–122.

Kovalsky, P., Wang, X., Bushell, G., Waite, T.D., 2008. Application of local material properties to prediction of constant flux filtration behaviour of compressible matter, Journal of Membrane Science 318, 191–200.

Lee, S.-J., Kim, J.-H., 2015. Effects of coagulation on the ceramic membrane fouling during surface water treatment. Journal of Environmental Engineering 141, 4014087.

Matsui, Y., Hasegawa, H., Ohno, K., Matsushita, T., Mima, S., Kawase, Y., Aizawa, T., 2009. Effects of super-powdered activated carbon pretreatment on coagulation and trans-membrane pressure buildup during microfiltration. Water Research 43, 5160–5170.

Matsui, Y., Sanogawa, T., Aoki, N., Mima, S., Matsushita, T., 2006. Evaluating submicron-sized activated carbon adsorption for microfiltration pretreatment. Water Science and Technology: Water Supply 6, 149–155.

Murić, A., Petrinić, I., Christensen, M.L., 2014. Comparison of ceramic and polymeric ultrafiltration membranes for treating wastewater from metalworking industry. Chemical Engineering Journal 255, 403–410.

Nagahoro Water Supply Authority, 2006. The First Water Treatment Plant, Hokkaido, Japan. http://www.nagahoro.jp/authority/plant_01/ (accessed 2.1.22).

Pan, L., Matsui, Y., Matsushita, T., Shirasaki, N., 2016. Superiority of wet-milled over dry-milled superfine powdered activated carbon for adsorptive 2-methylisoborneol removal. Water Research 102, 516–523.

Pan, L., Nishimura, Y., Takaesu, H., Matsui, Y., Matsushita, T., Shirasaki, N., 2017. Effects of decreasing activated carbon particle diameter from 30 Mm to 140 nm on equilibrium adsorption capacity. Water Research 124, 425–434.

Partlan, E., 2017. Superfine Powdered Activated Carbon (S-PAC) Coupled with Microfiltration for the Removal of Trace Organics in Drinking Water Treatment. Doctoral dissertations, Clemson University.
Pelekani, C., Snoeyink, V.L., 1999. Competitive adsorption in natural water: Role of activated carbon pore size. Water Research 33, 1209–1219.

Samaei, S.M., Gato-Trinidad, S., Altaee, A., 2018. The application of pressure-driven ceramic membrane technology for the treatment of industrial wastewaters – A review. Separation and Purification Technology 200, 198–220.

Shao, S., Liang, H., Qu, F., Li, K., Chang, H., Yu, H., Li, G., 2016. Combined influence by humic acid (HA) and powdered activated carbon (PAC) particles on ultrafiltration membrane fouling. Journal of Membrane Science 500, 99–105.

Tian, J., Ernst, M., Cui, F., Jekel, M., 2013. Correlations of relevant membrane foulants with UF membrane fouling in different waters. Water Research 47, 1218–28.

Zhao, P., Takizawa, S., Katayama, H., Ohgaki, S., 2005. Factors causing PAC cake fouling in PAC-MF (powdered activated carbon-microfiltration) water treatment systems. Water Science and Technology 51, 231–240.

Zhao, Y., Kitajima, R., Shirasaki, N., Matsui, Y., Matsushita, T., 2020. Precoating membranes with submicron super-fine powdered activated carbon after coagulation prevents transmembrane pressure rise: Straining and high adsorption capacity effects. Water Research 177, 115757.

Zhu, H., Wen, X., Huang, X., 2012. Characterization of membrane fouling in a microfiltration ceramic membrane system treating secondary effluent. Desalination 284, 324–331.

Chapter 5. Conclusions

In this study, the application of SSPAC on mitigating membrane fouling in microfiltration systems was investigated in detail. Compared to conventional PAC, SSPAC exhibits superior adsorption performance on membrane foulants (biopolymers). In addition, this study also developed an addition method for SSPAC: pulse dosing, which allows SSPAC to form a protective layer on the membrane surface at the initial stage of filtration to prevent it contacting with foulants in water body during the filtration. It was then revealed that the essential role of coagulation process in the application of pulse SSPAC dosing, which related to the removal of precoated layer by each backwash step (Chapter-2). Pulse dosing of SSPAC was tested under the circumstances of 1) a submerged membrane system that enables vacuum-driven outside-in filtration by a hollow fiber PVDF polymeric membrane or a tubular ceramic membrane and 2) a filtration system that enables pressure-driven inside-out filtration by a monolithic ceramic membrane (Chapter-4). In the case of 1) with a hollow fiber PVDF polymeric membrane, the precoating speed of pulse SSPAC dosing, coagulant dose timing and coagulant types were further investigated, attempting to obtain the optimum condition when applying pulse dosing of SSPAC with coagulation method (Chapter-3). Here, I would like to summarize the important findings from the study of each chapter:

1) Superior adsorption capacity of SSPAC.

The capacity of AC to adsorb biopolymers increases with a decrease in the AC particle size and hence follows the order as PAC < SPAC < SSPAC. SSPAC selectively adsorbs biopolymers form NOM compared with PAC and SPAC. The superiority of SSPAC for biopolymer adsorption suggests that it has potential application in the control of membrane fouling.

2) Straining effect by pulse dosing of SSPAC (precoating).

Biopolymers can be strained out by SPAC/SSPAC precoat layer on membrane surface. SSPAC precoating removes biopolymers with a stronger straining effect than SPAC precoating caused by the difference between AC particle sizes.

3) The importance of coagulation.

Coagulation is indispensable in AC precoat filtration process because coagulation removes biopolymers and facilitates the detachment of AC particles from the membrane during hydraulic backwashing, and in this way prevents hydraulically irreversible membrane fouling by AC itself.

4) Precoating speed of SSPAC.

Changing the precoat filtration flux after pulse dosing of SSPAC did not have a significant effect on suppression of TMP rise. However, a slow or constant flux rather than a high flux is recommended to suppress TMP rise because the formed precoat layer can be cleaned off by hydraulic backwashing more easily.

5) Coagulant dose timing with pulse dosing of SSPAC.

Dosing with PACl throughout the water feed and the whole filtration process was the most effective of the various dosing schedules of coagulant for suppressing TMP rise. Although pulse dosing of SSPAC was effective in suppressing TMP rise, pulse doing of PACl coagulant was not and resulted in excessively large floc particles that settled to the bottom of the membrane tank instead, where they influenced the formation of the precoat layer.

6) Coagulant types.

A sulfated PACl with high basicity (70%) seemed to be more effective in suppressing a rise of TMP than one with medium basicity (50%). However, for non-sulfated PACls, low-to-medium-basicity PACls (20% and 40%) effectively suppressed TMP rise rather than PACls with basicities of 0% and 70%.

7) Pulse dosing of SSPAC in ceramic membranes.

Pulse dosing of SSPAC prevented TMP rise more than continuous dosing of SSPAC in the submerged membrane filtration system with a ceramic membrane. A precoating layer composed of SSPAC formed evenly on the ceramic membrane surface and was peeled off cleanly by hydraulic backwashing in the case of the pulse dosing of SSPAC. High removal of NOM (including biopolymer and HS) and a uniform layer of SSPAC, which prevented attachment of NOM to the membrane surface at the beginning of filtration, was thought to be the cause.

In monolithic ceramic membrane systems, pulse dosing of SSPAC did not alleviate TMP rise better than continuous dosing of SSPAC and did not remove NOM better. The uneven distribution of pulse dosed SSPAC in the membrane channels was thought to be a cause of the lack of any difference between the efficacy of the pulse dosing of SSPAC over the continuous dosing. The higher backwash pressure in the monolithic ceramic membrane system versus the submerged membrane filtration was not the cause of the absence of a treatment effect.